Productivity surfaces for *Pinus radiata* and a range of indigenous forest species under current climatic conditions

MAF Technical Paper No: 2011/45

Full report prepared for Ministry of Agriculture and Forestry
By Landcare Research (CO9X0902)
2010

Authors: MUF Kirschbaum, NWH Mason, MS Watt, A Tait, AE Ausseil, DJ Palmer, FE Carswell

ISSN 2230-2794 (online)
ISBN 978-0-478-38415-4 (online)

June 2011

Ministry of Agriculture and Forestry
Te Manatū Ahuwhenua, Ngāherehere

BIOSECURITY NEW ZEALAND

NEW ZEALAND FOOD SAFETY AUTHORITY

Publisher

Ministry of Agriculture and Forestry
PO Box 2526
Pastoral House, 25 The Terrace
Wellington 6140
www.maf.govt.nz

Telephone: 0800 008 333

Facsimile: +64 4 894 0300

Productivity Surfaces for *Pinus radiata* and a range of indigenous forest species under current climatic conditions, and exploration of the effect of future climatic changes on *Pinus radiata* productivity.

Final Report

Contract: C09X0902

Landcare Research
Manaaki Whenua

Productivity Surfaces for *Pinus radiata* and a range of indigenous forest species under current climatic conditions, and exploration of the effect of future climatic changes on *Pinus radiata* productivity.

Miko U.F. Kirschbaum[1], Norman W.H. Mason[2], Michael S. Watt[3], Andrew Tait[4], Anne-Gaelle E. Ausseil[1], David J. Palmer[5], Fiona E. Carswell[6]

Prepared for:

Ministry of Agriculture and Forestry

PO Box 2526

Wellington

2010

[1]*Landcare Research, Private Bag 11052, Palmerston North 4442, New Zealand, Ph +64 6 353 4800, Fax +64 6 353 4801, www.landcareresearch.co.nz*

[2]*Landcare Research, Private Bag 3127, Hamilton 3240*

[3]*Scion, PO Box 29237, Christchurch 29237*

[4]*NIWA, Private Bag 14-901, Kilbirnie, Wellington*

[5]*Scion, Private Bag 3020, Rotorua 3046*

[6]*Landcare Research, PO Box 40, Lincoln 7640*

Reviewed by:	*Approved for release by:*
Ian Payton Research Leader Landcare Research	David Whitehead Science Team Leader Global Change Processes

Landcare Research Contract Report:	LCR0910/176

Contents

Executive Summary

The aim of the present work was to generate productivity surfaces for indigenous forest species and *Pinus radiata* for New Zealand. For *P. radiata*, these surfaces were generated for current and anticipated future climatic conditions. Simulations were performed under the assumption of constant CO_2 concentration and with increasing CO_2 as anticipated in line with future climatic conditions.

For indigenous forests, the work used predictive modelling techniques (boosted regression trees) to produce spatial models of tree diameter increment. Surfaces were produced for 10 indigenous species, *Beilschmiedia tawa, Dacrydium cupressinum, Elaeocarpus hookerianus, Myrsine australis, Nothofagus fusca, Nothofagus menziesii, Nothofagus solandri, Podocarpus hallii, Prumnopitys ferruginea* and *Weinmannia racemosa.* Models were developed based on diameter measurements from over 5000 0.04-ha plots in the NVS database that had been measured at least twice. Plots were scattered throughout New Zealand, but were mainly concentrated in moist montane regions which reflects the distribution of the majority of New Zealand's remaining indigenous forests. Mean carbon sequestration rates varied from 1.3 $tCO_2e\ ha^{-1}\ yr^{-1}$ for *Podocarpus hallii* to 6.5 $tCO_2e\ ha^{-1}\ yr^{-1}$ for *Dacrydium cupressinum.* Productivity surfaces were generated for all ten species at 0.05 degree resolution.

Productivity modelling for *P. radiata* was based on simulations with the physiologically based model CenW that was parameterised using growth data from permanent sample plots and a larger data set of less intensively measured growth plots covering a wide range of environmental conditions throughout New Zealand. The primary data set consisted of 101 sites with 1297 individual stand-level observations of height and/or basal area from which diameters and volumes could also be calculated. Model efficiencies were very high, 0.824-0.886 for the four growth indices that either were directly observed, or could be readily deduced from the data.

Modelled mean volume productivity, over the course of a 30 year rotation, for *P. radiata* was 24.9 $m^3\ ha^{-1}\ yr^{-1}$ and ranged from 0 to 50 $m^3\ ha^{-1}\ yr^{-1}$ for different regions. In terms of biomass increments, mean growth rate was 14.6 $tDW\ ha^{-1}\ yr^{-1}$ and ranged from 0 to 30.8 $tDW\ ha^{-1}\ yr^{-1}$. Growth rates were highest in the Taranaki region and lowest in Canterbury, Otago and the West Coast.

Responses to climate change were simulated under the climatic outputs of 12 different Global Circulation Models (GCMs) that had been forced by climate-change scenarios according to the SRES A1B, A2 and B1 scenarios and were conducted for 2040 and 2090 and compared against productivity in 1990. Regionally specific climate-change fields were available for each GCM/emission scenario combination, and those inputs were used as the base of climate change simulations. Humidity changes were calculated on the basis of the assumption that minimum and maximum temperatures would respond in the same way to climate change so that the diurnal temperature range would remain unaltered. There is some uncertainty as to the physiological response of trees to increasing CO_2 concentrations. Simulations were therefore run with either the CO_2 concentration representative of 1990 or that corresponding to future periods under the different emission scenarios.

Without considering changes in CO_2, responses to climate change were generally slight, with a net change across the country close to 0. There were detrimental effects in the North Island

owing to direct temperature stress and increasing water stress, but gains in the South Island, especially in cooler, higher altitude locations. For sites where *P. radiata* is currently grown, changes across the full suite of GCMs and scenarios ranged from –7.5 to 12.5% changes in productivity by 2040 and from –20 to +25% by 2090.

When the model was run with the inclusion of increasing CO_2 concentration, responses were generally positive, with increases in productivity of 15% by 2040 and 25% by 2090. These responses varied regionally, with minor positive effects in the North, but very significant growth increases in the South where the beneficial effect of increasing CO_2 combined with the beneficial effect of increasing temperatures. These relatively large responses to CO_2 were partly due to the assumption of maintenance of adequate fertility in plantations – as was largely observed for stands growing today. For stands growing with nutrient limitations, lesser growth responses to CO_2 have to be expected.

Growth enhancements did come at the expense of expected losses in soil carbon, mainly due to the increase in temperature, which is expected to stimulate organic matter decomposition. Average losses for the country are likely to range from 3–4% if CO_2 is held constant to 1–2% if CO_2 concentration is increased. Again, there are likely to be large regional differences, with larger losses in regions that experience lower growth enhancements, whereas in regions with greater growth enhancements, the effect of faster decomposition activity can be partly balanced by greater carbon input from litter.

1 Introduction

Plantation forests, primarily of *Pinus radiata*, in New Zealand currently occupy about 1.8 Mha, with 680 000 ha estimated as "Kyoto-compliant" (Wakelin and Beets 2009). Several Mha have been identified by various workers as being suitable for either indigenous forest regeneration (Beets et al. 2009) or additional exotic plantation forestry (Wakelin and Beets 2009). It is important to be able to estimate the growth rate of these forests accurately to help both in optimal siting of future plantations and in national policy formulation. It is particularly important to provide some guidance on likely future growth rates to either forewarn growers of potential problems or allow the industry to best capture future growth opportunities.

Forest growth varies as a function of climatic and soil characteristics (Madgwick 1994). While much has been learnt about the response of *P. radiata* and other tree species to these key drivers of productivity, this information has not often been put together in national analyses that allow a comparison of productivity between different regions, and assessment of variability in key limitations across the country. The information has also not been given in a form that would allow an assessment of the likely response of productivity to climatic changes.

Current productivity estimates are often based on growth estimates of *P. radiata* per region (MAF 2010), an approach that ignores the key productivity drivers, which vary not only between but also within individual regions. An advancement of that was provided by Watt et al. (2010) who generated productivity estimates for *P. radiata* for New Zealand based on identified key environmental variables. Watt et al. (2010) identified mean annual temperature, water availability, wind exposure, and slope and soil characteristics as the most important determinants of tree growth. These estimates provide a good approximation of growth of *P. radiata* under current climatic conditions.

The work of Watt et al. (2010) was, however, based on the use of an empirical model and thus does not allow the extrapolation of their findings to new combinations of environmental conditions. Important physiological determinants, such as atmospheric CO_2 concentration, were also not included in that modelling approach as there is no relevant variability in CO_2 under current conditions. The extrapolation of growth estimates to future climatic conditions instead requires a modelling approach based on a more mechanistic approach in which all expected changes can be simulated even if there is no present-day variability in those that would allow the parameterisation of an empirical model (Watt et al. 2008).

Such a physiologically based assessment of future productivity of pines has not yet been done for New Zealand, but various model assessments have been carried out in Australia (Kirschbaum 1999c; Simioni et al., 2009; Battaglia et al., 2009) and the Mediterranean region (e.g., Sabate et al. 2002; Magnani et al. 2004). Such analysis needs to combine the various direct physiologically important climatic changes, such as temperature and CO_2 concentration, with indirect changes, such as changes in soil-nitrogen mineralisation and water availability.

Productivity surfaces have also not yet been generated for indigenous species in New Zealand. Estimating productivity for indigenous species is more difficult than for plantation-grown *P. radiata* because species possess a variety of physiological attributes, and because

trees usually occur in mixed-species, multi-aged stands, actual growth rates tend to be affected by competitive interactions with other trees (especially for smaller trees) as much as they are affected by environmental drivers. Stand age can have a large influence on carbon gain at scale of both individuals and stands, with regenerating stands gaining carbon and mature stands having more-or-less constant carbon stocks (Payton 2007).

The productivity surface for New Zealand indigenous forests was developed based on comprehensive datasets provided through both the National Vegetation Survey (NVS) and the Land Use and Carbon Analysis System (LUCAS). Generation of a surface underpinned by such comprehensive data has not previously been attempted. Existing approaches have either calculated gross productivity (e.g., Whitehead et al. 2001) or have insufficiently accounted for the contribution of different indigenous species (e.g., Baisden 2006). Boosted regression trees are considered the most appropriate methods for modelling interactions between predictor variables in complex systems such as mixed-species, mixed-age forests (Elith et al. 2008) and offer an excellent solution for modelling productivity under current climatic conditions.

2 Model description

Plant productivity surfaces represent the potential C sequestration across the country as a function of identifiable environmental drivers. Potential annual carbon sequestration was modelled as a two-step process for 10 indigenous tree species. First, annual diameter growth of individual trees was modelled based on individual tree diameter and the total basal area of the 0.04 ha plot in which they occurred using non-linear least absolute deviances regression. Then, for each plot in which the species occurred, the mean deviance of individual tree growth was taken across the trees of the relevant species occurring within the plot. Boosted Regression Trees (BRTs) were used to predict mean deviance in annual diameter growth of plots, as a means of modelling environmental effects on tree growth.

Productivity modelling for *P. radiata* was based on simulations with the physiologically based model CenW that was parameterised against growth data from permanent sample plots covering a wide range of environmental conditions throughout New Zealand. Both models were used to generate productivity surfaces under current climatic conditions. The CenW model was also used to generate productivity surfaces for *P. radiata* under changed climatic conditions, including and excluding the effect of elevated CO_2 concentration.

2.1 Indigenous forest productivity methods

2.1.1 Forest plot data and quality control

Diameter measurements from over 5000 20 m × 20 m (0.04 ha) plots that had been surveyed at least twice were extracted from the NVS database. Plots were scattered throughout New Zealand, but were mainly concentrated in moist montane regions (Figure 1). This reflects the distribution of the majority of New Zealand's remaining indigenous forests. The plots covered a range of vegetation types, with types including or dominated by beech (*Nothofagus spp.*) being especially well represented (Figure 1). Forest types containing kamahi

(*Weinmannia racemosa*) and podocarp species were also well represented. Most plots were first measured in the 1970s or 1980s, and most measurements occurred after 2000.

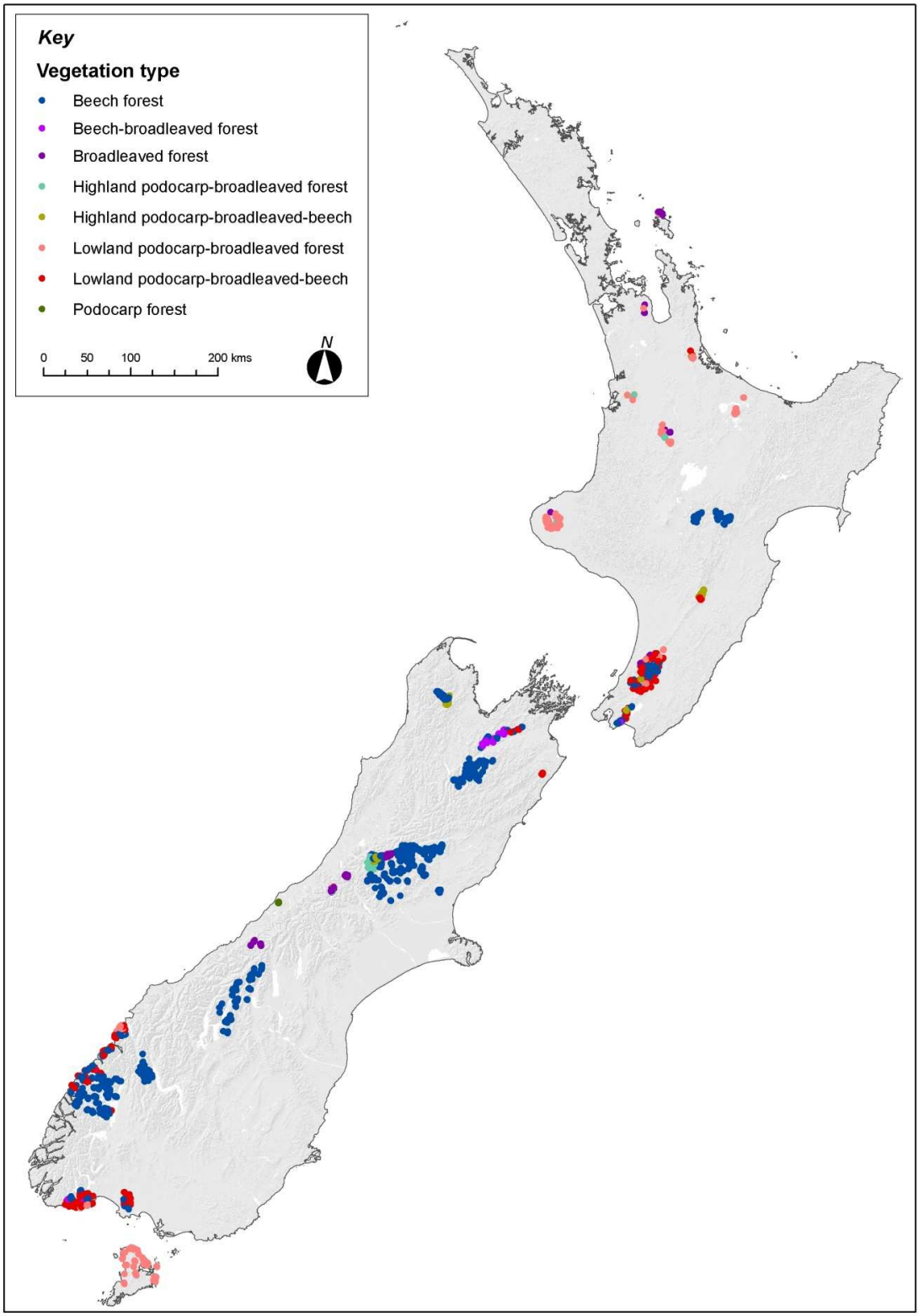

Figure 1 Location of indigenous forest plots used for the growth analysis of indigenous forests.

Diameter data have been thoroughly checked for errors, with special attention paid to ensuring that individual stems were correctly matched between surveys. Possible errors in diameter records were removed by excluding any stems that decreased in diameter by more than 0.5 cm per year or grew by more than 1 cm per year. This represented less than 0.01 percent of stems in the dataset. No differentiation was made between individuals with a single trunk and those with multiple leaders.

2.1.2 Diameter growth modelling

Non-linear diameter at breast height (dbh) growth models were fitted for all species represented by more than 200 remeasured stems with diameter <30 cm. These models predicted diameter growth in all stems <30 cm using the stem initial diameter and the initial stand basal area by minimising absolute deviances (equivalent to fitting a quantile non-linear regression through the median) for the expression:

$$\Delta D = \frac{D_{t2} - D_{t1}}{t_2 - t_1} = \mathrm{d} + \mathrm{a}D_{t1}{}^{\mathrm{b}} + \mathrm{c}BA_{t1}$$

where ΔD is annual change in dbh, t_1 and t_2 are the times of the initial and final measurements (expressed in years), D_{t1} and D_{t2} is dbh at time t_1 andt_2, respectively and BA_{t1} is total basal area in the 0.04 ha plot at time t_1, and a, b, c and d are fitted parameters. Stems over 30cm dbh were excluded since it is unlikely trees would reach this size over the length of time modelled and past work has found the slope of the relationship between diameter and growth rate changes at or around this diameter in several common indigenous tree species (Hurst et al. 2007).

Table 1 *Specifications for key climatic variables used in BRT models*

Name	Data Source	Interpolation Method	Number of Weather Stations
Mean annual rainfall (mm)	*Rainfall Normals for New Zealand 1951 to 1980, N.Z. Meteorological Service Miscellaneous Publication 185, + misc. rain gauge records*	*Anusplin – easting, northing, PCA as splines + elevation as a covariate*	*Stations – 2202*
Mean vapour pressure deficit at 0900 hours (kPa)	*Summaries of Climatological Observations to 1980, N.Z. Meteorological Service Miscellaneous Publication 177*	*Anusplin – easting, northing, PCA as splines + elevation as a covariate*	*Stations – 287*
Mean annual and Mean June daily solar radiation ($MJ/m^2/day$)	*Summaries of Climatological Observations to 1980, N.Z. Meteorological Service Miscellaneous Publication 177*	*Anusplin – easting, northing & humidity as spline variables*	*Stations – 21 solar radiation, 91 sunshine hours*
Mean annual temperature (℃)	*Summaries of Climatological Observations to 1980, N.Z. Meteorological Service Miscellaneous Publication 177*	*Anusplin – easting, northing & elevation as splines*	*Stations = 300*
Mean minimum temperature in the coldest month of the year (℃)	*Summaries of Climatological Observations to 1980, N.Z. Meteorological Service Miscellaneous Publication 177*	*Anusplin – easting, northing & elevation as splines*	*Stations = 300*

Diameter was included since previous work has suggested that growth in diameter may be strongly related to initial diameter in indigenous New Zealand tree species (e.g., Coomes & Allen 2007). Basal area was included as an indicator of competition (mainly for light), and since it has been demonstrated as a key factor influencing individual stem growth (Coomes & Allen 2007). For biological interpretability, a and b were constrained to be non-negative, while c was constrained to be non-positive. This model was chosen since it received the strongest AIC weight support (Burnham & Anderson 2002) for almost all species among the models examined. Other models examined included all possible combinations of log, linear power and exponential relationships between initial diameter, basal area and ΔD. In some instances a combination of a power relationship between initial diameter and growth, and a logarithmic relationship between plot basal area and growth yielded a better fit. However, when extrapolating to stands of lower basal area than the minimum values in the observed data, these models gave unrealistically high estimates of carbon sequestration, making them unsuitable for the present work.

2.1.3 Modelling growth responses to environmental heterogeneity

For species where diameter growth was well or moderately well predicted by basal area and initial diameter, and which occurred in at least 100 plots, deviance in growth from that predicted by the model described above due to environmental variables was modelled using boosted regression trees (BRTs). BRTs have the advantage of modelling interactions between predictor variables well, which generally confers increased accuracy in prediction relative to alternative techniques. A drawback is that relationships between individual predictors and the response variable within BRT models can be difficult to describe. BRTs are a machine-learning modelling method based on classification and regression trees (CARTS), with the important difference that BRTs iteratively fit new models to explain residual variance left by previous models. Two key parameters can affect the efficiency of BRTs. The first is tree complexity, which sets a limit to the complexity of interactions that can be modelled. The second is learning rate, which determines the rate at which the influence of models on the final prediction decreases with each iteration. For this work we used a tree complexity of 5 (which allows interactions between as many as five predictors to be modelled), and a learning rate of 0.001. Models were optimised to minimise absolute deviance in cross validation. Here, the dataset was divided into 10 even-sized groups. Each group was sequentially removed from the dataset, models were fitted on the remaining data and deviance calculated by comparing predicted with observed values for the group that had been removed. Cross validation is vital in validating complex models like BRTs, since their flexibility means they can easily find solutions that fit the training data perfectly, but they do not predict well on to independent data. In this way, the cross validation deviance or correlation between observed and predicted values provides an accurate indication of the ability of models to predict on to independent data.

The response variable used was the plot-level mean deviance in observed annual diameter growth from that predicted by the initial diameter-basal area model. Means were calculated for each species separately. The influence of plots in BRT models was weighted by the number of stems in the plot, so that individual stems did not have a disproportionate effect on predictions if they occurred in plots with relatively few stems of the species in question. Plot weights were calculated as:

$$w_{is} = \frac{n_{is}}{\sum_{j=1}^{N} n_{js}}$$

where n_{is} is the is the number of stems of species s in plot i and N is the number of plots. 11 predictor variables were included in the BRT models. Climatic variables are listed in Table 1. In addition, soil phosphorous, slope and drainage were obtained from GIS layers associated with Land Environments New Zealand (Leathwick et al. 2003). These variables were chosen for their known importance in the growth and distribution of indigenous tree species (Leathwick & Whitehead 2001). The contribution of predictors in BRT models was recorded as the percentage of times a variable was used to make the dichotomous splits in the dataset that constitute individual regression trees. Once models had been fitted, deviance in diameter growth was predicted for each species for the entire country at a resolution of 0.05° latitude and longitude.

2.1.4 Predicting carbon sequestration during afforestation

For these predictions a scenario of single species even-aged stands was assumed. Initial stem density was held constant at 2500 stems ha^{-1}. All stems were assumed to have a starting diameter of 2.5 cm, the minimum size of measured stems in the forest plot data. Growth of individual stems was calculated based on diameter and basal area using the coefficients fitted during stem growth modelling. The predicted deviance from the BRT models was then added to give an environmentally adjusted annual increment in diameter. These calculations were performed in annual steps for a total of thirty years. Carbon sequestration at the end of this period was recorded at tonnes of CO_2 equivalents per hectare.

The carbon contained in individual stems was estimated using the allometric equations of Hall et al. (2001), which link stem diameter and height to stem volume and biomass in leaves and branches. To obtain carbon contained in stems, stem volume was multiplied by wood density values used in Mason et al. (2010). Stem heights were derived from models based on diameter produced by Mason et al. (2010).

$$\text{Stem Volume} = 0.0000598\ (\text{dbh}^2 \times \text{Height})^{0.946}$$

$$\text{Stem carbon (kg)} = \frac{1}{2}\text{Wood density}\ (1.0 - 0.0019 \times \text{dbh}) \times \text{Volume}$$

$$\text{Branch mass (kg)} = 0.03 \times \text{dbh}^{2.33}$$

$$\text{Foliage mass (kg)} = 0.0406 \times \text{dbh}^{1.53}$$

Root mass was assumed to be 25% of the live above-ground tree biomass following Hall et al. (2001). Finally, tree biomass was assumed to be comprised of 50% carbon (Coomes et al. 2002).

2.2 Modelling the productivity of *Pinus radiata*

We used the process-based model CenW to derive a productivity surface for *P. radiata*. This model has been used extensively in Australia to predict the growth of pine stands in response to silvicultural management options, climate and land-use change (Kirschbaum 1999a, b; Kirschbaum & Paul 2002; Kirschbaum et al. 2003; 2008a, b; Simioni et al. 2008, 2009). The model has also been used to derive productivity surfaces for all of Australia under current and future climatic conditions (Kirschbaum 1999c; Lucas & Kirschbaum 1999; Roxburgh et al. 2004).

CenW is a physiologically based model that allows the incorporation of key environmental drivers, including those that are likely to change in the future. The model was parameterised against a large set of site-specific data from plots throughout New Zealand. This allows modelling of climate-change simulations that lie outside the realm of empirical observations against which a regression-based model can be parameterised. CenW has been developed primarily for climate-change investigations and is therefore an ideal tool to model forest growth in response to multiple changes and multiple interacting factors. Even with that attribute, the extrapolation of simulations beyond the range over which the model can be tested against empirical data always retains an element of doubt. This is discussed further below.

The simulations used the model CenW 3.1 as described by Kirschbaum (1999, 2004) and Kirschbaum and Paul (2002). Further modifications to the model were added as part of the present work, and it is now designated as version 4.0. The model was originally developed and parameterised for *P. radiata*, which made it an ideal choice for the present work. The model and its source code are available at: http://www.kirschbaum.id.au/Welcome_Page.htm , with a full list of relevant equations available at http://www.kirschbaum.id.au/CenW_equations.pdf.

The model runs on a daily time step and simulates stand characteristics, such as leaf-area development, stand height, basal area development, litter fall and exchange of both water and CO_2. Stand-level dynamics are explicitly linked to carbon and nitrogen cycling in the soil and plants. This linkage allows multiple factors to constrain estimates of growth and carbon exchange of the stand at daily or longer time scales. For the present work, only nitrogen was included as a limiting nutrient as analysis of our primary observational data set showed no sign of phosphorus limitation (data not shown).

The model can be easily run over periods of several decades, which was necessary for the simulation of *P. radiata* forests that are typically grown for periods of 25–30 years. As external drivers, the model requires daily minimum and maximum temperature, solar radiation, a measure of atmospheric humidity and precipitation. The model was initialised by setting soil nitrogen levels proportional to those observed at our test sites, or, for simulations beyond our test sites, by extractions from a surface of soil nitrogen (W.T. Baisden, pers. comm.) developed from the National Soils Database (Wilde et al. 2000). In addition, soil water holding capacity and percentage of silt plus clay were also obtained from the National Soils Database.

A number of modelling changes were required and are described below. Other new routines required for the present simulations are described in Appendix 2. A set of key parameter values is given in Appendix 1. A brief description of the model is given in Sections 2.2.1-2.2.5, but readers are referred to the original publications or the web site for full modelling details.

2.2.1 Photosynthesis and Respiration

Photosynthetic calculations were based on combination of the photosynthesis model of Farquhar and von Caemmerer (1982) with the simple stomatal model of Ball et al. (1987). Maximum photosynthetic capacity was controlled by foliar nitrogen status and further restricted by temperature limitations, water stress and constraints imposed by water logging and excess rainfall. The Farquhar and von Caemmerer photosynthesis model also embodies a CO_2 response function, which was important for our climate change simulations. This response function is well-calibrated against short-term photosynthetic measurements. In longer term CO_2 enrichment experiments, photosynthetic rates often decline. To the extent that this phenomenon is due to nutrient feedback limitations, it is accounted for through the integrated structure of the model. Other possible feedback limitations are not well characterised and have not been included in the present work. The existence of further limitations cannot be excluded, but there is no established theory through which they could be included.

Instantaneous leaf-level equations were scaled up to the canopy and to a daily time scale using the equations of Sands (1995). These equations calculate daily canopy photosynthesis from parameters of single-leaf photosynthetic light response, canopy extinction coefficient, leaf area index, day length and daily solar irradiance. The calculations assume that light absorption within the canopy follows Beer's law that maximum photosynthetic rate within the canopy is proportional to light absorption and that light varies sinusoidally throughout the day. It is an efficient algorithm for calculating canopy photosynthesis while minimising systematic scaling errors.

2.2.2 Water relations

Daily transpirational water loss was calculated with the Penman-Monteith equation with canopy conductance explicitly linked to photosynthetic carbon gain based on the Ball-Berry model (Ball et al. 1987). Soil water-holding capacity was obtained from the National Soils Data base (Wilde et al. 2000).

2.2.3 Allocation

Plant stands were sub-divided into foliage, branches, sap- and heartwood, bark, pollen, cones and fine and coarse roots. This sub-division was found necessary as each of these pools is unique with respect to their nutrient concentration, longevity, physical location (above or below ground) and physiological function.

Carbon allocation to different plant organs was determined by plant nutrient status, tree height and species-specific allocation factors. It was assumed that the ratio of above- to below-ground allocation increased with foliar nitrogen concentration and that the allocation ratio of stem wood to foliage increases with increasing tree average height, but that allocation ratios between branches, bark and coarse roots and stem wood remain invariant with height or nutrient status. Nitrogen allocation was treated in a similar way except that it was further assumed that the nitrogen concentration in each biomass compartment scaled linearly with foliar nitrogen concentration.

Our primary calibration data set consisted of detailed height and basal area measurements from which tree diameters could be deduced. In order to adequately describe the growth in height and diameter across stands of different ages and stand densities and across regions with different temperatures and fertilities, we found it necessary to refine the allometric relationships that were used by CenW to calculate the relative allocation of carbon to height and diameter growth, respectively. Details of this work are given in Appendix 3.

From the measurements of height and diameter, wood volume, *V*, was calculated, following Kimberley and Beets (2007), as:

$$V = HB[0.942(H\text{-}1.4)^{-1.161} + 0.317]$$

where volume is in $m^3 ha^{-1}$ of wood, H is tree height in metres and B is basal area in $m^2\ ha^{-1}$.

For generating productivity surfaces, mean annual increment was calculated as the wood volume increment over 30 years under a standardised thinning regime. Wood weight increment was calculated as the woody biomass increment over the final years of growth.

These two measures thus differ primarily by the change in wood density with environmental variables, by the peculiarities of weather conditions in the final year of growth, and by the differential effect of environmental variables in controlling growth of mature stands versus the effect of the same variables over the whole rotation length.

Wood weight and wood volume increments are provided as alternatives in some of the following graphs, but neither is inherently better than the other. Growth can be expressed in many different ways, and two options are given below. The effect of climate change is given as the proportional effect on wood volume production as that is the measure of greatest direct relevance to forestry.

2.2.4 Organic matter dynamics

Organic matter dynamics were calculated with a version of the CENTURY model (Parton et al. 1987) that had been slightly modified to better describe the dynamics of forest soils and litters with their often wider C:N ratios than found in agricultural and grassland soils (Kirschbaum & Paul, 2002). As such, the model contains a complete and coupled nitrogen cycle, with nitrogen taken up by stands following decomposition and nitrogen mineralisation. Nitrogen was then either retained in plant pools or returned to the soil through senescence of plant organs, especially foliage and fine roots.

The amounts of organic matter at our test sites were scaled based on measured soil nitrogen concentrations (0–5 cm depth). For constructing national surfaces, organic matter amounts at different sites were scaled based on a national surface for soil nitrogen concentration (W.T. Baisden, pers. comm.). The rate at which that organic matter decomposes and makes nitrogen available for plant uptake was determined by temperature and the soil water status and as such is responsive to any changes in climatic conditions.

2.2.5 Weed unit

Initial runs of the model strongly over-estimated early stand growth. This was thought to be related to weed competition which had originally not been included in the model. In the original version of the model, stands were modelled as uniform stands, with all site resources, light, water and nutrients being available to developing stands of trees. In reality, of course, trees have to compete for site resources with weeds, which managers try to minimise in order to maximise tree growth.

However, weeds are not generally completely eliminated so that some reduction of early growth by weed competition has to be expected. Trees eventually overtop the weed layer so that weeds become strongly suppressed, and at later stages of growth, the original assumption of trees having sole access to site resources becomes valid again. To deal with the period of partial growth reduction by weeds, a new weed routine was introduced into CenW. This routine has been described in Appendix 2.

2.2.6 Model fitting

The present work aimed to get the best constrained estimates of the growth of *P. radiata* across New Zealand. We had access to observations from 101 sites at which height and/ or

basal area was measured repeatedly. There were 1297 independent stand-level observations. For each stand, stocking and the time for specified silvicultural operations were recorded, which included either thinning or branch pruning. On most sites, there was also a small amount of additional natural mortality. The model run from planting to the age at which the last observations on individual stands were available. These ages varied from 14 to 32 years for the observations from different stands. Modelled silvicultural manipulations followed the recorded sequence for individual stands.

Parameter values of the model were originally chosen based on past work in Australia (Kirschbaum 1999; Kirschbaum et al. 2008a; Simioni et al. 2007), but were modified further to achieve greatest possible agreement with respective observations. Parameter values were, however, constrained to remain within plausible bounds to retain the physiological integrity of the simulations. The output of this work was the estimation of growth, with parameter values used primarily as a tool to constrain growth estimates and allow a more confident extrapolation to future climatic conditions

We also used a second dataset of growth estimates (as 300 Index) that spanned a wider range of climatic conditions, especially in high-rainfall regions. From that dataset only a final growth estimate was available rather than detailed height and diameter observations. This data set consisted of observations from 1764 independent plots. Each stand was mapped onto our 0.05° data grid and, with a large number of observations duplicating other observations on that grid, only 548 grid locations were represented. Where multiple observations for the same grid location were available, we calculated and used the mean of all observations for that grid point. We had less confidence in the veracity of all the observations in this data set, but used it for additional constraints under the climatic conditions where our primary dataset had a poor representation.

2.2.7 Statistical analysis

The goodness of fit in respective comparisons between model and data was assessed by calculating model efficiency, which is the extent of variation explained by the model (or by a 1:1 relationship between observed and predicted values of the response). Hence, it assesses not only the closeness of the correlation between model and data, but also whether there is any consistent bias in the relationship. High model efficiency can only be achieved when model and data are consistently closely related and when there is little systematic bias in the model.

Formally, model efficiency, EF, was calculated as (Nash & Sutcliffe 1970; Soares et al. 1995):

$$EF = 1 - \frac{\sum (y_o - y_m)^2}{\sum (y_o - \bar{y})^2} \quad (1)$$

where y_o are the individual observations, y_m the corresponding modelled values and $\bar{y}$ the mean of all observations. Parameters were generally optimised to maximise the average of model efficiencies of all observations.

2.3 Climate data, including climate change projections

Daily data from the Virtual Climate Station Network (VCSN) from NIWA (National Institute of Water and Atmospheric Research Ltd.) were used in this study. Daily VCSN data are estimated for the whole of New Zealand on a 0.05° latitude/longitude (approximately 5 km) grid, using a spatial interpolation model (Tait et al. 2006; Tait 2008; Tait & Liley 2009). Daily estimates of rainfall begin in January 1960, for wind speed in January 1997, and for nine other variables data begin in January 1972. VCSN data are automatically updated every night using all the available climate station observations from the previous day, held in the NIWA climate database. A thin-plate smoothing spline model is used for the spatial interpolations. This model incorporates two location variables (latitude and longitude) and, for some variables, a third "pattern" variable (usually elevation) is included. For rainfall, the 1951–1980 mean annual rainfall digitised from an expert-guided contour map is used to aid the interpolation (Tait et al. 2006). The software used for the interpolations is ANUSPLIN (Hutchinson 2010).

For the purposes of this study, the 20-year period 1980–1999 was used to define the "current climate" and the climate variables used to model forest productivity were daily rainfall, maximum and minimum air temperature, global solar radiation and absolute humidity (calculated as the 9 a.m. vapour pressure).

For the climate change projections used in this study, outputs from 12 Global Climate Models (GCMs) were used to statistically downscale mean monthly temperature and rainfall changes for New Zealand at the same resolution as the VCSN data (0.05° latitude/longitude) following the methodology described in MfE (2008). The 12 GCMs are described in MfE (2008) and are noted in this study in shorthand as: CNRM (France), CCCma (Canada), CSIRO Mk3 (Australia), GFDL CM 2.0 (USA), GFDL CM 2.1 (USA), MIROC32 (Japan), ECHOG (Germany/ Korea), ECHAM5 (Germany), MRI (Japan), NCAR (USA), UKMO-HadCM3 (UK), UKMO-HadGEM1 (UK). Temperature and rainfall were statistically downscaled for each GCM; for the three emission scenarios B1 (low), A1B (mid-range) and A2 (high); and for two future periods 2030–2049 (midpoint reference year = 2040) and 2080–2099 (midpoint reference year is 2090).

To calculate future values of absolute humidity, dew-point temperature corresponding to the absolute humidity was calculated. This dew-point temperature was then changed according to the given projected changes in air temperature, and the new dew point temperature was used to calculate the changed absolute humidity. As methodology check, the calculated relative humidity under current and future conditions were compared, and we found that it barely changed, which is consistent with theory. Solar radiation was not changed for the future climate projections.

The daily values from the VCSN for 1980–1999 were then adjusted according to the mean monthly changes from the above projections. For maximum, minimum and dewpoint temperature, the mean monthly anomalies were directly applied to the daily values. For rainfall, the mean monthly rainfall change (in mm) was evenly distributed to all the days with rainfall in the corresponding month in the 1980–1999 dataset. For projections of decreasing or increasing mean monthly rainfall, it means that the number of "dry" and "wet" days remained unchanged.

3 Productivity of indigenous forests

3.1 Results

3.1.1 Stem diameter growth models

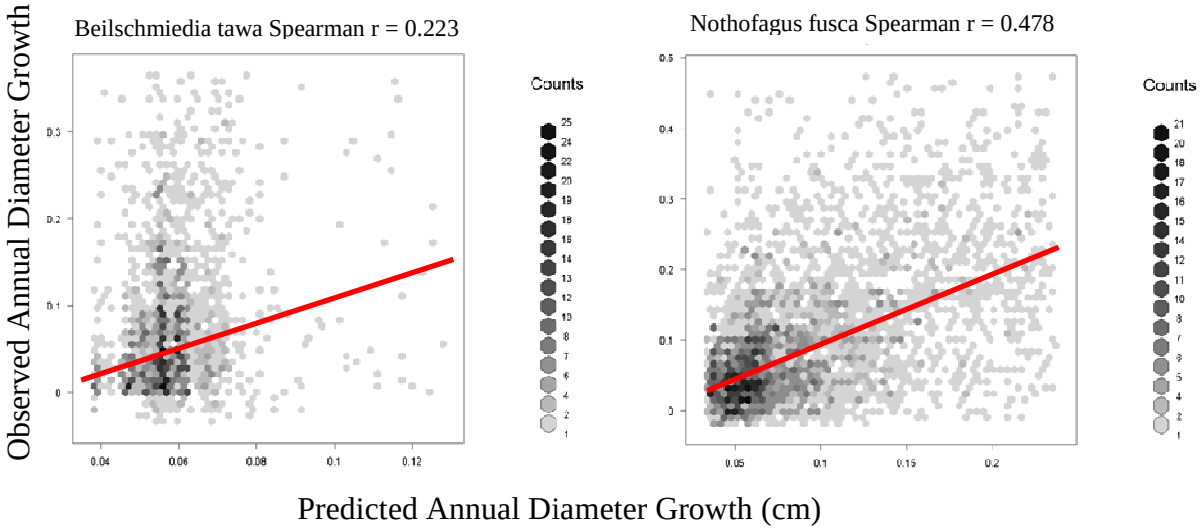

Figure 2 Examples of observed and predicted annual growth in diameter (cm) clipped to 95% confidence intervals for both observed and predicted. Red lines indicate a 1:1 relationship between observed and predicted. The full set of comparisons for all species is given in Appendix 5.

Growth models based on initial diameter and plot basal area had moderate to poor predictive accuracy (Appendix 5, Table 2). Generally, predicted values spanned only a small portion of the range of observed values (Figure 2).

To better reveal the distribution of individual stems in the plot, stems are grouped into hexagons. Darker hexagons contain more stems (in accordance with the legend for each plot). Here we show two extreme examples – *Beilschmiedia tawa* where the bulk of the data are poorly aligned with the 1:1 line, while for *Nothofagus fusca*, hexagons with high stem density are clustered evenly around the 1:1 line despite the large amount of scatter. The *N. fusca* example indicates that an unbiased estimate of stem diameter growth was obtained despite the large amount of error. This is an advantage of quantile regression, which is less sensitive to outliers than ordinary least squares regression.

Table 2 *Spearman correlations and parameters fitted in models of individual tree annual diameter growth including basal area and initial diameter. The model has the form Growth =* $\mathrm{d} + \mathrm{a}D_t^{\mathrm{b}} + \mathrm{c}BA_t$ *where t is the time if the initial measurement (expressed in years),* D_t *is d.b.h. at time t,* BA_t *is total basal area in the 0.04 ha plot at time t and a, b, c and d are fitted parameters*

Species	a	b	c	d	Spearman
BEITAW	$3.21e^{-08}$	4.5950	-0.0092	0.0787	0.223
DACCUP	0.1131	0.1718	-0.0399	0.0032	0.493
ELAHOO	$1.96e^{-08}$	4.4435	-0.0159	0.0664	0.417
MYRAUS	$5.93e^{-08}$	4.4023	-0.0106	0.0756	0.292
NOTFUS	0.0026	1.3033	-0.0125	0.0635	0.478
NOTMEN	0.0007	1.4437	-0.0070	0.0388	0.262
NOTSOL	0.0048	0.9947	-0.0183	0.0600	0.380
PODHAL	$2.02e^{-08}$	0.0001	-0.0034	0.0339	0.213
PRUFER	0.4982	0.0477	-0.0073	-0.4640	0.271
WEIRAC	0.0108	0.6731	-0.0018	0.0127	0.260

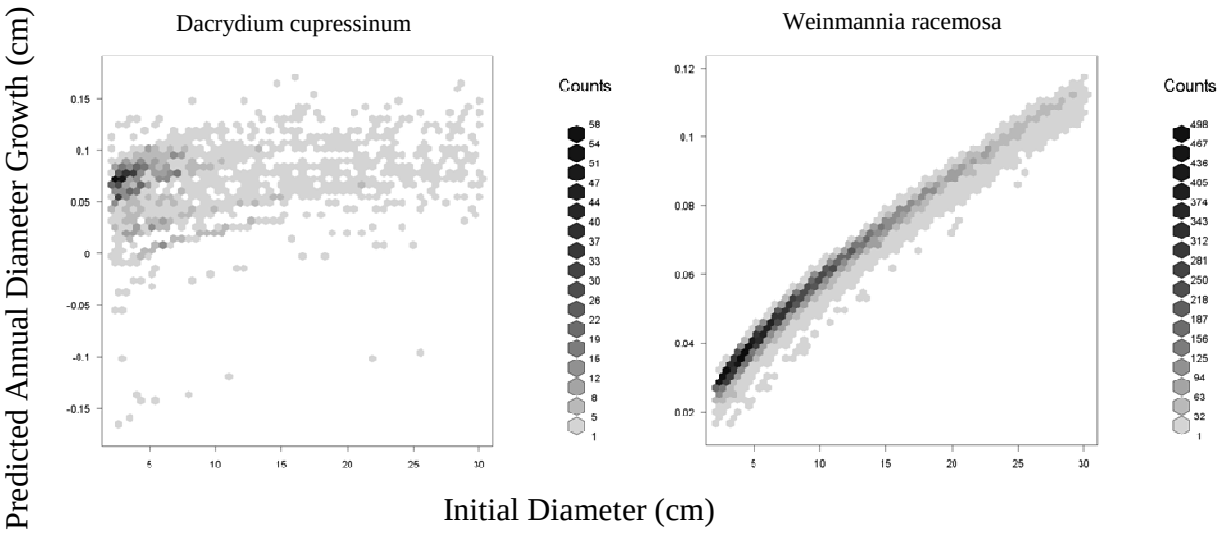

Figure 3 Predicted annual growth in diameter (cm) of individual stems against their initial diameter (cm) for selected species. A function, Growth = a +b(Diameter)^c + d(Basal Area) was fitted, with b and c constrained to be non-negative, and d constrained to be non-positive. Shading indicates density of stems within each hexagon according to the legend for each species.

Species differed markedly in the relative importance of diameter and basal area for predicted growth values. All the *Nothofagus* species, as well as miro (*Prumnopitys ferruginea*), kamahi (*Weinmannia racemosa*) and tawa (*Beilschiedia tawa*) were most strongly influenced by initial diameter. At the other extreme, growth in rimu (*Dacrydium cuppresinum*), mountain totara (*Podocarpus hallii*) and pokaka (*Elaeocarpus hookerianus*) was only weakly related to initial diameter. Examples of each extreme are given in Figure 3 (See Appendix for graphs of all species). That initial diameter had little effect on predicted growth values in the final model for *Dacrydium cupressinum* is shown by the large amount of scatter in the figure. Contrast this with *Weinmannia racemosa* where the relationship is very tight.

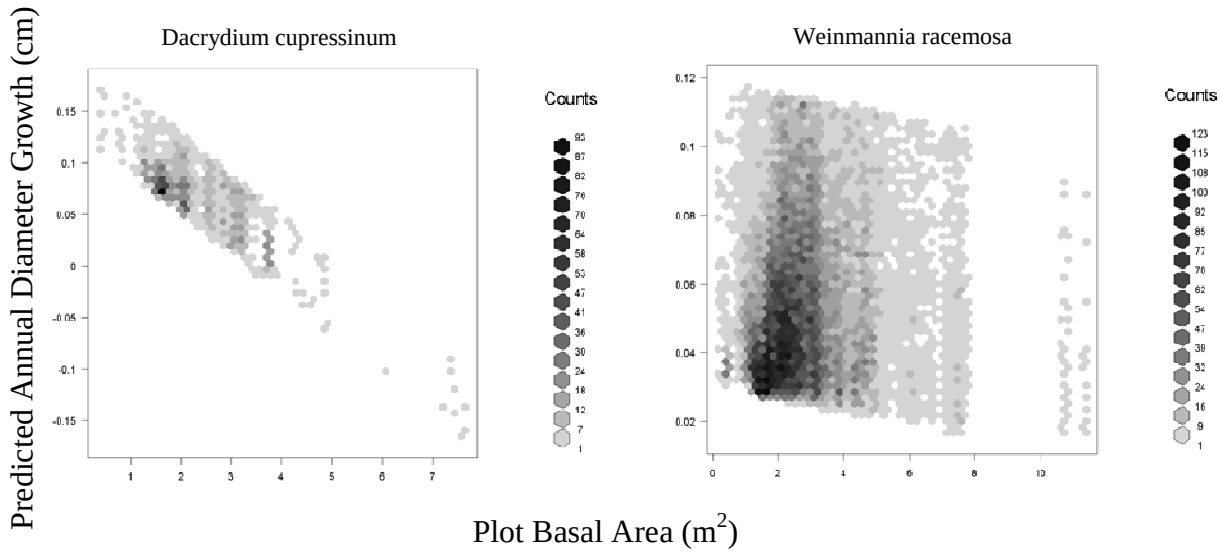

Figure 4 Predicted growth in diameter (cm) of individual stems against initial total basal area within the 0.04 ha plots in which they occurred. Predictions were obtained by fitting the model described in Figure 3. Here the strong effect of plot basal area on predicted growth values in the final model for *D. cupressinum* is seen in the tight, steep relationship between the two, in contrast to the scattered relationship for *W. racemosa*.

For basal area, the inverse was true, with all the species showing strong responses to diameter having only a diffuse relationship with basal area, while those species that did not respond to diameter had predicted growth values closely linked to stand basal area. Extreme examples given in Figure 4 (all species presented in Appendix 5). This indicates that the species studied may be roughly divided into groups of greater or lesser sensitivity to light competition.

3.1.2 BRT models of deviance in annual growth from diameter-basal area models

For most of the species studied, BRT models provided moderate accuracy in predicting on to independent data (as indicated by cross-validation correlation between observed and predicted values, Figure 5). The two exceptions were red beech (*Nothofagus fusca*) and *Myrsine australis*. Red beech had the second most accurate diameter-basal area growth model, so that the poor performance of the BRT model may be due to the relatively limited residual deviance left over from this model. There is no obvious explanation for the poor performance of the *Myrsine australis* model. For all species, there was no evidence of bias in predictions.

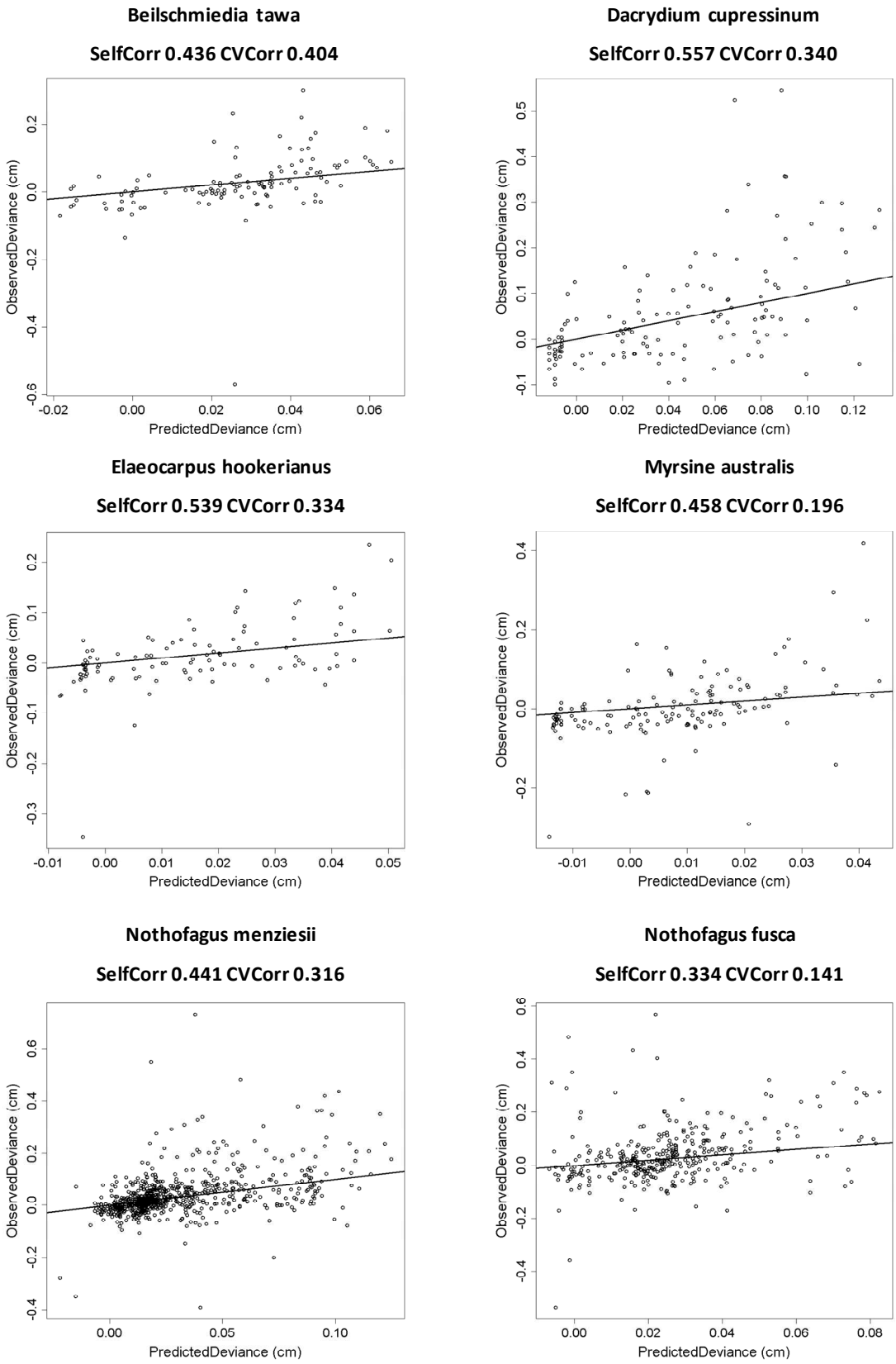

Figure 5 Observed and predicted mean deviance in annual diameter growth for 0.04 ha plots from boosted regression tree models. Lines indicate a 1:1 relationship between observed and predicted. SelfCorr refers to Spearman correlation based on training data, while CVCorr refers to Spearman correlation in cross validation (where BRT models were fitted on 90% of the data and validated on the remaining 10%). For all

species, plots were evenly distributed around the 1:1 line indicating that there was no evidence of bias in predictions.

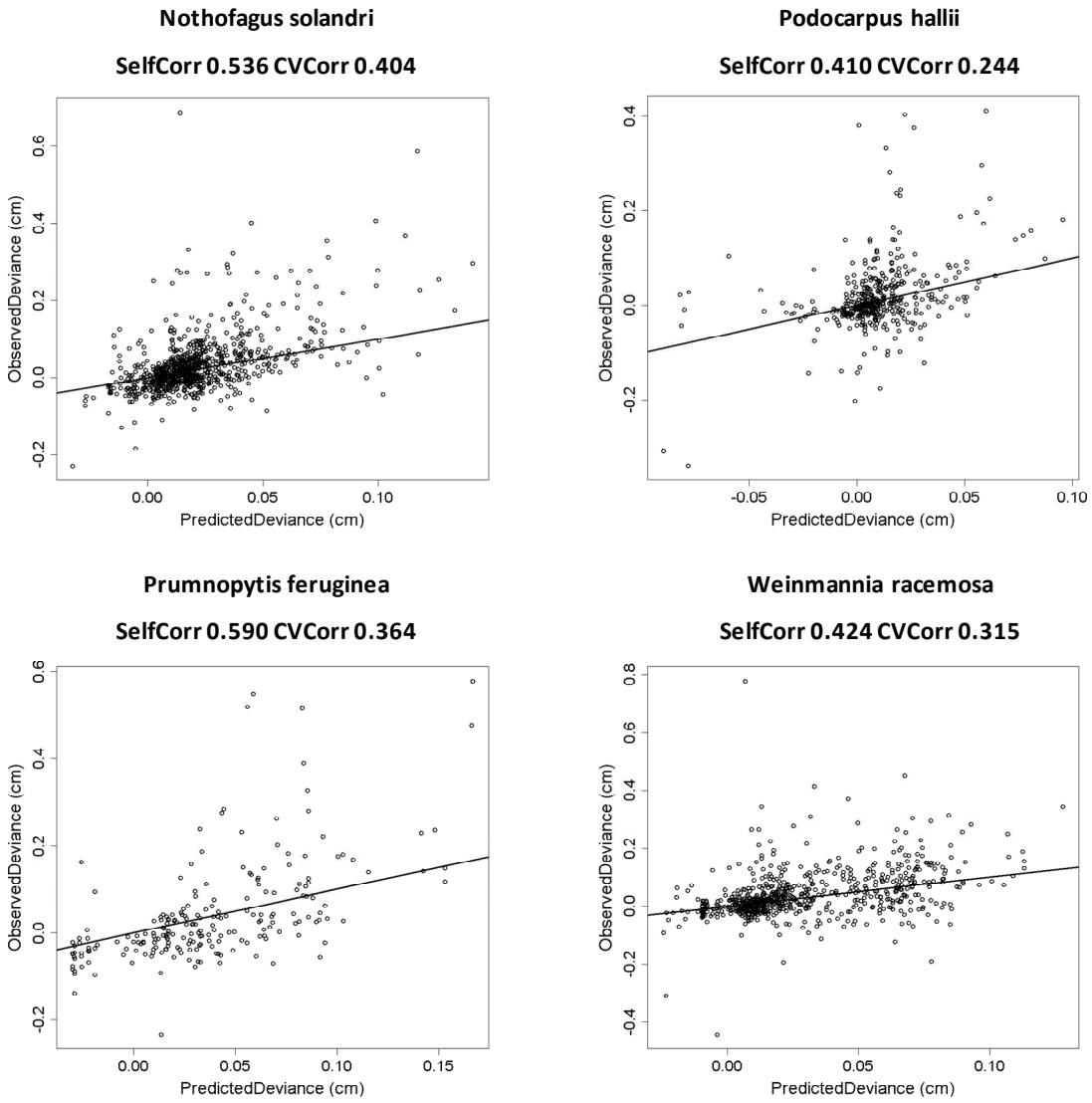

Figure 5 (continued).

Mean deviance (within plots) in growth from the diameter-basal area model in most species had a monotonic positive relationship with either mean or minimum temperature and mean annual or mean June solar radiation. One exception was tawa, where deviance showed a monotonic negative relationship with each of these variables. Responses to rainfall were more varied, with most species showing more negative deviance in growth with increasing rainfall, but with tawa and mountain totara showing monotonic increases and silver beech (*Nothofagus menziesii*) and kamahi showing parabolic relationships. These parabolic relationships are most likely due to correlations between predictor variables. Responses of mean deviance (taken across stems) in annual diameter growth within 0.04ha plots to mean annual temperature and rainfall are shown in Figures 6 and 7, respectively. Figures of deviance in diameter growth response to these and other key environmental variables are listed in Appendix 5.

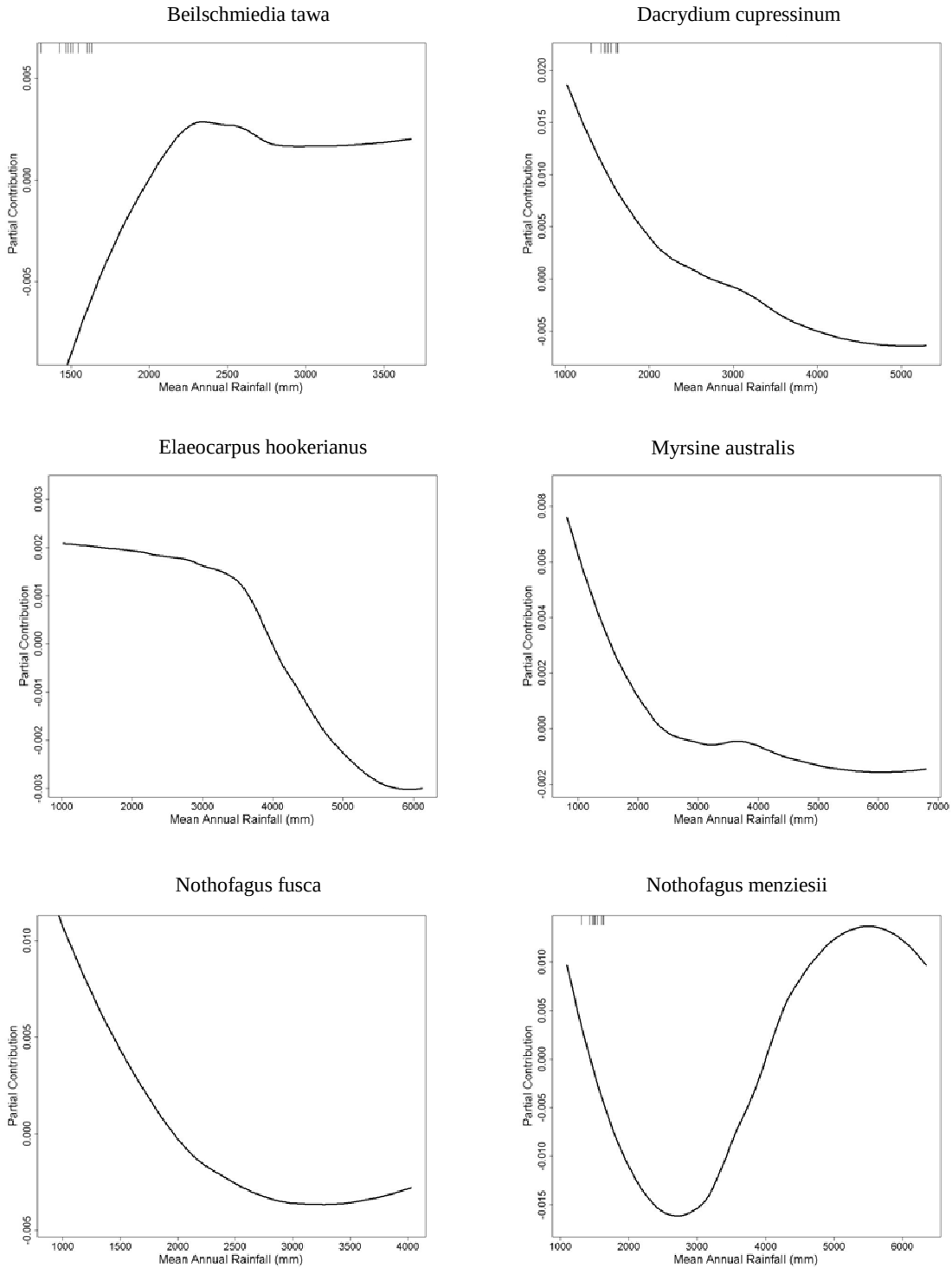

Figure 6 Partial contribution of mean annual rainfall in Boosted Regression tree models to deviance in annual stem diameter growth for 0.04 ha plots. Partial contributions are obtained by calculating the effect of mean annual rainfall on deviance in growth while holding the effects all other predictor variables constant.

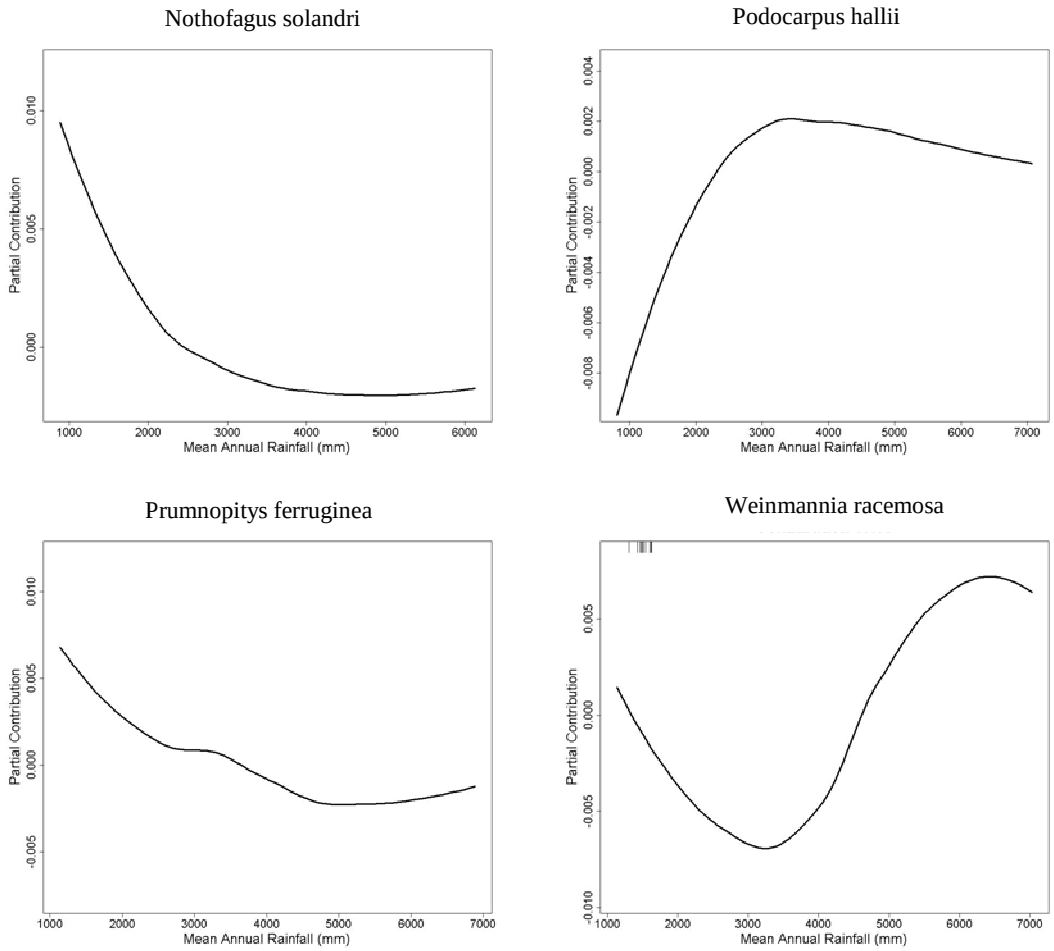

Figure 6 (cont).

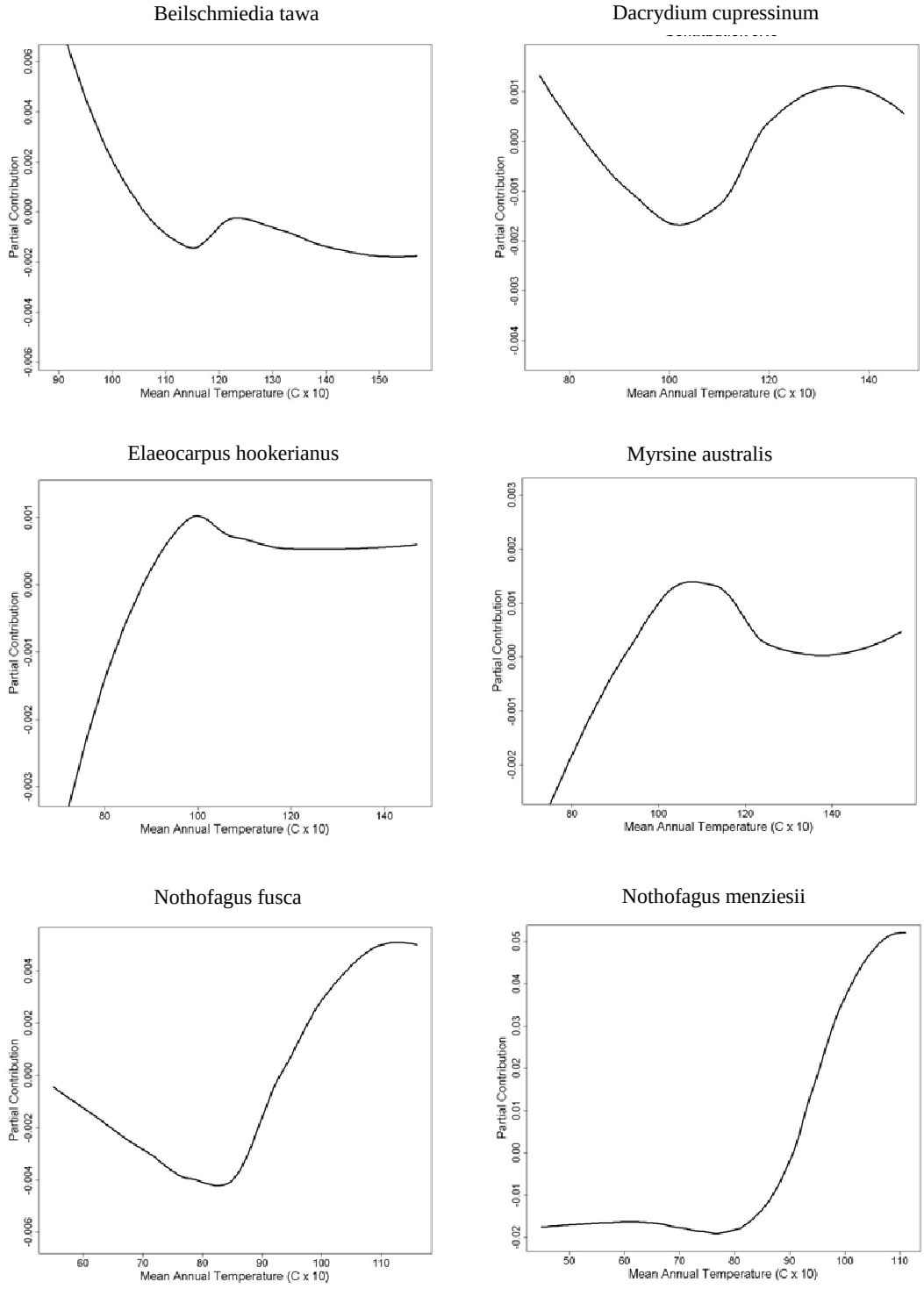

Figure 7 Partial contribution of mean annual temperature in Boosted Regression tree models to deviance in annual stem diameter growth for 0.04 ha plots. Partial contributions are obtained by calculating the effect of mean annual rainfall on deviance in growth while holding the effects of all other predictor variables constant.

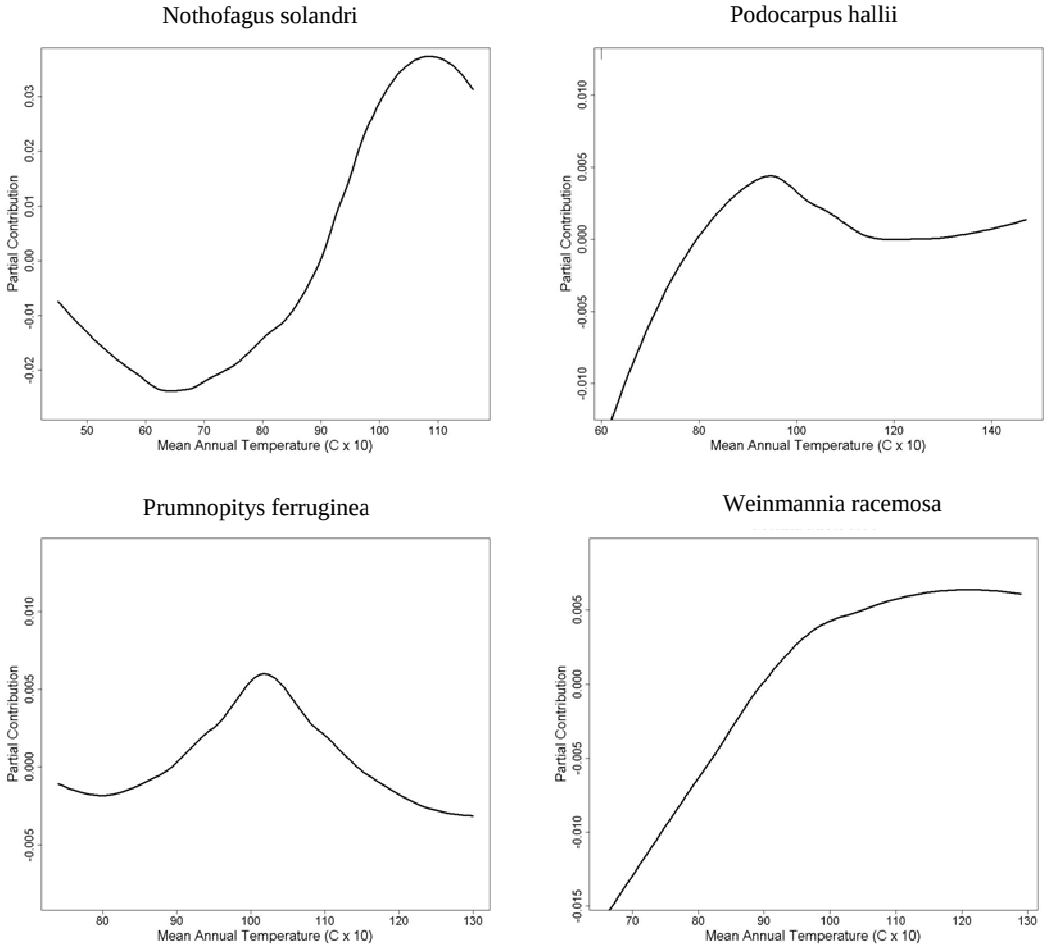

Figure 7 (cont.)

3.1.3 Predicted indigenous forest productivity

For estimating carbon gain of indigenous forest species, we used a stem density of 2,500 stems ha^{-1}. This stem density is commonly used in indigenous forest restoration planting. A variety of stem density values were tried, varying from 1,500 to 10,000 stems per hectare. Estimated carbon gain did not vary considerably across different densities since growth became rapidly constrained by stand basal area at higher densities.

In simulated even-aged stands, mean carbon sequestration rates varied across species from 1.26 tonnes CO_2e $ha^{-1}year^{-1}$ for *Podocarpus hallii* to 6.47 tonnes CO_2e $ha^{-1}year^{-1}$ for *Dacrydium cupressinum* (Table 3). When the species giving the maximal sequestration rate for each pixel was selected, the national mean carbon sequestration was 6.50 tonnes CO_2e $ha^{-1}year^{-1}$. Maps of spatial variation in carbon sequestration for each species are presented in Figures 8–17, and Figure 18 gives the sequestration potential of the most productive species at each location.

Table 3 *Mean and standard deviation of annual carbon sequestration for each species ($tCO_2e\ ha^{-1}\ yr^{-1}$), and when taking the species that gave the maximum sequestration at each pixel*

Species	Mean	S.D.
Beilschmiedia tawa	2.94	0.36
Dacrydium cupressinum	6.47	1.49
Elaeocarpus hookerianus	1.87	0.35
Myrsine australis	2.02	0.21
Nothofagus fusca	3.31	0.93
Nothofagus menziesii	2.89	1.10
Nothofagus solandri	3.68	1.27
Podocarpus hallii	1.26	0.59
Prumnopitys ferruginea	3.15	1.38
Weinmannia racemosa	1.63	0.44
Maximum	6.50	1.46

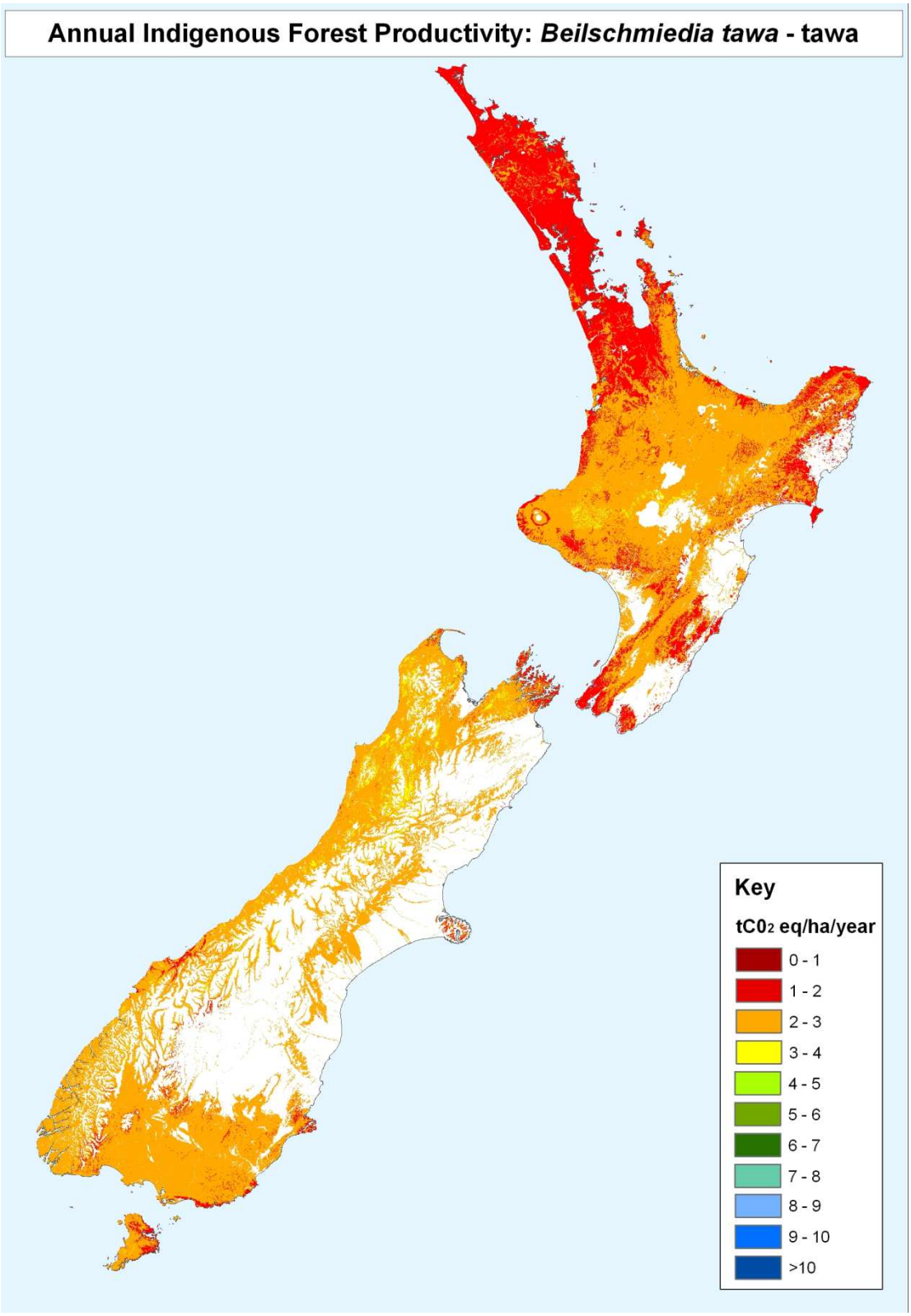

Figure 8 Modelled productivity of *Beilschmiedia tawa* throughout New Zealand. Carbon gain predictions were restricted to areas with sufficient rainfall to support rapid tree growth (i.e. outside the dryland zones identified by Walker et al. 2009) and below 1000m altitude.

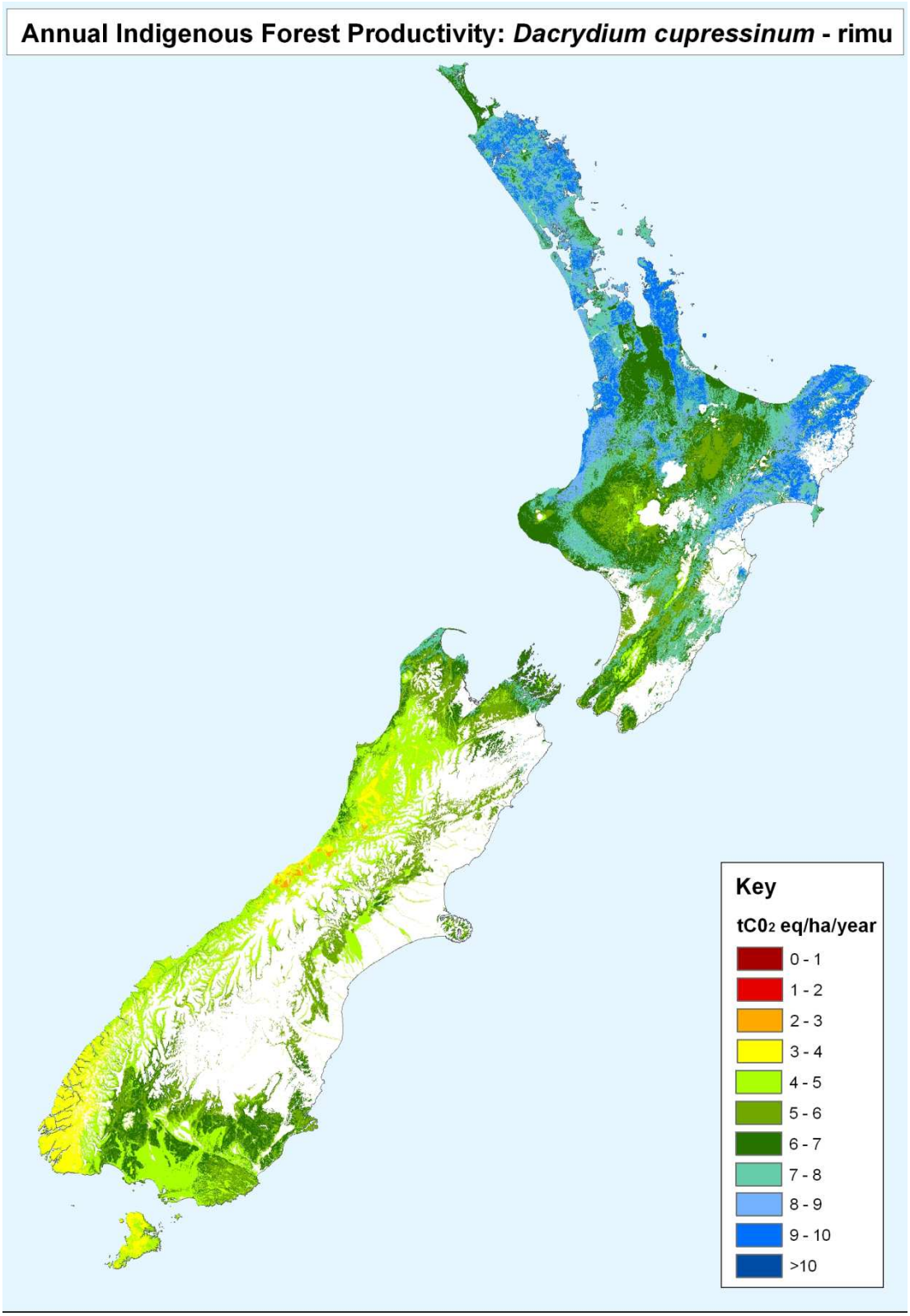

Figure 9 Modelled productivity of *Dacrydium cupressinum* throughout New Zealand. Carbon gain predictions exclude dryland and high-altitude zones (as for Fig. 8).

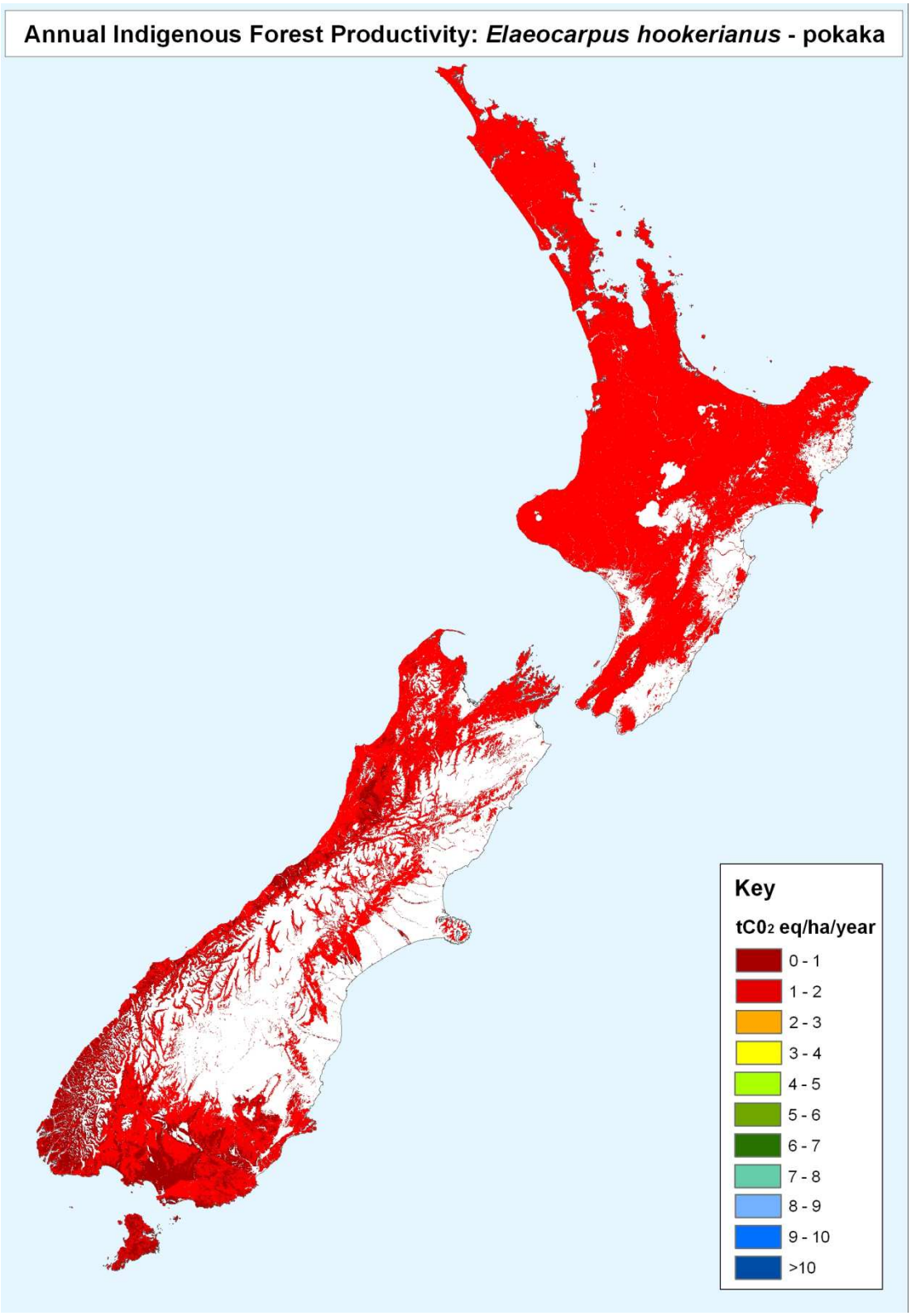

Figure 10 Modelled productivity of *Elaeocarpus hookerianus* at 0.05° resolution throughout New Zealand. Carbon gain predictions exclude dryland and high-altitude zones (as for Fig. 8).

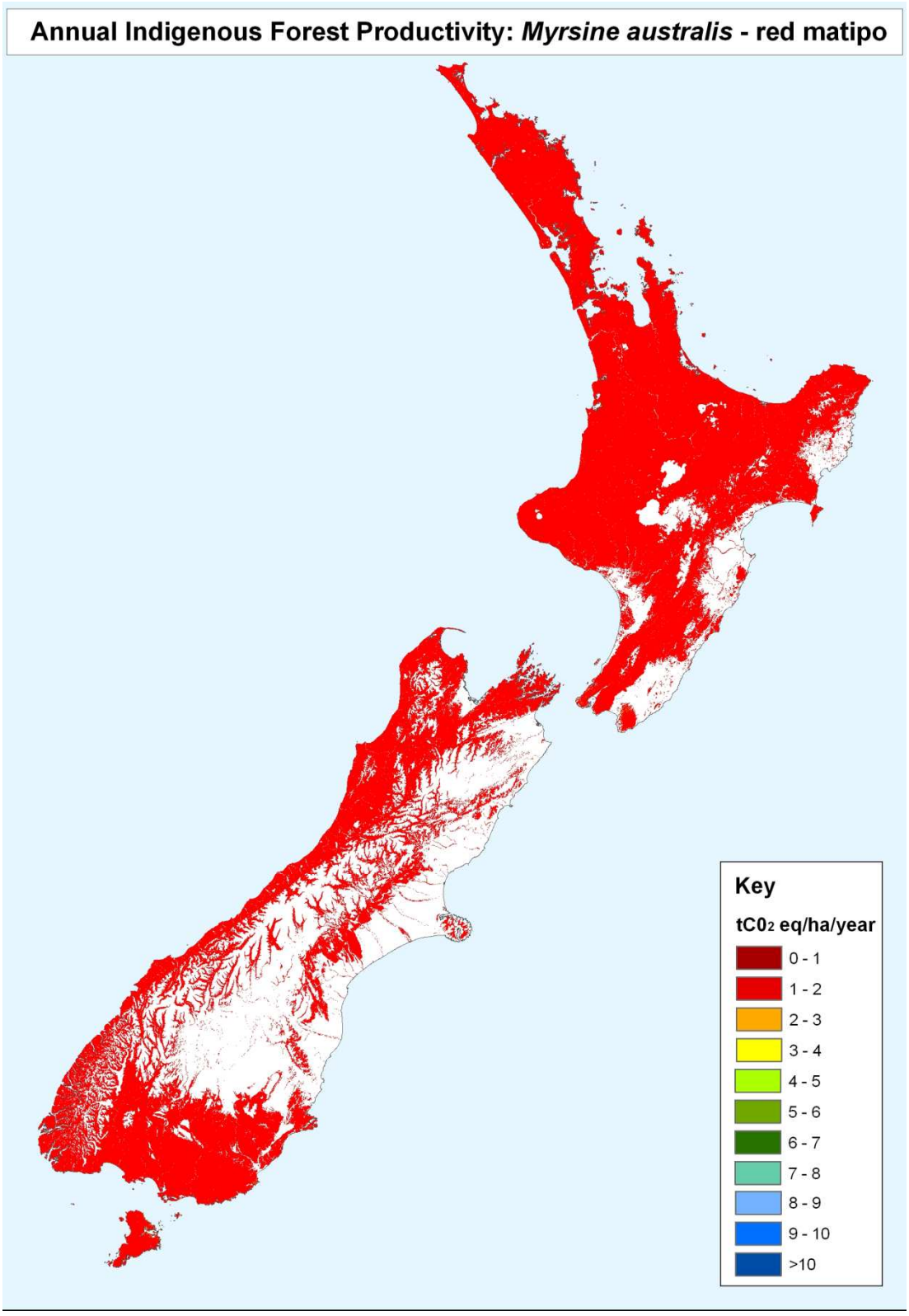

Figure 11 Modelled productivity of *Myrsine australis* at 0.05° resolution throughout New Zealand. Carbon gain predictions exclude dryland and high-altitude zones (as for Fig. 8).

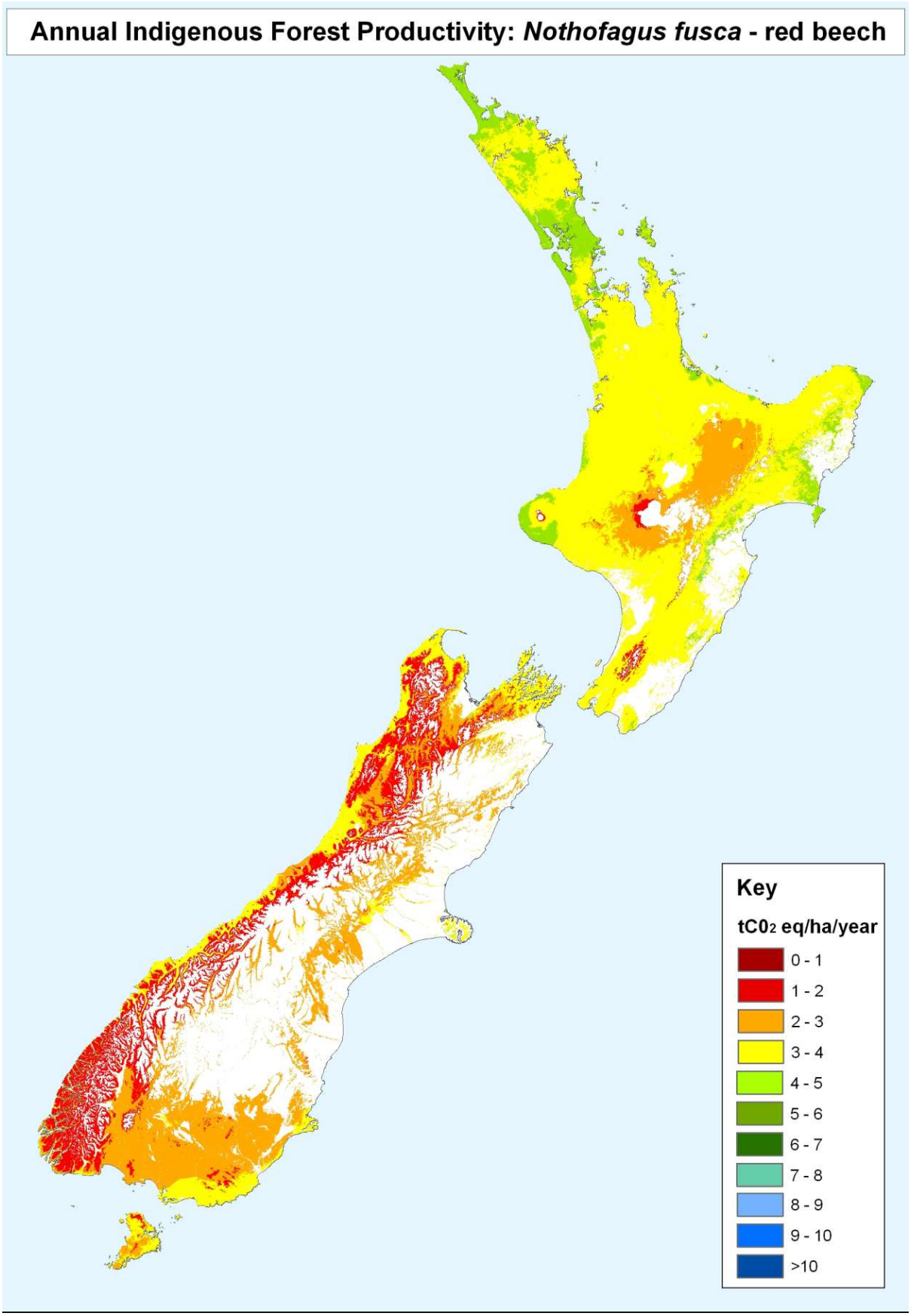

Figure 12 Modelled productivity of *Nothofagus fusca* at 0.05° resolution throughout New Zealand. Carbon gain predictions exclude dryland and high-altitude zones (as for Fig. 8).

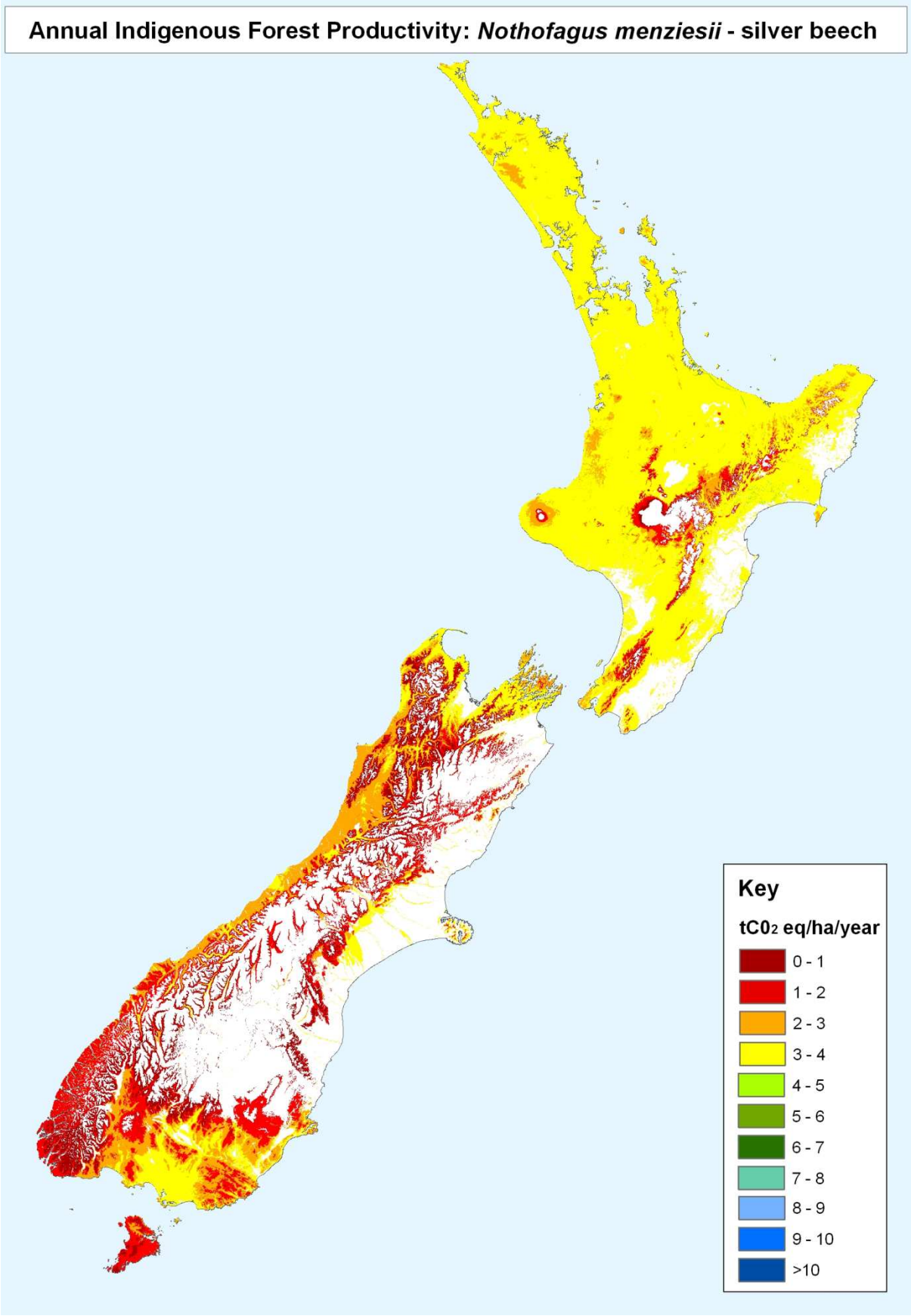

Figure 13 Modelled productivity of *Nothofagus menziesii* at 0.05° resolution throughout New Zealand. Carbon gain predictions exclude dryland and high-altitude zones (as for Fig. 8).

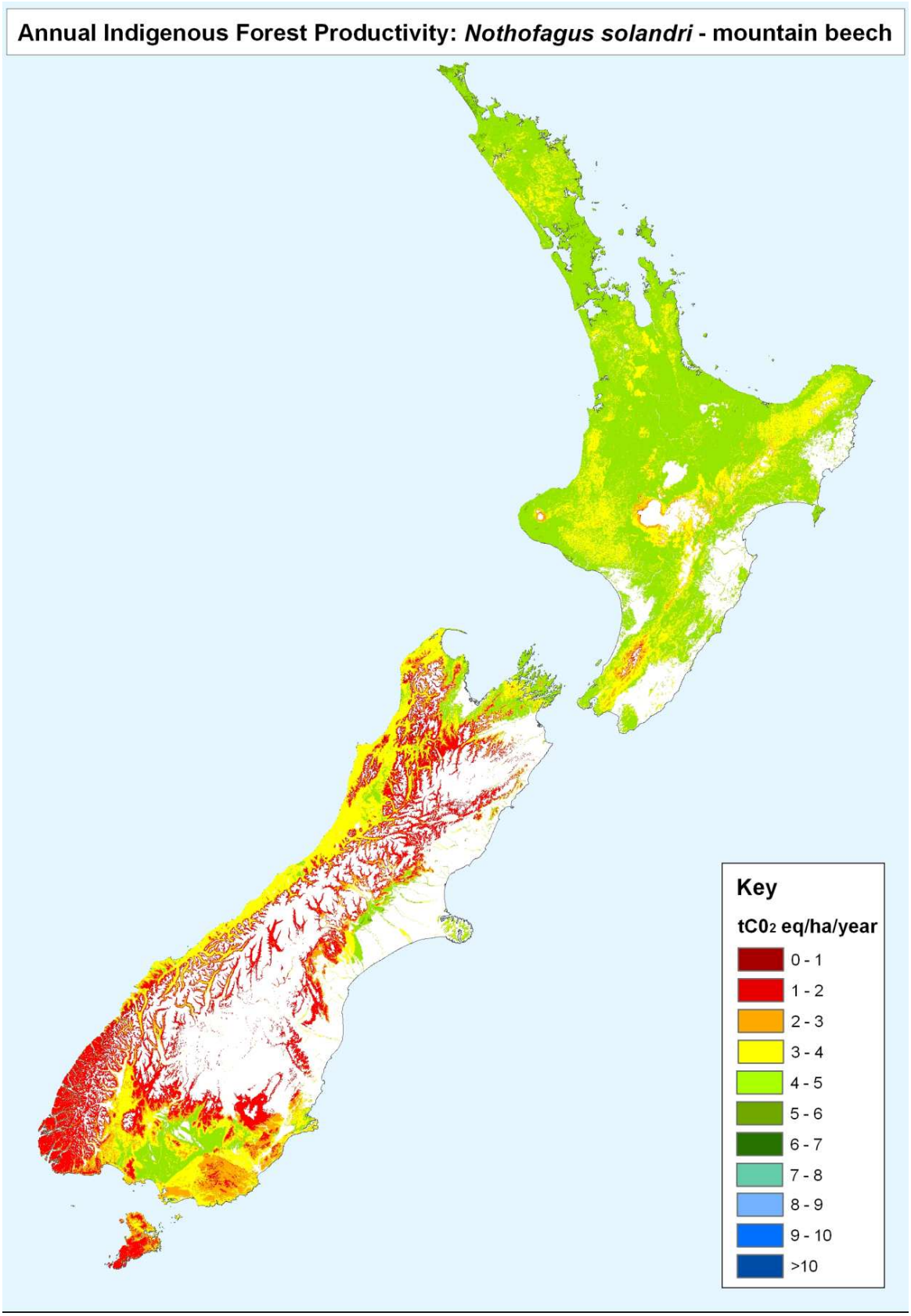

Figure 14 Modelled productivity of *Nothofagus solandri* at 0.05° resolution throughout New Zealand. Carbon gain predictions exclude dryland and high-altitude zones (as for Fig. 8).

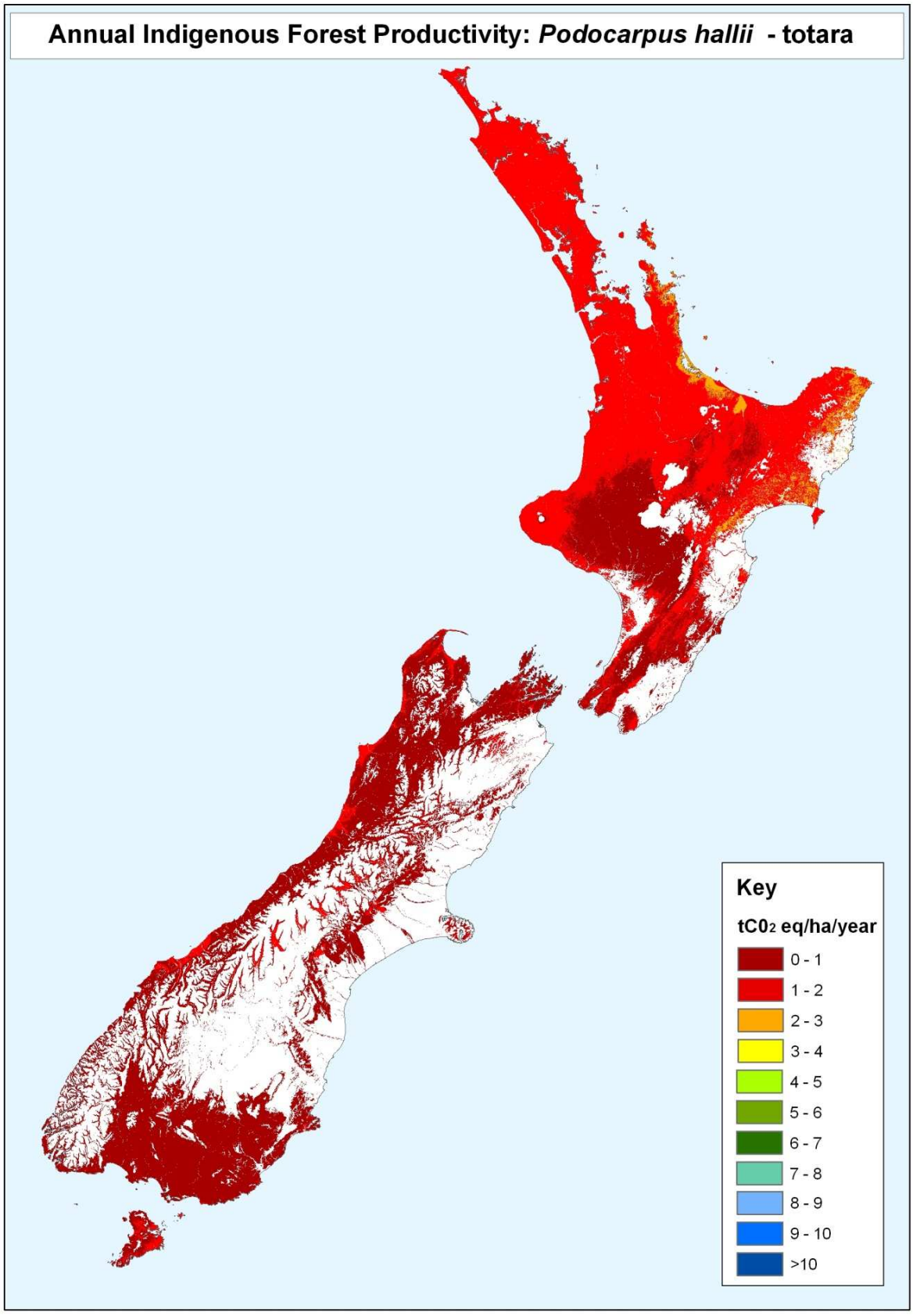

Figure 15 Modelled productivity of *Podocarpus hallii* at 0.05° resolution throughout New Zealand. Carbon gain predictions exclude dryland and high-altitude zones (as for Fig. 8).

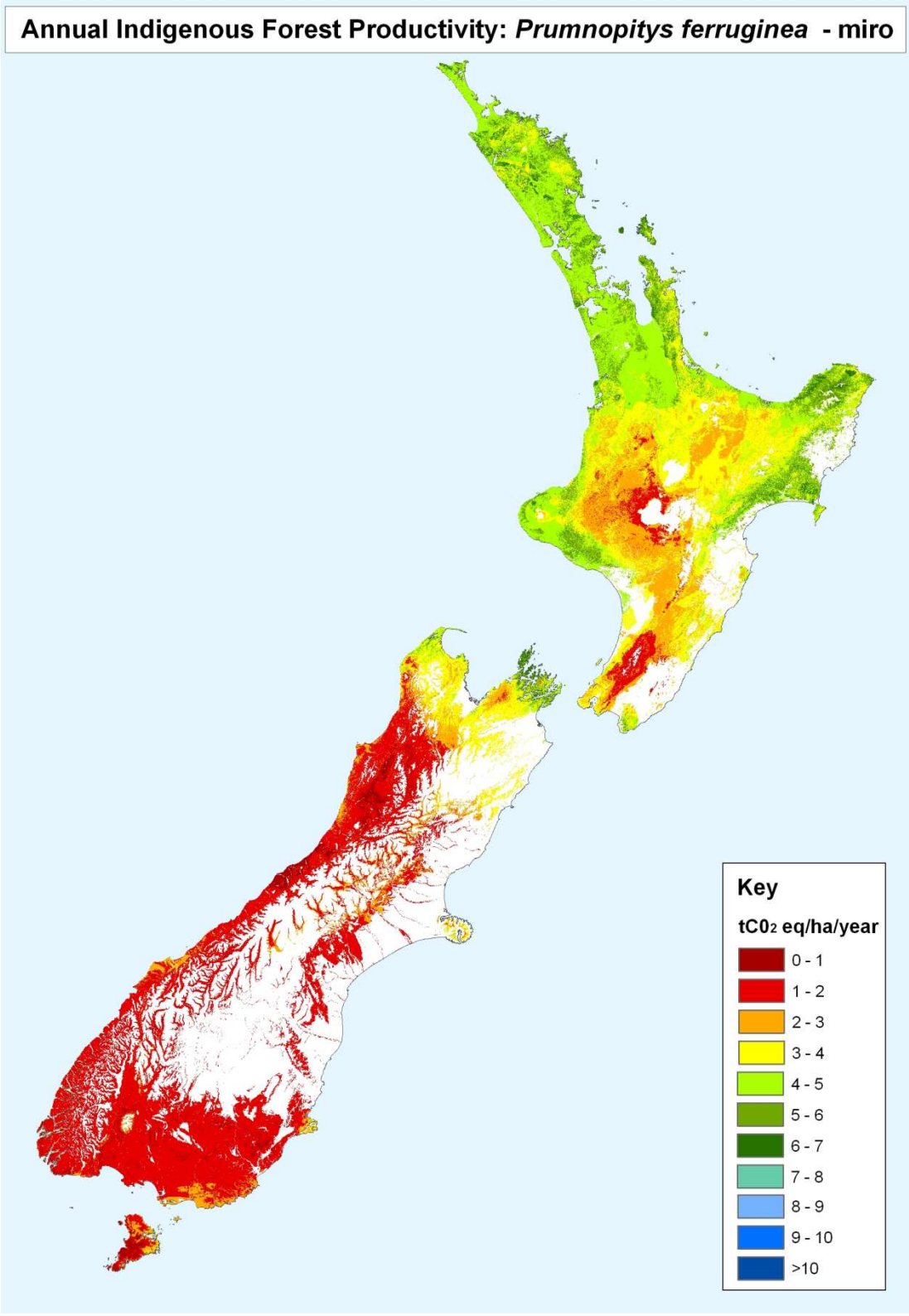

Figure 16 Modelled productivity of *Prumnopitys ferruginea* at 0.05° resolution throughout New Zealand. Carbon gain predictions exclude dryland and high-altitude zones (as for Fig. 8).

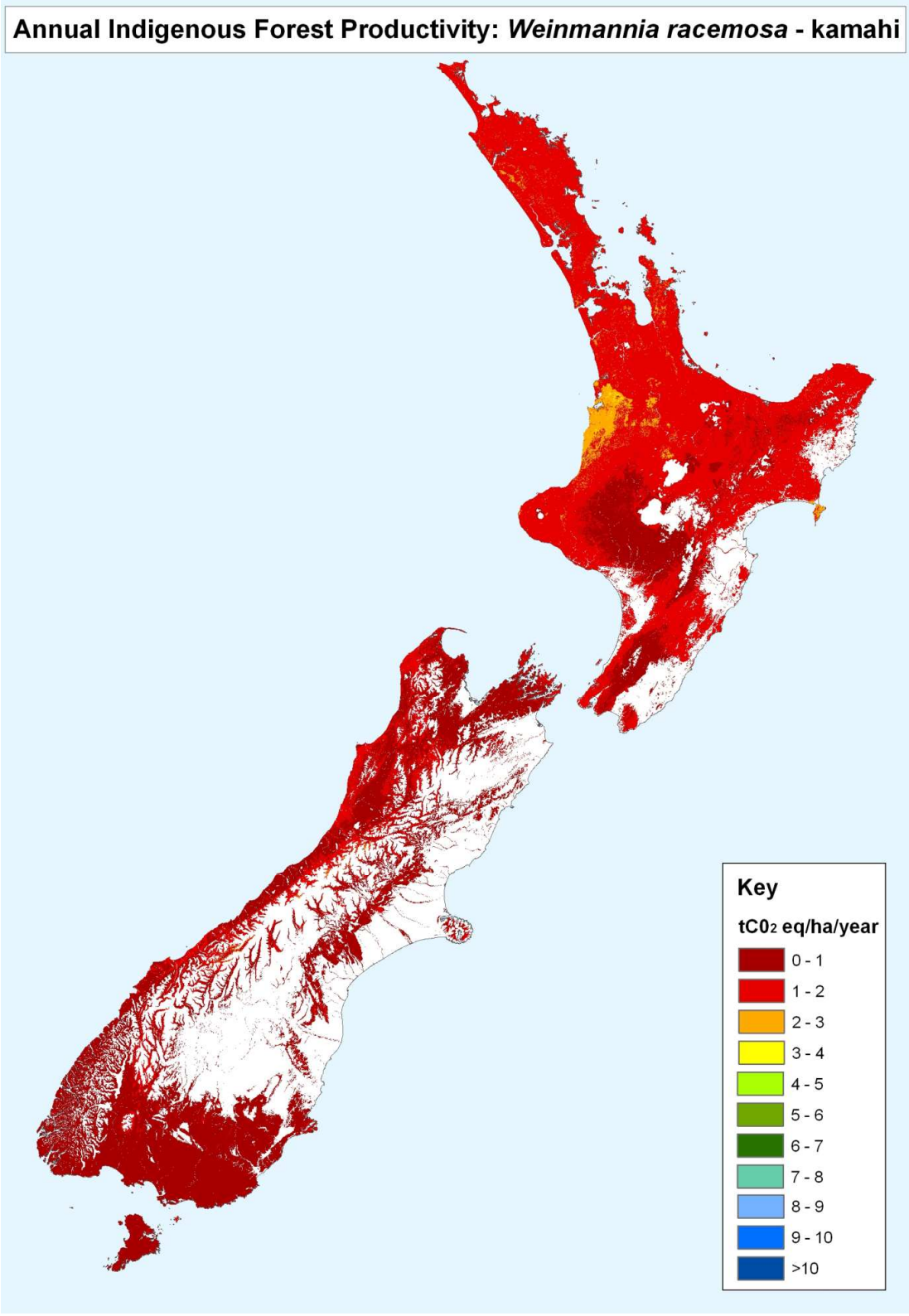

Figure 17 Modelled productivity of *Weinmannia racemosa* at 0.05° resolution throughout New Zealand. Carbon gain predictions exclude dryland and high-altitude zones (as for Fig. 8).

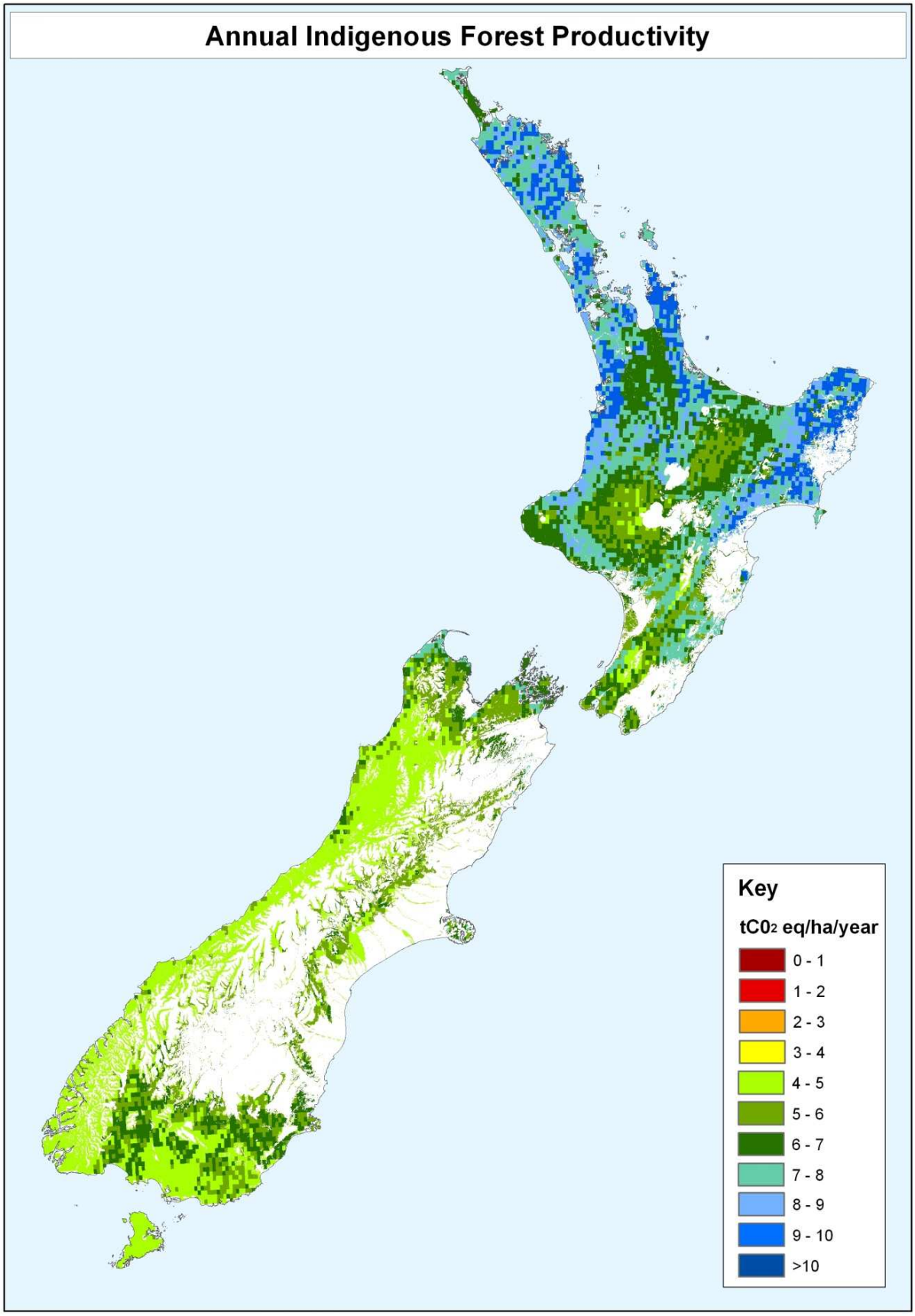

Figure 18 Modelled productivity where the species giving the highest sequestration rate is selected for each pixel.

3.2 Discussion

The complexity of forest successional dynamics, and the limitations of available data impose constraints on our ability to model carbon gain realistically through natural regeneration. Below we detail some of the drawbacks of the approach used to model indigenous forest productivity and make some suggestions to how these could be ameliorated.

3.2.1 Distribution and successional stage of forest plots

Most of the plots used to model stem growth occur in the moist montane regions of New Zealand. This is a consequence of the small area of lowland habitats still covered by indigenous forest. Consequently, in predicting tree growth in warm, highly productive areas we are often extrapolating outside the range of our observed data. In taking a national-level approach, we have modelled carbon gain for some species in areas where they do not occur naturally, or would be unlikely to form a dominant component of early-successional forests. These factors will need to be considered when interpreting our carbon gain predictions.

Also, there are very few remeasured plots in successional vegetation. This is particularly important for our tree growth models, since stand basal area is an important predictor of growth for some species, and in using models to predict growth in an afforestation scenario we are extrapolating to basal area values much lower than for the majority of remeasured plots. For example, the results for *Dacrydium cupressinum* may to a certain extent be due to this effect, since increasing basal area had a strong negative effect on *D. cupressinum* growth, so that extrapolating to lower basal area values than in the observed data might yield unrealistically high growth rates. While the modelling approach used may have some drawbacks in predicting productivity in early successional forests, it would be very well suited to predicting the productivity of existing forests, since this would not require extrapolation outside the range of the observed data.

3.2.2 Complexities of modelling forest dynamics

Our modelling approach makes no attempt to account for species' potential natural distributions, dispersal limitation, changes in species composition due to succession or variation in size between individual trees. It would be relatively simple to incorporate potential natural distributions using existing predictive models (e.g. Leathwick et al. 2001). One of the most challenging issues in modelling forest productivity through afforestation is coping with dispersal limitation (Dungan et al. 2001). Data on dispersal rates for New Zealand tree species are rare so that any attempt to model dispersal would be speculative. Also, dispersal is an inherently difficult process to model, since rare long distance dispersal events can have large long term consequences. Models of natural indigenous afforestation would greatly benefit from further empirical studies of tree species dispersal.

Another difficult property of forest dynamics to model is species replacement, and different forest models have tried to cope with this in different ways. One of the difficulties in modelling succession in forests is that it occurs over a time scale longer than we can observe, making it difficult to validate the model predictions. Another issue is that species replacement can be greatly affected by stochastic processes, such as dispersal, catastrophic disturbance

(e.g., floods, earthquakes, landslides), and individual tree mortality through disturbances such as wind throw (Hall & McGlone 2006).

The LINKAGES model (Post & Pastor 1996) copes with species replacement by assigning species to particular successional stages. It is unclear whether its New Zealand derivative LINKNZ (Hall & Hollinger 2000) replicates this (and it makes no provision for dispersal limitation). The SORTIE model (Pacala et al. 1996) avoids this kluge, but has the drawback that a huge parameterisation effort is required for the model to yield accurate predictions even for a single stand.

A version of the SORTIE model has been constructed for a small area of forest in Southland, New Zealand (Easdale & Kunstler 2010), but as with the original SORTIE model, it requires a large effort in empirical observation to estimate the necessary parameters. As a consequence it is not a realistic candidate for simulating forest regeneration and productivity at a national scale. Modelling variation in tree size is challenging since microsite variation can greatly influence tree growth. Also, mortality is a highly stochastic process, with our ability to model mortality in mature individuals of common New Zealand tree species (especially podocarps) being severely limited by the small number of tree deaths observed in remeasured forest plots (Hurst et al. 2007). In general, building a nationwide forest dynamics model remains an ongoing challenge, which will require much more research than was possible in this report.

4 Productivity of *Pinus radiata* and its response to climate change

4.1 Results

4.1.1 Model-data comparisons

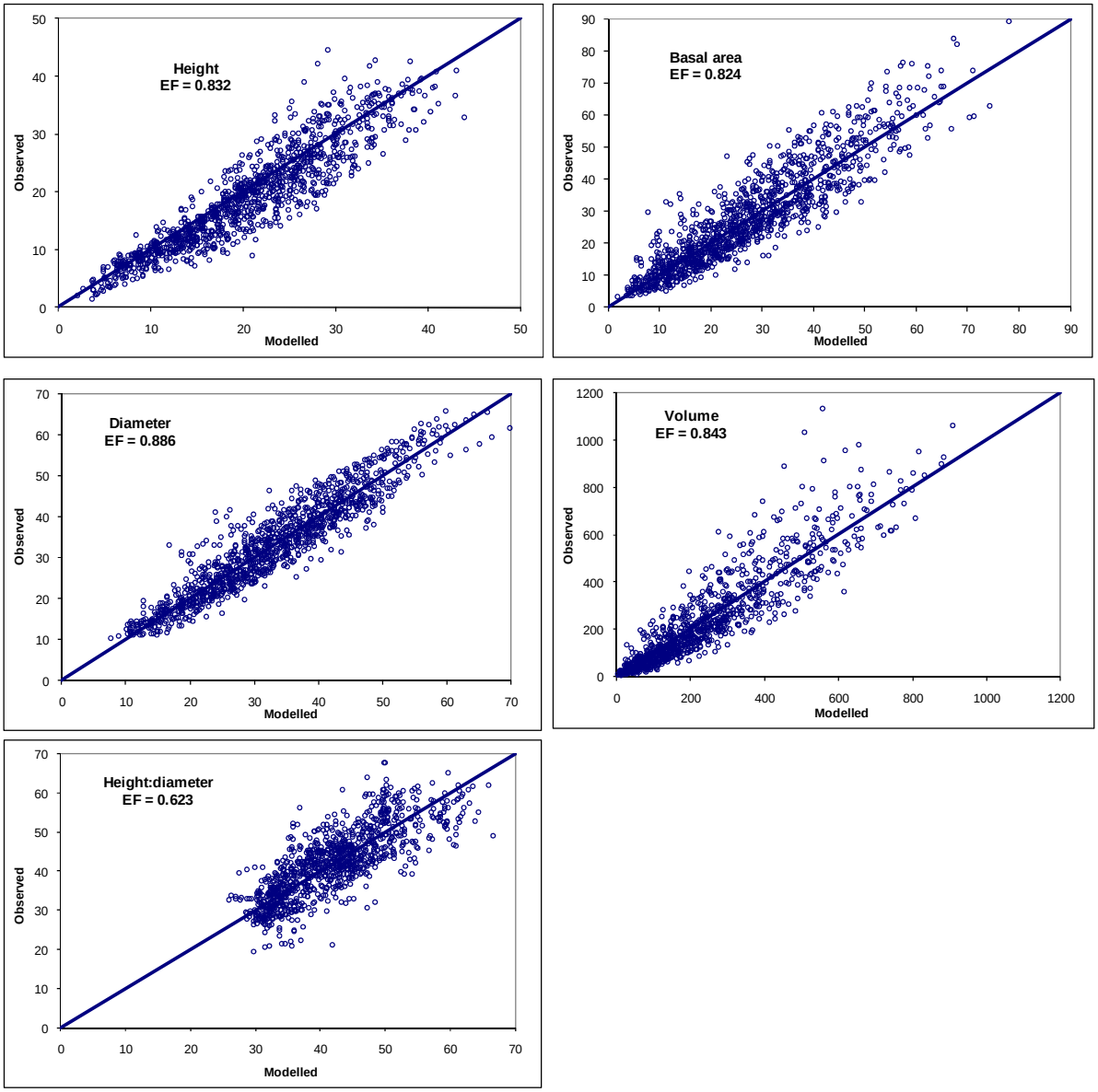

Figure 19 Comparison between modelled and observed stand properties for 101 PSP sites, comprising 1297 individual observations of basal area, stem diameter, or both. Lines in each graph give a 1:1 line, and EF refers to model efficiency, or the extent of variation explained by the 1:1 line.

From the data comparisons, the model gave excellent predictions against the data in the 101 PSP plots (Figure 19). Model efficiencies were very high, 0.824 – 0.886 for the four growth indices that were either directly observed or could be readily deduced from the data. Model efficiency for the ratio of height:diameter was somewhat lower but, given the narrower data range, this is also considered to be a very good data fit. None of the data comparisons show any significant residual bias (i.e. consistent over- or underprediction of the data).

There was also no remaining bias in the plot of residuals (modelled – observed volume) against temperature and precipitation, the two key environmental drivers (see Appendix 4).

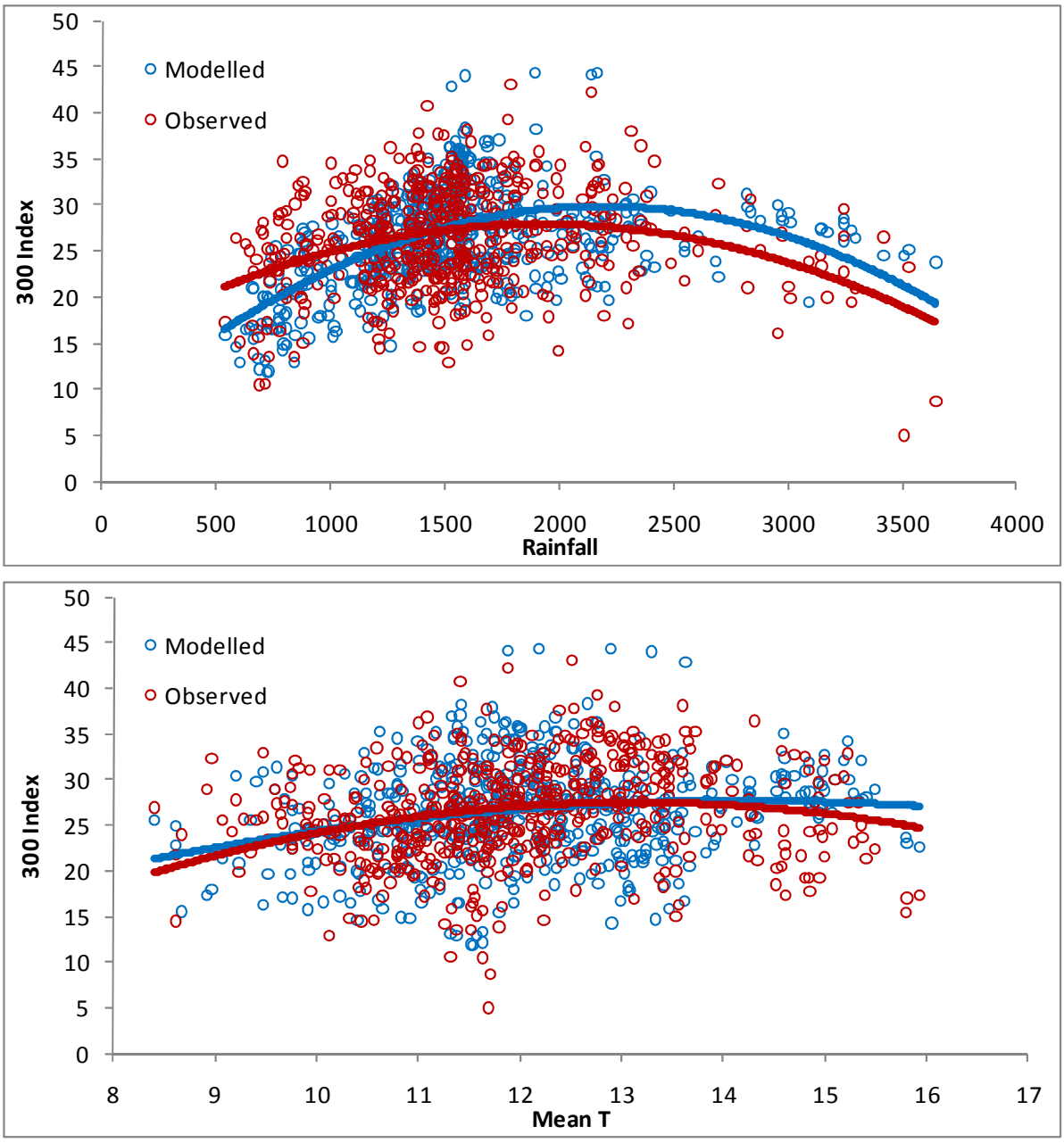

Figure 20 Modelled and observed growth rates from a set of 1764 observations from 548 individual 0.05° locations in New Zealand. Where multiple observations were available from the same 0.05° locations, the average of the observations was taken. The red and blue lines have been fitted to the observed and modelled relationships, respectively. 300 Index is a calculated growth index for a 30-year old stand, with a stand stocking of 300 stems ha^{-1} (Watt et al. 2010). As individual stands are measured at different ages and with different stocking, 300 Index provides a standardisation to assess site productivity.

The comparison in Figure 20 shows that the model follows fairly well the trend in the observations. It also shows that productivity increases only up to about 1500–2000 mm precipitation, but falls quite markedly with further increases in rainfall. The two sites with lowest observed productivity received more than 3500 mm yr^{-1} in rainfall. It is not well known what causes the down-turn at high rainfall, and special routines had to be added to CenW to be able to emulate that decrease.

In contrast, the response to temperature is fairly flat across the observed temperature range in New Zealand from 8.5 to 16 degrees, with only slight down-turns at the highest and lowest temperatures.

4.1.2 Productivity surfaces under current climatic conditions

Productivity can be measured in terms of wood volume (Figure 21a) or in terms of woody dry weight increment (Figure 21b). The principle difference between the maps across the country is the effect of wood density, with wood being denser in trees grown at higher temperatures, so that in the north there is relatively greater carbon gain whereas in the south, there is relatively greater wood volume increment. Apart from that, maps are, of course, similar, as all factors other than temperature affect carbon and wood volume increments in the same way.

Height is relatively more uniform, but shows a north–south gradient, with the tallest trees growing in Northland. Basal area, on the other hand, displays more small-scale variability but less of a consistent gradient with temperature.

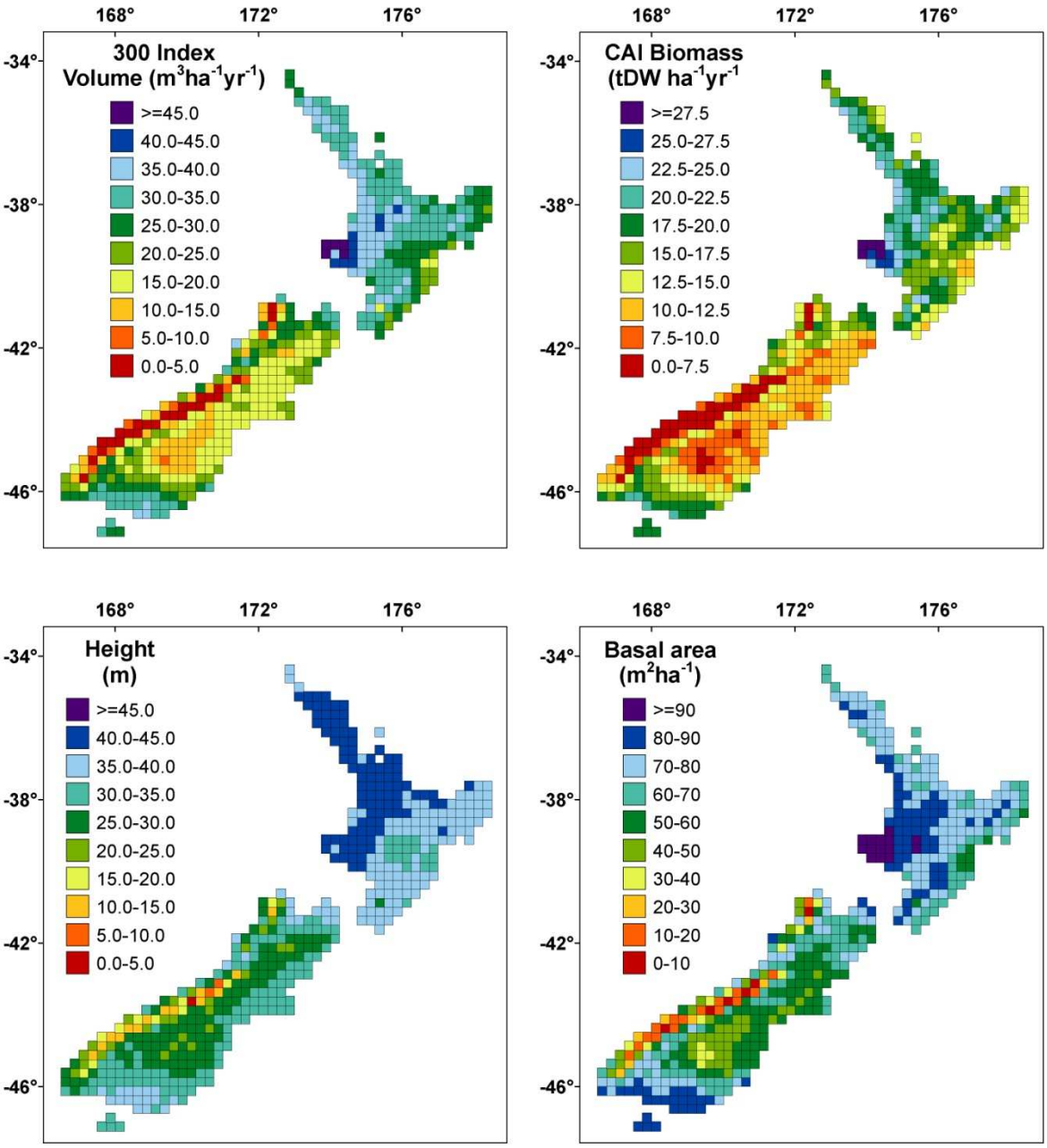

Figure 21 Modelled *P. radiata* productivity in New Zealand at ¼ degree resolution. Data are expressed either as annual wood volume increment, averaged over the growth over 30 years and including wood losses due to thinning (designated as 300 Index), or as dry weight increment calculated over the final year of growth at age 30 (designated as current annual increment, CAI). The other panels show height and basal area of 30-yr old stands.

Growth in either volume or biomass increment is also shown by regional district in Table 4. Modelled growth is highest in the Taranaki region owing to moderate temperatures, high rainfall and good soil conditions. Most other regions in the North Island also achieve good growth rates. Lowest growth rates are modelled for the Canterbury regions because of water limitations, the Otago region because of dry and cold conditions and the West Coast Region because of excess rainfall. Biomass increments display a similar pattern (Table 4).

Table 4 *Modelled P. radiata wood volume and biomass productivity by region in New Zealand*

Region	Volume increment (m^3 ha^{-1} yr^{-1})		Biomass increment (tDW ha^{-1} yr^{-1})	
	Mean	S.D.	Mean	S.D.
Northland Region	33.2	3.1	18.8	2.3
Auckland Region	33.8	3.5	20.0	2.8
Waikato Region	34.4	3.3	19.2	2.6
Bay of Plenty Region	32.4	2.3	18.6	2.3
Gisborne Region	30.2	3.2	17.5	3.3
Hawke's Bay Region	28.1	4.6	15.9	2.9
Manawatu-Wanganui	33.8	5.0	18.5	2.9
Taranaki Region	41.9	4.5	24.8	3.5
Tasman Region	19.9	8.1	12.8	4.1
Wellington Region	30.0	5.3	17.1	3.3
Nelson Region	26.2	1.6	15.5	1.0
Marlborough Region	22.7	5.4	13.3	3.1
Canterbury Region	16.2	5.6	9.7	3.0
West Coast Region	13.7	9.8	8.6	5.3
Otago Region	18.1	7.6	10.8	4.1
Southland Region	22.7	10.0	13.9	5.3

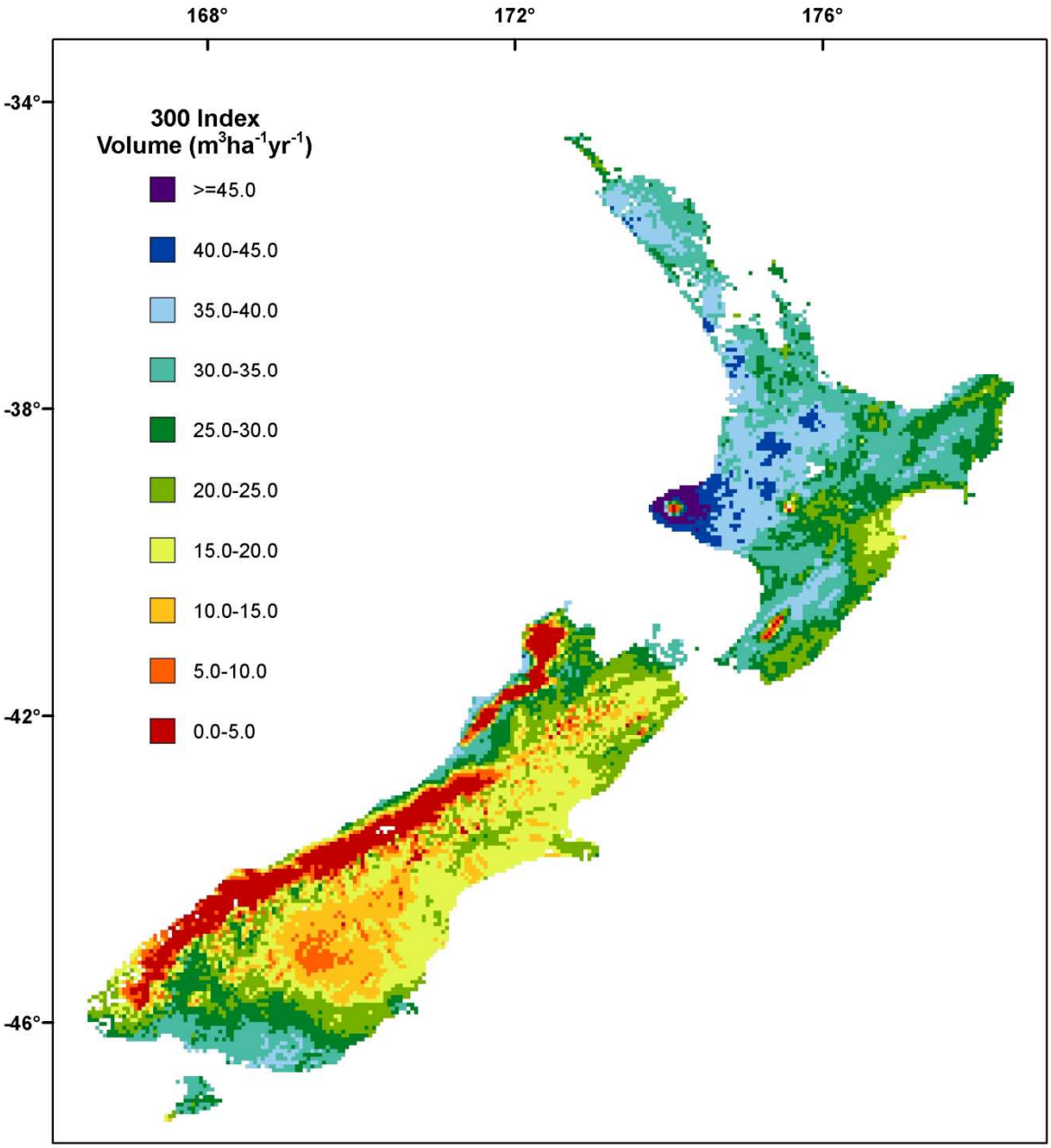

Figure 22 Modelled *P. radiata* wood volume productivity in New Zealand at 0.05° resolution. Data are expressed as annual wood volume increment, averaged over 30 years of growth and including wood losses due to thinning (designated as 300 Index).

Figure 22 shows the same simulations as Figure 21a but at the finer resolution of 0.05 degrees (about 5 × 5 km). The patterns are the same but it is easier to relate specific productivity classes to the underlying landscape patterns.

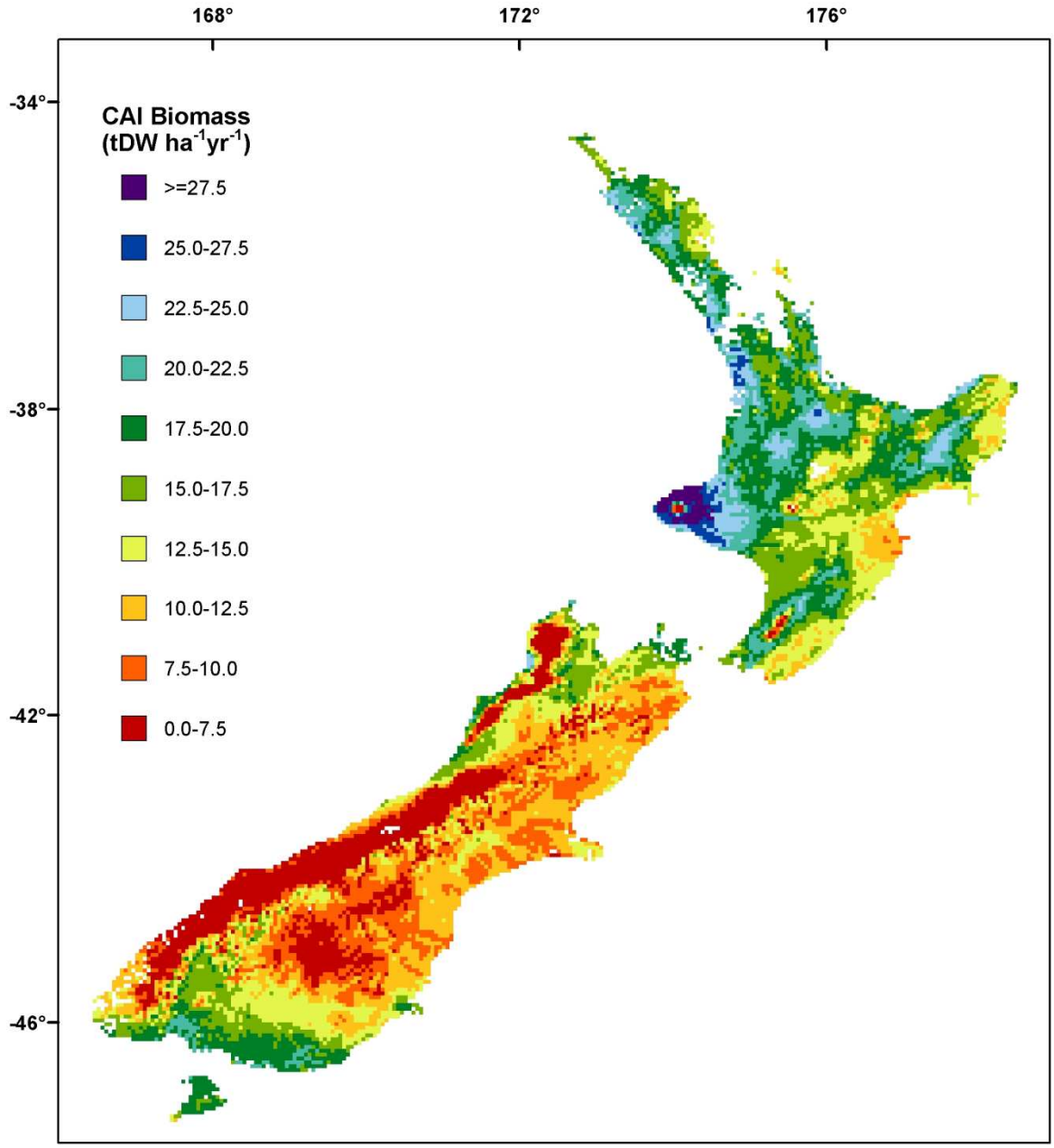

Figure 23 Modelled *P. radiata* current annual increment at 0.05° resolution. Data are expressed as wood dry weight increment over the last year of growth.

As in Figure 22, Figure 23 shows the data at a higher resolution. Because of the number of simulations involved, it was not practical to run climate-change simulations at such a fine resolution. Simulations under future climate change scenarios were therefore run at only ¼ degree resolution.

4.1.3 Sensitivity to climate change

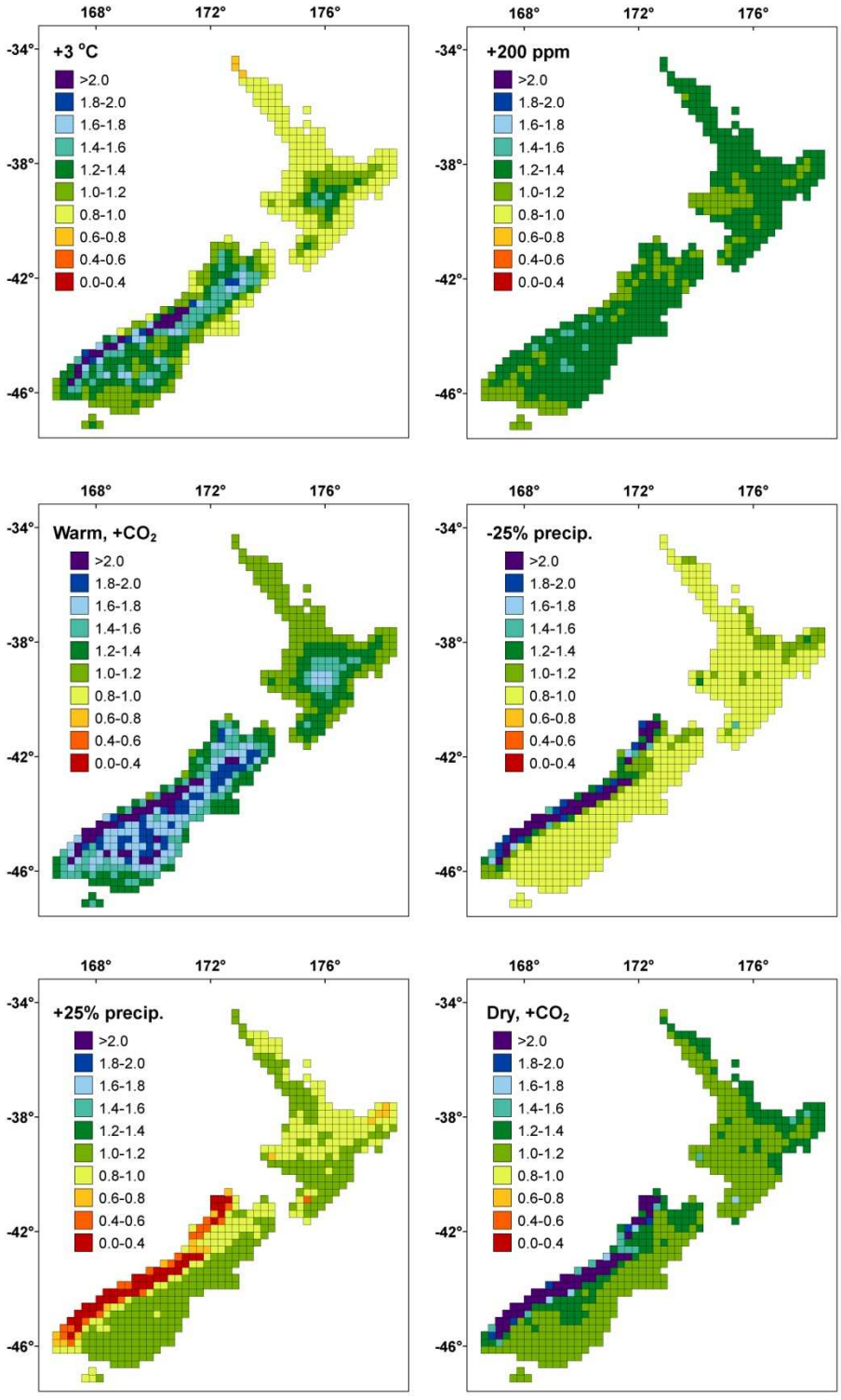

Figure 24 Modelled response of *P. radiata* wood volume production to increases in temperature (3°C), CO_2 concentration (+ 200 ppm), both CO_2 and temperature increase (warm, +CO_2), or changes in rainfall (–25% or +25%), or drying by 25% together with increasing CO_2. Responses are expressed relative to volume production under current climate. A value of 1.1, for example, means a 10% enhancement in productivity.

In response to temperature, growth is reduced over much of the North Island as trees begin to experience increasing high-temperature stress. Responses are generally positive in the cooler

regions of the Central Plateau of the North Island and over most of the South Island. Very positive responses are seen over some of the very cold mountain regions. Responses are negative over parts of the already water-limited Canterbury planes as increasing temperature leads to increasing water loss.

Responses are broadly, and fairly uniformly, positive in response to increasing CO_2 concentration, with responses slightly higher in the warmer part of the country. Responses are particularly positive with increasing temperature and CO_2 concentration, with increasing temperature benefiting cool parts of the country, and increasing CO_2 benefiting the warmer regions, especially where increasing temperature would cause water stress to develop

Reductions in rainfall generally lower productivity for much of the country, except along the already very wet West Coast of the South Island, where *P. radiata* would actually benefit from a reduction in rainfall. This general detrimental effect of reduced precipitation can be negated almost entirely by a concomitant increase in CO_2 concentration.

4.1.4 Climate change for New Zealand

Further simulations were based on a set of regionally-specific climate change scenarios. Detailed change fields of temperature and precipitation were available from 12 global circulation models, forced with greenhouse gas concentration according to three IPCC greenhouse gas emission scenarios (SRES 2002). We used the B1, A1B and A2 SRES scenarios to represent an optimistic low-emission (B1), an intermediate (A1B) and a high-emission 'Business as usual' scenarios (A2). Simulations were run for 30-year rotations from 1975 to 2005 (mid-point reference year 1990) designated as "current" climatic conditions, and for 2025–2055 (reference year 2040) and 2075–2105 (reference year 2090). All simulations either used CO_2 concentrations corresponding to the different emission scenarios or kept to the 2075–2105 values (as indicated in respective Sections below).

Figure 25 shows the climatic change corresponding to the mean response of the 12 GCMs for 2090, shown separately for each of the three emission scenarios. Changes in temperature and the proportional change of precipitation are shown. For temperature, only changes in average temperature were available but the diurnal temperature range had to be assumed to remain the same. Vapour pressure under future climatic scenarios was calculated based on the assumption that dew point temperature changed in line with the average change in temperature. There was no information about possible changes in solar radiation.

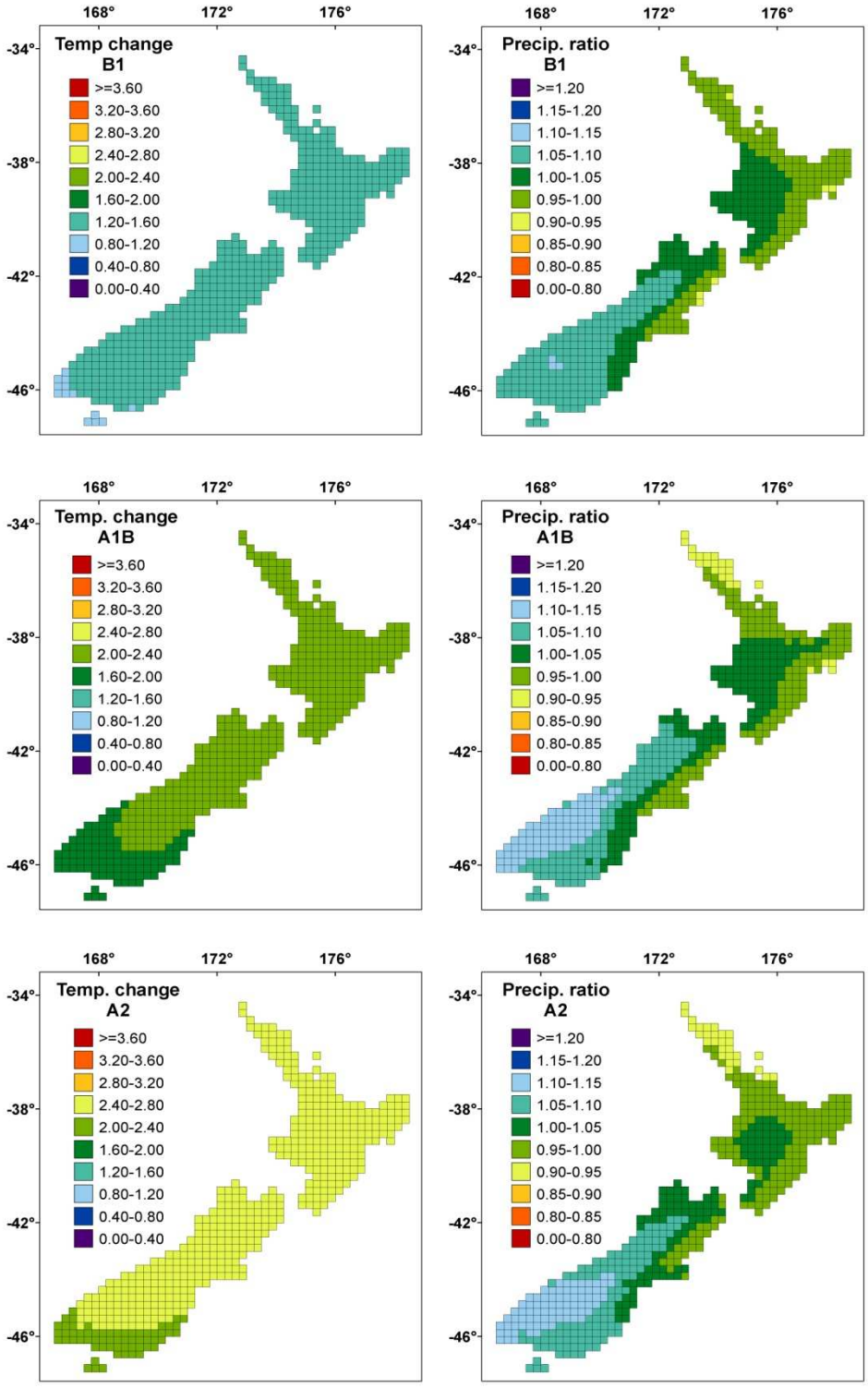

Figure 25 Average climatic changes to 2090 under the 12 GCMs, shown by emissions scenario. Temperature changes are expressed in degrees Centigrade, while changes in precipitation represent the change relative to current climate.

The climate-change scenarios are fairly mild for New Zealand, with projected temperature increases from 1990 to 2090 ranging from about 1.5°C under the SRES B1 scenario over most of the country to an also fairly uniform temperature increase of about 2.5°C under the SRES A2. The projected increase is marginally greater in the North than the South. Precipitation changes over the same period are also fairly slight, ranging from a decrease of

between 5 and 10% over northern regions of the North Island to an increase of between 10 and 15% in the south-western part South Island. Changes in rainfall relative to current climate are least extreme under the B1 scenario and most extreme under the A1B and A2 scenarios (Fig. 25).

At the same time, the averaged changes hide a considerable range of divergence between the different GCM runs, and Figure 26 shows the temperature and precipitation patterns under the two GCMs that give the smallest and largest changes, respectively.

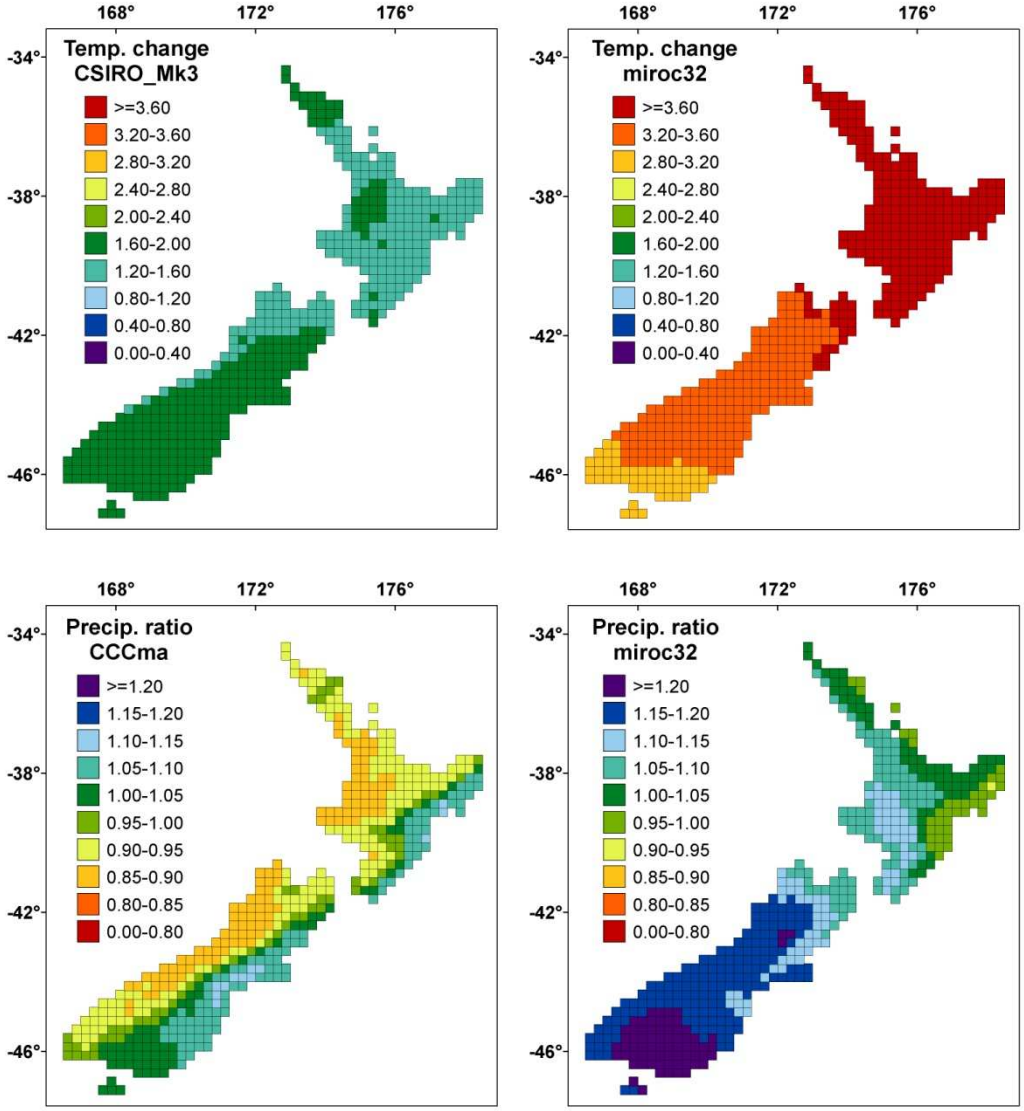

Figure 26 Temperature and precipitation changes under two extreme GCMs for the SRES A2 scenario for 2090. The GCM outputs shown are for the GCMs that showed the smallest and greatest temperature changes, and the greatest wetting and drying, respectively. Temperature changes are expressed in degrees Centigrade while changes in precipitation represent the change relative to current climate.

Individual GCM provide a more divergent pattern of changes than is apparent from the average of all GCMs. With respect to temperature, CSIRO Mk 3 shows not only much smaller temperature increases than the other GCMs, but also slightly greater temperature increases in the south than the north. Under MIROC32, on the other hand, projected temperature increases are not only twice as high as those projected under the CSIRO Mk3 runs, but are also greatest in the north and slightly less in the south.

With precipitation, similarly, there are differences in both magnitude and regional patterns. CCCma projects the greatest drying, although even that is fairly mild, with drying for most of the west of the country, but wetting along the east coast, whereas MIROC32 projects the greatest wetting, especially in the south but a drying trend in the north and northeast. Further details are given in Table 5.

Table 5 *Summary of responses under the 3 emission scenarios and 12 GCMs. Averages give the average response of all 12 GCMs across all quarter-degree grid points within New Zealand. Minimum and maximum refer to the GCM scenario with the lowest and highest averages across all grid points. Site min and site max refer to the quarter-degree location in New Zealand experiencing the highest and lowest changes, respectively*

Emission scenario		mean	min	max	Site min	Site max	mean	min	max	Site min	Site max	CO_2 conc.
	Year	Temperature change (°C)					Precipitation change (%)					
	1990											352
A1B	2040	0.93	0.35	1.30	–0.03	1.71	2.1	0.0	5.0	–23	+22	483
A2		0.93	0.31	1.30	0.00	1.71	0.9	–5.6	4.3	–17	+15	481
B1		0.73	0.43	1.22	0.17	1.53	1.6	–2.1	5.6	–15	+16	457
A1B	2090	2.07	1.18	3.39	0.94	3.96	3.2	–1.5	12.9	–31	+44	674
A2		2.56	1.65	3.58	1.42	4.18	3.0	–3.8	11.5	–21	+30	754
B1		1.32	0.70	2.30	0.43	2.72	2.6	–4.7	7.9	–17	+25	538

An important aspect for the CenW simulations is the relatively mild climate change projected for New Zealand, especially with respect to changes in precipitation.

4.1.5 Productivity response to climate change

These simulations show adverse effects of climate change on productivity in northern and low altitude regions within the North Island. Reductions in volume productivity are especially marked for the high-emission SRES A2 scenario and are more pronounced for 2090 than for 2040. In contrast, productivity is likely to be improved in the cool parts of the country, including most of the South Island and the higher altitude regions of the North Island. The magnitude of anticipated changes is moderate, ranging from productivity losses of more than 20% over some North Island locations to gains of more than 40% over the cooler sites, especially in the South Island.

The average response depicted in Figure 27 hides a large amount of overall and regional divergence evident under individual GCMs (Figure 28). Under the ECHAM5 model, overall changes are the worst from the 12 GCMs, contributed mainly by large reductions in productivity along the South Island West Coast, whereas changes for most of the North Island are still negative but relatively mild.

The CCMA model, on the other hand, predicts the overall most beneficial changes, mainly because it does not lead to adverse outcomes for the West Coast even though it does show greater reduction in the far north than the ECHAM5 model.

Much of the change depicted in the Figures above is in regions that are basically unsuitable for growing *P. radiata* so that any changes in hypothetical productivity are only marginally relevant. It is more important to assess what productivity changes might be expected in those regions where plantations currently grow well and where any changes in productivity are of more tangible importance for the industry. This is shown in Figure 29, which depicts the probability of sites with current productivity in excess of 25 m^3 ha^{-1} yr^{-1} experiencing specified changes in productivity by 2040 and 2090. Also shown are productivity changes weighted by the distribution of the current forestry estate.

For these data the outcomes under each of the three emissions scenarios and under each of the 12 GCMs were considered equally likely so that the Figure depicts the probability of sites having productivity shifts by the indicated magnitudes.

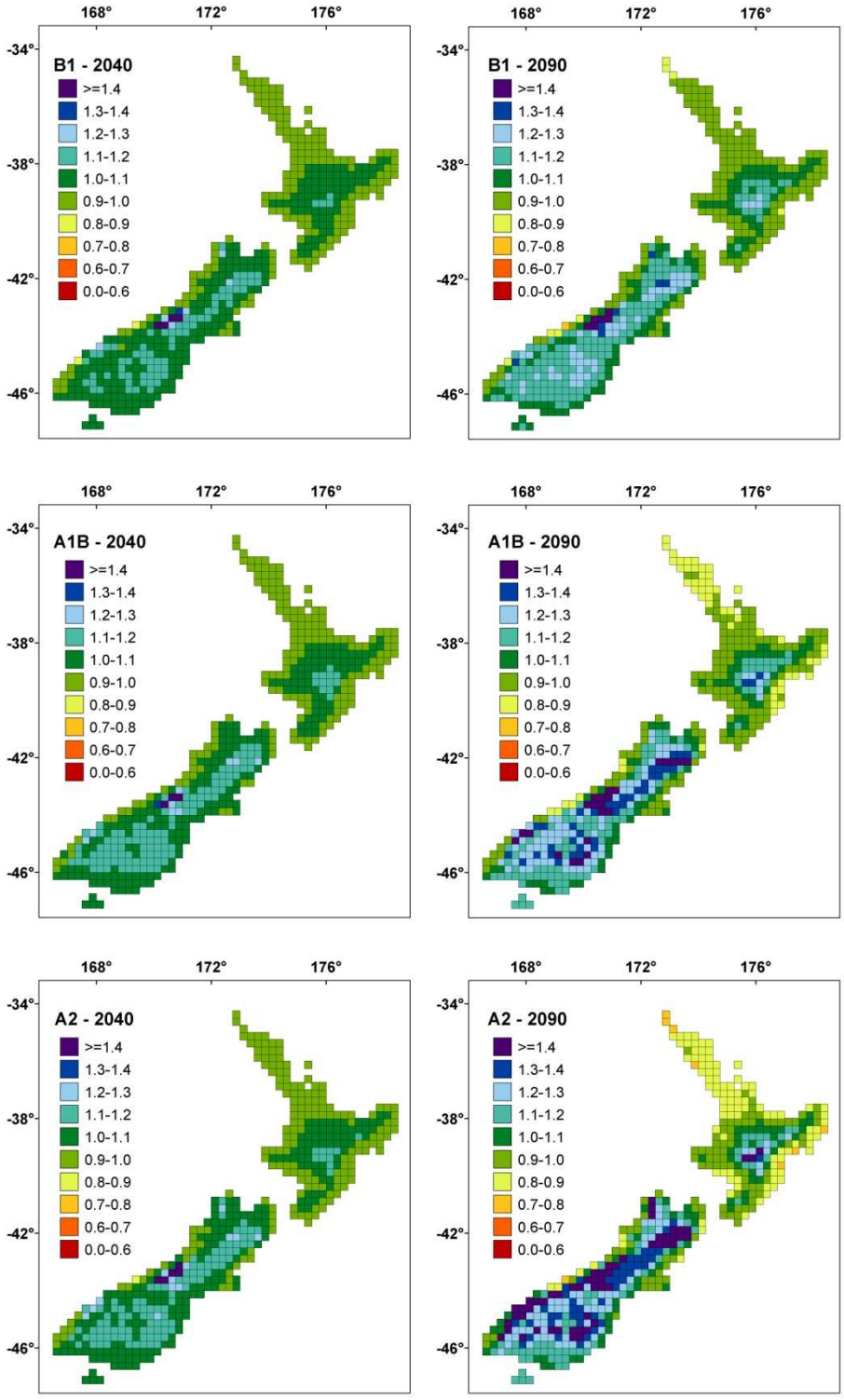

Figure 27 Climate change impacts on volume production under three emission scenarios for 2040 and 2090 relative to simulations for 1990. For each time period/ emission scenario, simulations were run independently under climate change prediction under each of the 12 GCMs. Shown here are the averages of responses generated under the new climates of the 12 GCMs. These simulations use CO_2 concentrations at 1990 for all runs.

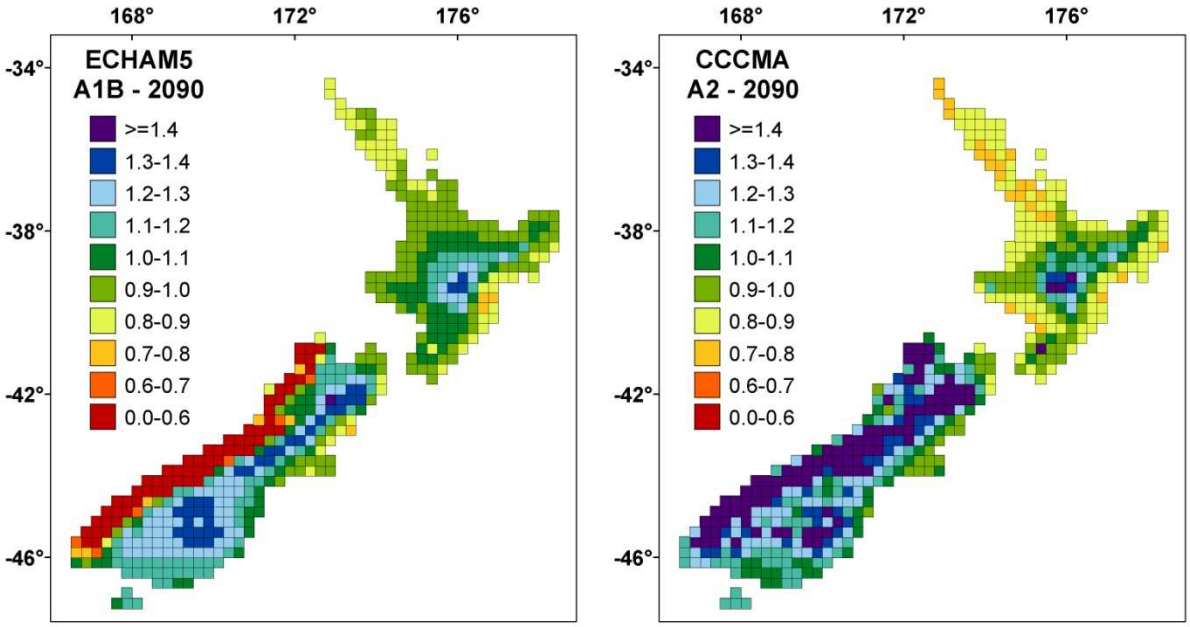

Figure 28 Climate change impacts on volume production under the two most divergent scenarios for 2090 relative to simulations for 1990, shown for the scenarios that show the most adverse and most beneficial overall changes. These simulations use CO_2 concentrations at 1990 for all runs.

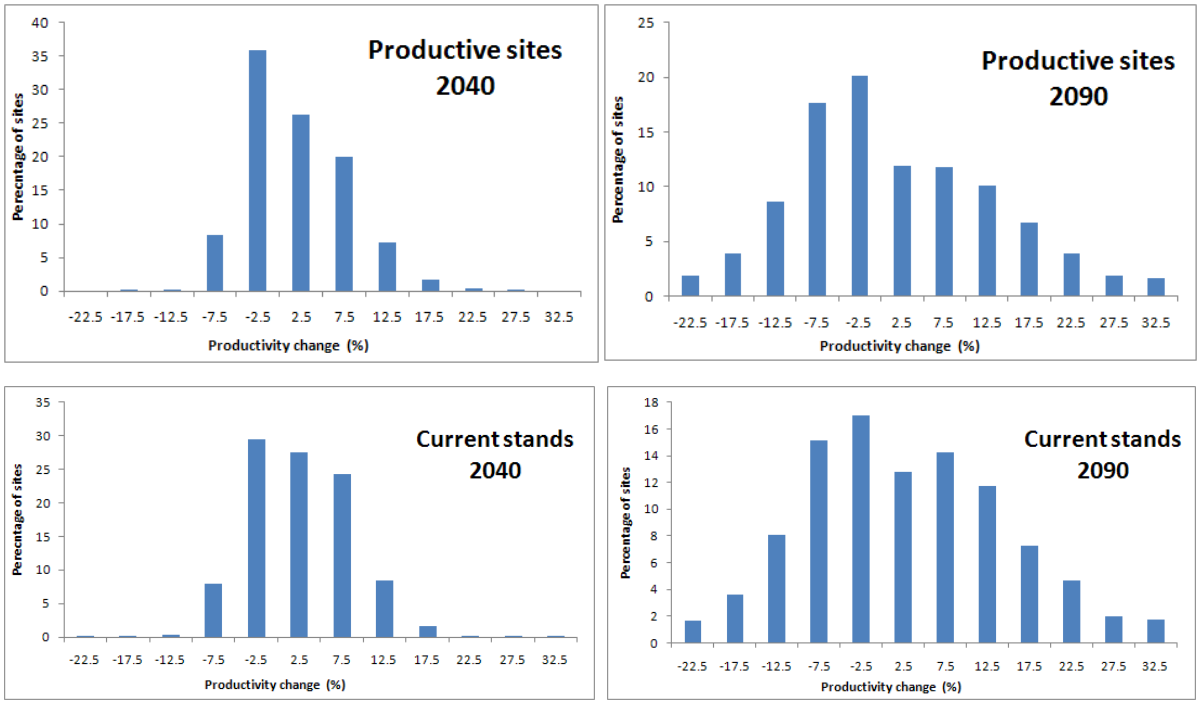

Figure 29 Proportion of sites that are modelled to currently be highly productive (top panels) or weighted by the current distribution of the P. radiata estate (bottom panels) experiencing specified productivity changes by 2040 (left panels) and 2090 (right panels) under any of the three emission scenarios and all 12 GCMs. These simulations use the same CO_2 concentrations for all runs. 'Highly productive' sites are defined as sites with current modelled productivity above 25 m^3 ha^{-1} yr^{-1}.

It shows that under only climatic changes (but ignoring increases in CO_2 concentration), nearly half of all sites could expect some decrease in productivity, but losses in productivity are generally slight and unlikely to be more than 10%. At the same time, a similar proportion of sites are likely to benefit from expected changes. A small number of those sites are likely to benefit more substantially, with almost 10% likely to benefit by more than 10% in productivity. The outcome is similar whether it is based on currently highly-productive sites or on the current distribution of the plantation estate.

The average change is much the same by 2090, but the spread becomes wider, with almost 15% of sites experiencing 10% reduced productivity and almost 10% also experiencing gains of more than 20%. Although the distribution is somewhat skewed, with a majority of sites experiencing productivity losses, the average of all changes points to a slight overall increase in productivity. In other words, sites experiencing gains are, on average, experiencing greater gains than the sites expected to have reduced productivity.

The simulations shown above have a solid basis as only temperature and rainfall were changed. It thus constitutes little more than an interpolation between the observations under current climatic conditions that had been used to parameterise the model.

4.1.6 Productivity response to climate change including elevated CO_2

Future climatic conditions will include not only changed temperature and rainfall but also higher CO_2 concentrations, and since there are no observations of tree growth under naturally varying CO_2 concentrations, growth predictions have to be based on observation under experimentally varying CO_2 concentrations or a small number of observations of trees growing near natural CO_2 springs with naturally elevated CO_2 concentrations. Simulations with increasing CO_2 concentrations therefore have to be conducted with less confidence than the simulations with constant CO_2 and where the response against changes in other environmental variables could be constrained more tightly by the existing observations. Nonetheless, because CO_2 is certainly going to increase into the future, and since we know of the importance of CO_2 for plant growth, climate-change simulations were also conducted with increasing CO_2 concentrations.

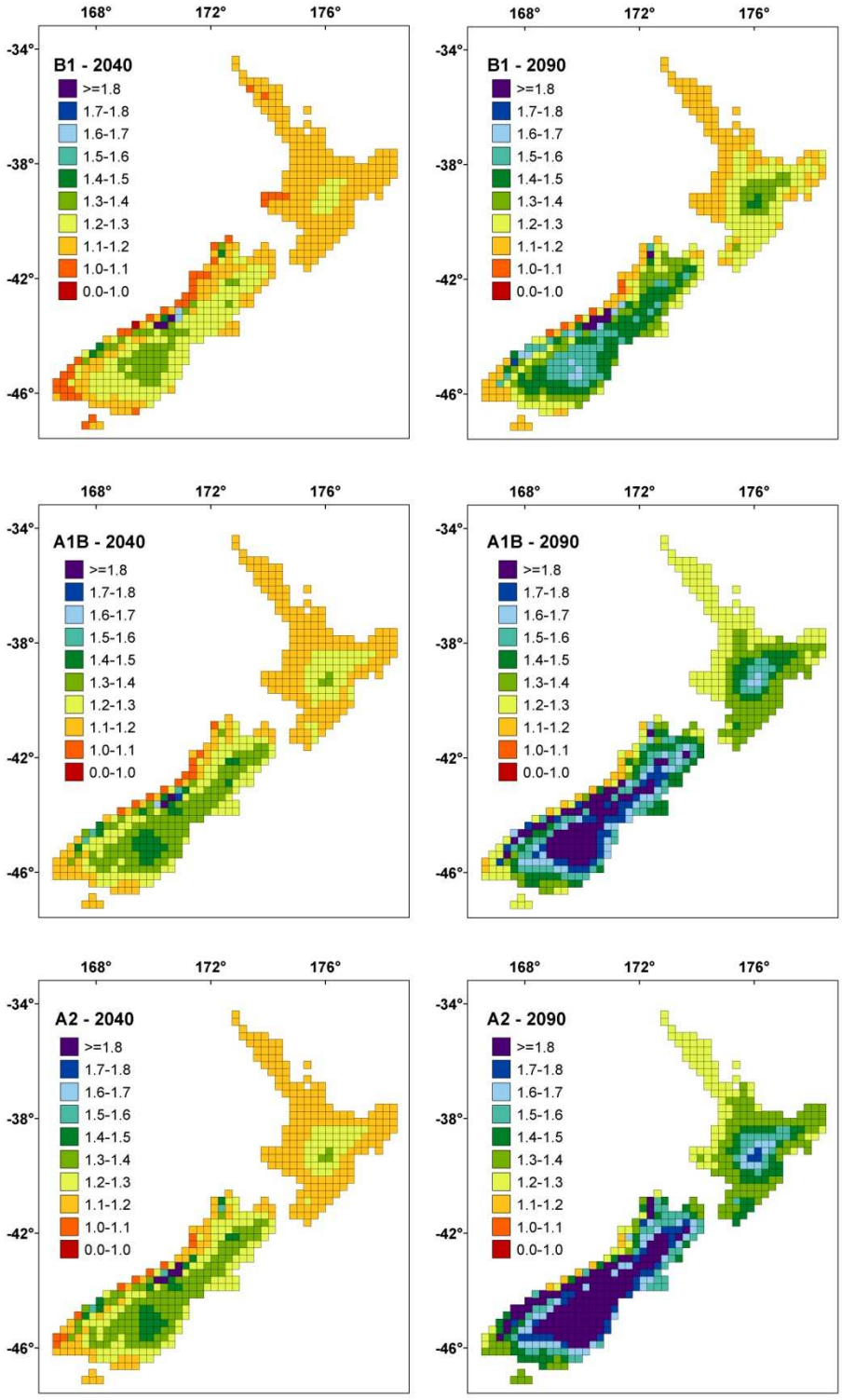

Figure 30 Climate change impacts on volume production under three emission scenarios for 2040 and 2090, including increases in CO_2 concentration, relative to simulations for 1990. For each time period/ emission scenario, simulations were run independently under climate change predictions under each of the 12 GCMs. Shown here are the averages of responses generated under the new climates of the 12 GCMs.

When simulations included increasing CO_2 concentration, resultant impacts on productivity were generally positive across all emissions scenarios and for both 2040 and 2090, with the positive effect further increasing from 2040 to 2090 (Figure 30). While increasing temperature had generally caused negative responses for most of the low altitude North

Island when CO_2 changes had not been considered (see Figure 27), increasing CO_2 completely offset these losses resulting in growth enhancements even for the far north. For the South Island, the stimulatory effect of elevated CO_2 added to the positive effect of warming to lead to substantial overall enhancements of growth.

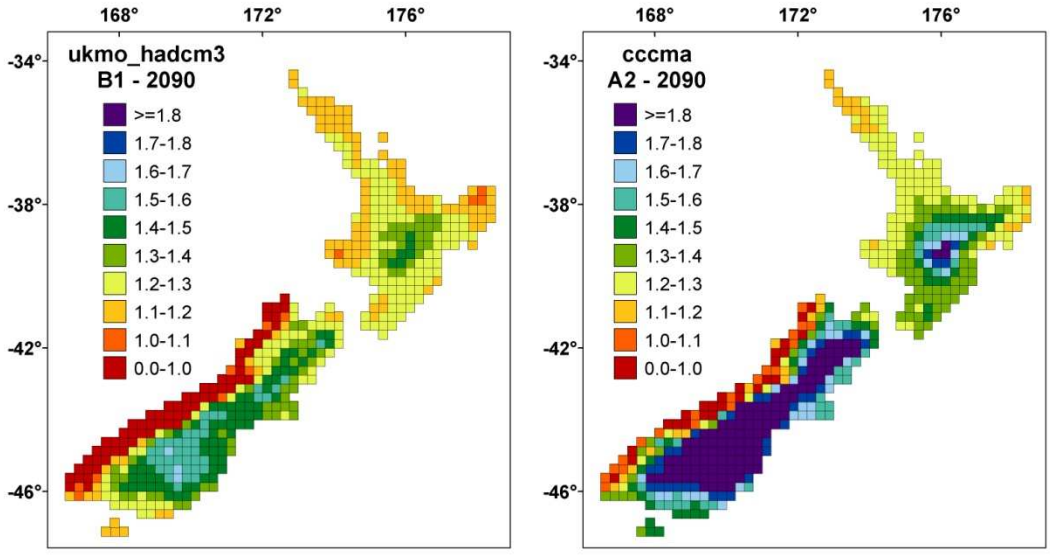

Figure 31 Climate change impacts on volume productivity, including the effect of elevated CO_2, under the two most divergent scenarios for 2090 relative to simulations for 2000, shown for the scenarios that show the least and most beneficial overall changes.

The average responses shown in Figure 30 again hide considerable regional divergence if simulations are based on specific GCM data (Figure 31). Divergence is particularly strong for the West Coast of the South Island, where model simulations vary between prediction of significant losses to significant gains in productivity. For other regions of New Zealand, predictions are for gain under all GCM runs, with only the magnitude of gains diverging.

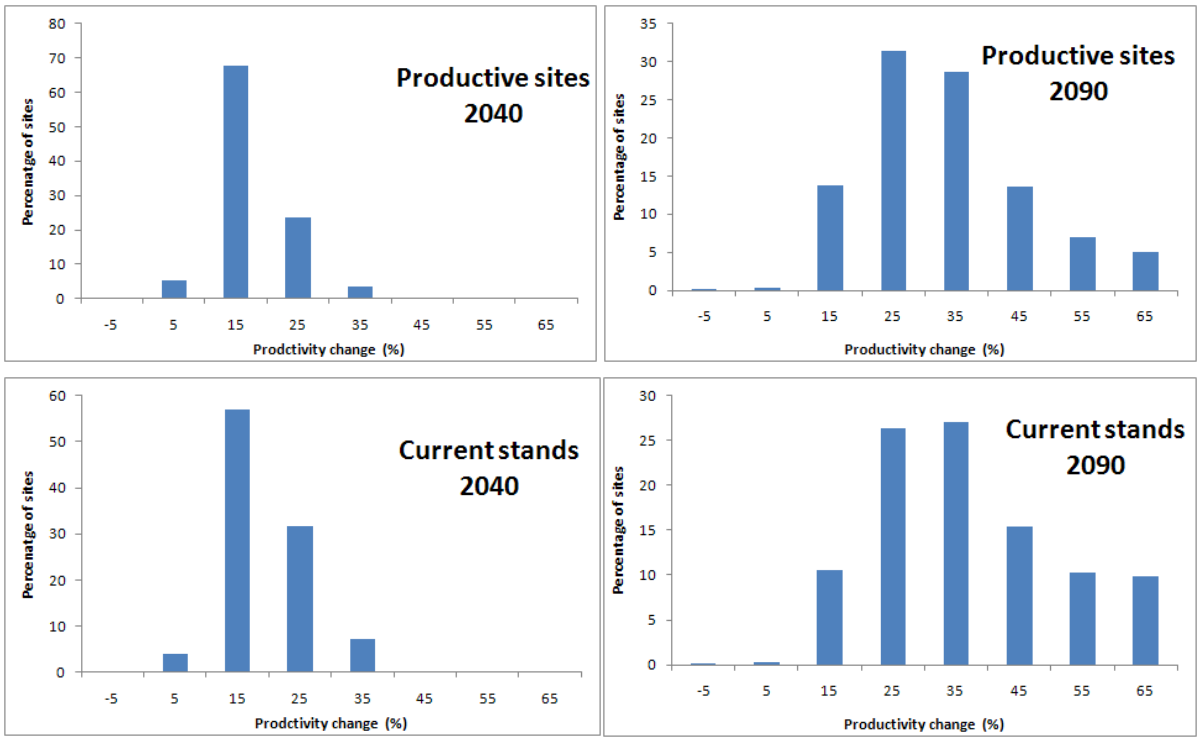

Figure 32 Proportion of currently highly productive sites (top panels) or weighted by the current distribution of the *P. radiata* estate (bottom panels) experiencing specified productivity changes by 2040 (left panels) and 2090 (right panels) under any of the three emission scenarios and all 12 GCMs and including any increase in CO_2 concentrations. 'Highly productive' sites are defined as sites with current productivity above 25 m^3 ha^{-1} yr^{-1}.

When the effects of increasing CO_2 are factored in, productivity is likely to increase for most sites and all future scenarios, with productivity enhancements increasing markedly from 2040 to 2090 (Figure 32). Only a very small fraction of site-scenario combinations are likely to experience adverse effects on productivity. The same picture emerges whether results are confined to all projected high productivity sites in New Zealand (regardless of current land use) or uses only productive areas currently in plantation forests.

4.1.7 Effects on soil organic carbon stocks

Climatic changes, together with the climate-induced changes in productivity, also lead to changes in soil organic matter. Changes are only slight by 2040 and are therefore shown only for 2090 (Figure 33).

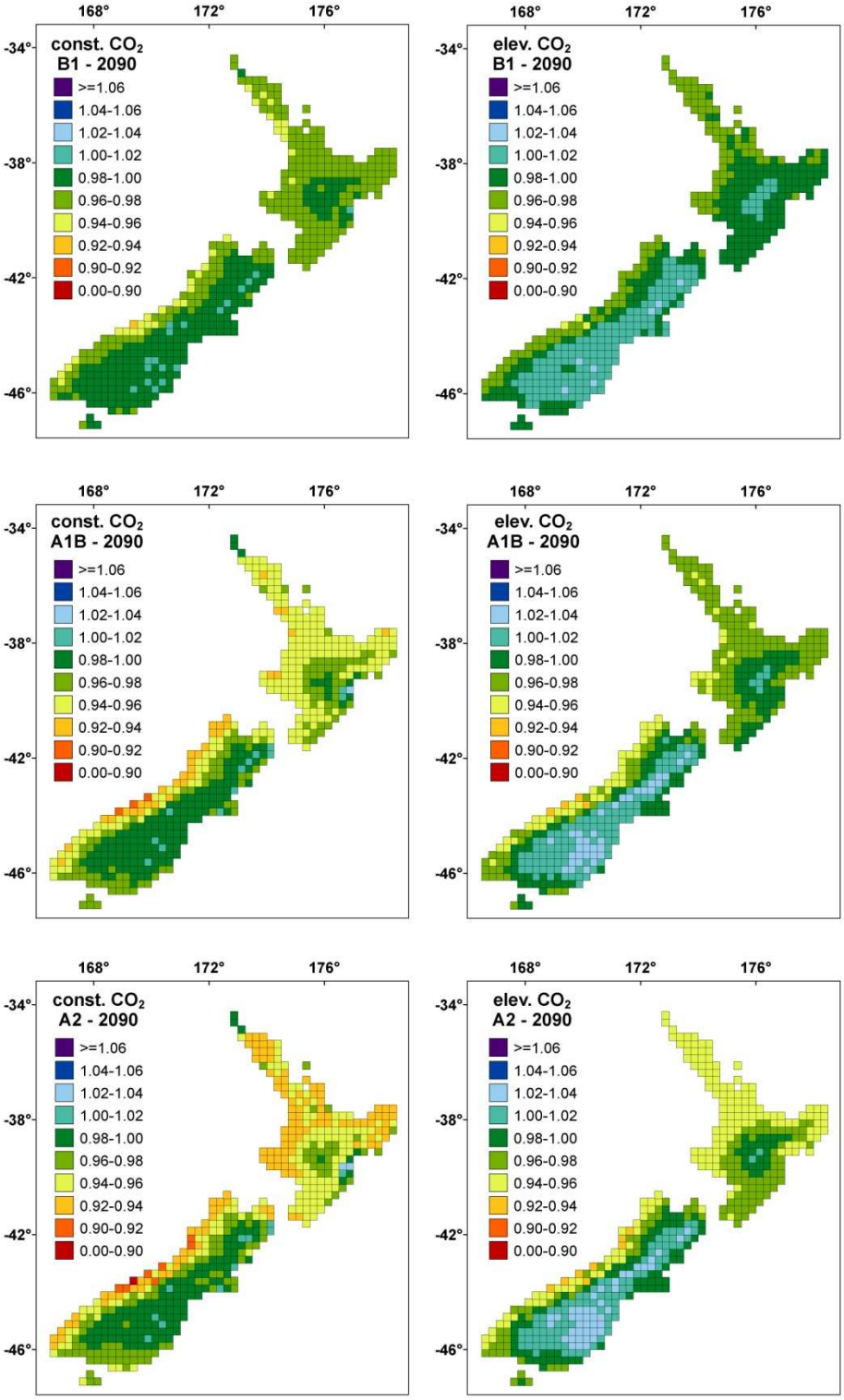

Figure 33 Changes in soil organic matter under three emission scenarios for 2090, for simulations with and without inclusion of increases in CO_2 concentration, relative to simulated amounts of organic matter under the climatic conditions of 1990. Soil organic matter here includes the sum of all organic matter pools, both above and below the soil surface and including litter pools. A value of 1.02, for example, means that soil organic matter would be 2% higher under climate change than currently.

There are likely to be losses of soil organic carbon for runs with both constant and increasing CO_2 concentration, but losses are likely to be slightly higher if CO_2 is held constant. Soil

carbon losses occur primarily over most of the North Island, the West Coast, and parts of Southland, whereas most of the eastern part of the South Island is expected to experience slight increases in soil carbon.

Losses of soil carbon also release nitrogen from soil organic matter. This nitrogen is mainly needed to satisfy the growth of trees, with stands accumulating 1000 m^3 ha^{-1} likely to accumulate something like 1000 kg N ha^{-1}. With greater growth potential under changed climatic conditions, the need for nitrogen and other nutrients is also likely to increase. This will be partly sourced from the soil and growth enhancements may consequently require increased fertilizer additions to be able to realise the projected potential. It is likely there will also be some increased nitrogen leaching under these anticipated climatic conditions.

4.2 A physiological discussion of modelled forest growth responses to climate change

4.2.1 Growth response to temperature

Photosynthesis and plant growth can be strongly affected by temperature but under New Zealand conditions, comparisons of productivity under current conditions showed that temperature is mostly favourable for the growth of *P. radiata*. There are exceptions, however, and growth in cooler locations in the far south and in mountainous regions are likely to be reduced by cool temperature. Current evidence for the positive effect of warmer temperatures on the growth of *P. radiata* in New Zealand is expressed through an increased site index and mean annual increment on sites with sufficient water supply and differences in annual mean temperatures (Hollinger 1990). It has to be highlighted that such field studies and the results of these are always the result of combined influence of several environmental variables, including temperature, solar radiation and humidity.

Jackson and Gifford (1974) described differences in productivity resulting from differences in rainfall, nutritional status of soils and growing temperatures. Rook and Whitehead (1979) studied the effects of temperature on young *P. radiata* seedlings in controlled environment chambers, but the effects are again complex because of the dependencies on diurnal and seasonal temperature ranges, exposure periods and stages of development. For older trees, Rook and Corson (1978) found the greatest photosynthetic carbon gain at an air temperature of 10°C, although this temperature was considered sub-optimal for growth. Air temperatures over 25°C, on the other hand, resulted in much lower photosynthetic rates. These findings did not allow for plant acclimation or for changes over the lives of trees and have to be carefully interpreted.

Also, *P. radiata* has no distinct dormant period in most parts of New Zealand. This makes it susceptible to frost damage but also creates the potential of additional growth under warmer winter conditions. Whitehead et al. (1994), working in the central North Island, recognised two months in early winter were no stem growth (diameter growth) occurred (May and June) and showed that needle elongation is related to thermal time (growing degree days above a base temperature of 6°C). With the shifting of the growth period because of increased temperatures, increased annual growth rates may be possible.

An interesting observation was made by Hellmers and Rook (1973) who found that the growth of pine seedlings was greatest with warm day temperatures and cool nights. Analysis

of residual error in the comparison of the model runs against observations confirmed the finding in that the greatest deviation between model and observations was found as a function of the difference between day and night temperature (i.e. the diurnal temperature range, Figure 34).

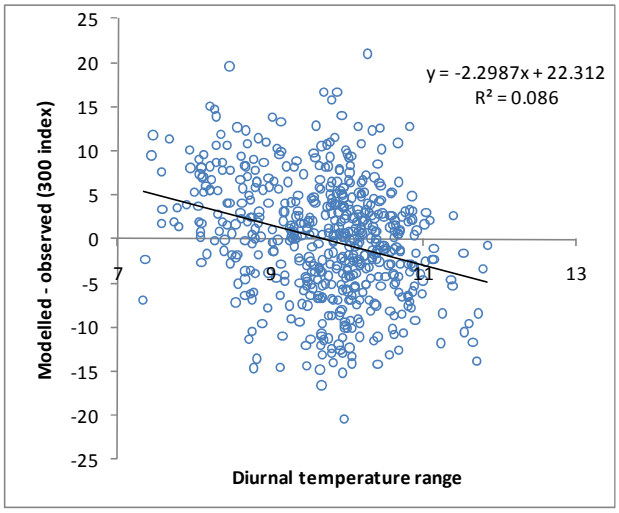

Figure 34 Deviations between modelled growth predictions and observations plotted against the diurnal temperature range at those sites.

Model simulations generally appear to overpredict growth where the diurnal temperature range is less than 9°C. This is a weak but significant relationship (r^2 = 0.086), especially given the narrow range in diurnal temperatures, but much stronger than the relationships obtained for the residuals against any other environmental variable (data not shown). It is not clear what the effect of diurnal temperature range means physiologically, or why there is such an effect at all.

This effect has not been included in the present modelling but constitutes a possible avenue for possible further refinement of the model in the future. Inclusion of this effect would not have any impact on modelled climate-change responses as the available climate-change scenarios do not quantify changes in the diurnal temperature range.

4.2.2 Water relations

Soil water balance has long been recognised as a major determinant of *P. radiata* growth at specific locations where trees experience seasonal water deficits (McMurtrie et al., 1990; Arneth et al., 1998a, 1998b; Richardson et al., 2002; Watt et al., 2003, 2010). These studies have all shown reductions in growth with declining root-zone water storage as estimated by soil water balance models. This was also shown in the present study, which showed a gradual reduction in productivity with decreasing precipitation for annual precipitation falling below about 1200 mm yr^{-1}.

For forest stands, even summer droughts often lead to little loss of productivity as water availability can be buffered through large soil-water resources that maintain trees' access to water even when water stores are not replenished by rainfall over extended periods. The extent of this buffering is determined by the physical properties of the soil, which determines the amount of available water that can be held per unit of soil volume, and by soil and rooting depth. These characteristics define the volume of soil that can be accessed by plants and the extent to which the available reservoir is fully replenished during periods with high precipitation. Using the National Soils Data base, we estimated soil water storage for different regions and thus explicitly accounted for this variability across the country.

For the present work, the impact of climate change on water availability of forest stands was assessed by combining predicted changes in precipitation with changed water-loss rates as

determined by the combination of factors that together determine evapotranspiration rates from plant canopies (see next Section).

The observations also showed a reduction in productivity with increasing rainfall in areas where annual rainfall is high. In fact, the two observations with lowest measured 300 Index both received rainfall in excess of 3500 mm yr^{-1} (Figure 2). This low productivity is not related to temperature or reduced solar radiation as they are explicitly included as drivers of modelled productivity. Hence, there is some aspect related to excessive rainfall that is detrimental to the growth of *P. radiata*. We were not able to relate it to an explicit physiological factor so that it had to be included as a simple empirical adjustment factor.

4.2.3 Evapotranspiration rate as a function of temperature

Water can be lost from stands of trees by evaporation from water on the surface of foliage, trunks, branches or the soil surface or by transpiration, which is the loss of water from the inside of leaves or needles, from where it is replenished from soil-water if that is available. These two processes are often jointly described as evapotranspiration. The replenishment of soil water resources during wet periods, and the extent to which the soil can store water, are, however, also of critical importance in determining the ability of forest stands to sustain productivity, or at least avoid tree mortality, over extended dry periods.

Evapotranspiration is strongly affected by temperature because warmer air can hold more moisture. This is diagrammatically shown in Figure 35, which shows saturated vapour pressure as a function of temperature.

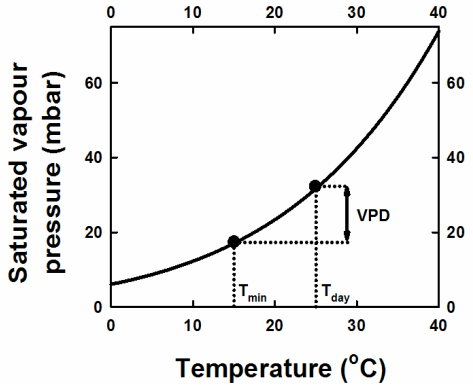

Figure 35 Saturated vapour pressure shown as a function of temperature, together with diurnal minimum and daytime temperatures.

As a generalised approximation, the absolute humidity in the air can be taken to be the vapour pressure that was at equilibrium with the previous night's minimum temperature. The vapour pressure at equilibrium with daytime temperatures determines the humidity of the air inside the leaves of plants. The difference between those two vapour pressures gives the vapour pressure deficit (VPD) of the air, which is the principle driving force for transpiration from plant canopies.

As a first approximation, warmer temperatures will increase water loss by evapotranspiration. With global warming, both overnight minimum and daytime temperatures are likely to increase. If the diurnal temperature range does not change, it will lead to an increase in vapour pressure deficit because the saturated vapour pressure curve is steeper at higher than lower temperatures (Figure 35).

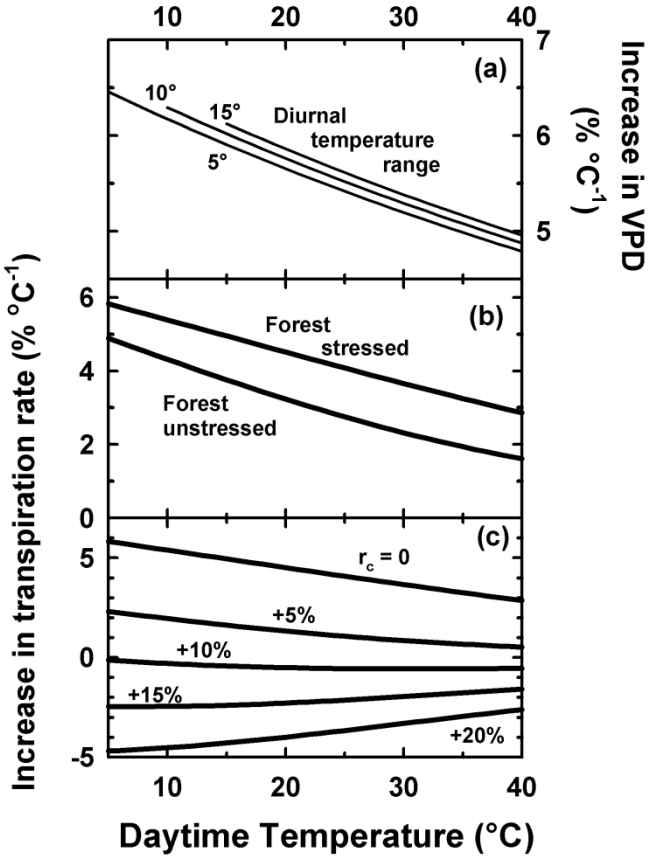

Figure 36 Change in vapour pressure deficit, VPD (a), transpiration rate with warming (b) and with warming plus stomatal closure due to increased CO_2 concentration (c). Change in vapour pressure is calculated as a function of daytime temperature and for a range of diurnal temperature ranges. Transpiration rate was calculated with the Penman-Monteith equation, with an assumed diurnal temperature range of 10°C, net radiation = 400 Wm^{-2}, and with parameters for aerodynamic and canopy resistance representative for unstressed (25; 50 s m^{-1}) and stressed forests with increased canopy resistance because of some kind of stress (25; 200 s m^{-1}). For calculations in (c), canopy resistance, r_c, was increased by 0, 5%, 10%, 15% or 20% as indicated in the figure.

Figure 36a shows the increase in vapour pressure deficit of the air with warming. The increase in vapour pressure deficit with increasing temperature is only marginally different for different diurnal temperature ranges or daytime temperatures, with increases in VPD being between 5 and 6% $°C^{-1}$ over most temperature combinations. Only at very low temperatures does the increase in VPD exceed 6% $°C^{-1}$, or be less than 5% at very high base temperatures (Figure 36a).

These changes in VPD can then be used to compute increases in transpiration rate with warming. The calculations were done with the Penman-Monteith equation (Monteith 1965; Martin et al. 1989), which is used as a sub-model in CenW. McKenney and Rosenberg (1993) compared a range of equations for calculating changes in evapotranspiration and concluded that only the Penman-Monteith equation includes sufficient of the underlying physics to properly capture likely changes under a range of climate-change scenarios. Canopy and aerodynamic resistances were used as given in the figure legend to represent typical values for different canopy types.

Canopies differ in the way transpiration rates respond to environmental drivers. Forest canopies tend to be relatively open so that transpiration rates tend to vary primarily as a function of changes in vapour pressure deficit (Jarvis & McNaughton 1986). These differential effects are formalised through canopy and aerodynamic resistances included in the Penman-Monteith equation.

For forests, the simulations suggest increases in transpiration rate in forest systems (Figure 36b) as transpiration rate in these systems is primarily controlled by VPD rather than absorbed net radiation. Calculated increases in transpiration ranged from 5% at 5ºC^{-1} to 2% $°C^{-1}$ at 40°C. The increases were even greater for forest systems under stress, with increases in transpiration rate ranging from 3 to 6% $°C^{-1}$ because transpiration rate in stressed forests is even more strongly controlled by VPD. These calculations imply that under warmer conditions, systems limited by the availability of water are likely to use any available water

faster. This will then allow less plant growth for the same amount of precipitation as it gets warmer.

Under increased CO_2 concentration, however, stomata of most plants are observed to close to some extent. The effect of such partial stomatal closure is illustrated in Figure 36b, for which the Penman-Monteith equation was run for a 1° increase in temperature and with some stomatal closure as indicated in the figure. Stomatal closure by 10% would have the effect of almost completely negating the effect of increasing temperature by 1ºC (Fig. 36b). Stomatal closure by more than 10% would lead to net reductions of transpiration rates, whereas stomatal closure by less than 10% would lead to increased transpiration rates, but by less than the increase if there were no adjustments in stomatal conductance (Figure 36c).

This raises the question of the extent of stomatal closure that can be expected in future. Stomatal adaptation has been shown on herbarium specimens in which the number of stomata on leaves has decreased with historical increases in global CO_2 concentration (Woodward, 1987; Rundgren & Björck 2003; Kouwenberg et al., 2003). The carbon isotope discrimination between $^{13}CO_2$ and $^{12}CO_2$ can also be used to infer changes in the intercellular CO_2 concentration and that can be related to historical changes in atmospheric CO_2 (Dawson et al. 2002) Using this approach, Arneth et al. (2002) and Duquesnay et al. (1998) reported data that inferred some stomatal closure in response to increasing atmospheric CO_2, but Marshall and Monserud (1996) and Monserud and Marshall (2001) found no evidence of stomatal closure in their data sets.

Morison (1985), Allen (1990) and Urban (2003) compiled a range of observations from the literature, and showed that stomatal conductance across a range of species was reduced by about 40% when CO_2 concentration was doubled. Stomatal conductance in woody species, however, is generally observed to be somewhat less sensitive to CO_2 concentration, with Curtis and Wang (1998) reporting stomatal closure by just 11% and Medlyn et al. (2001) reporting 21% stomatal closure across a range of studies.

Medlyn et al. (2001) also reported that the response appeared to be weaker in older rather than younger trees and weaker for conifers than deciduous trees. Changes in stomatal conductance usually mirror changes in CO_2 assimilation rate so that the ratio of intercellular to ambient CO_2 concentration is usually found not to change under conditions of elevated CO_2 (Drake et al. 1997). Medlyn et al. (2001) further assessed that question by fitting the Ball et al. (1987) model to the available data. In the Ball et al. (1987) model, stomatal conductance is described explicitly as a function of CO_2 concentration and photosynthetic rate. Medlyn et al. (2001) found that under non-water-stressed conditions, the same model parameters held under ambient and elevated CO_2 which implied that the functional relationships between photosynthesis and stomatal conductance is not altered by growth in elevated CO_2. Since the short-term response of photosynthesis to elevated CO_2 is well understood, the key uncertainty thus relates to the extent of a possible long-term acclimation of photosynthesis to growth in elevated CO_2, which is discussed in the next Section.

Figure 36 only indicates the sensitivity of the system to the indicated changes, but ultimate outcomes will depend to a large extent on the relative rates of increases in CO_2 concentration and temperature and the extent of physiological adjustment, if any. Greater relative temperature increases will lead to greater increases in transpiration rate, whereas greater relative increases in CO_2 concentration will lead to less increase in transpiration rate, or even a reduction. Similarly, species in which stomata are more sensitive to CO_2 concentration will

experience less increase in transpiration rate than species with less sensitive stomata. Stomatal opening also tends to be linked to photosynthetic rates, and conditions that increase or decrease photosynthesis, such as more or less favourable temperatures, or access to more or less nutrients, also flow through to changes in stomatal conductance.

Since some of these parameters are directly linked to temperature. Others, such as nutrition, can be indirectly linked to climate change. Because of these multiple dependencies, it is not possible to be too definite in assigning a value to the extent of stomatal conductance under specific climate change simulations. Only the full integrated simulations in CenW provide that. However, if one assumes canopy carbon gain does not change with climate change, and calculates changes in transpiration rate based solely on the Ball-Berry formulation for stomatal conductance (Ball et al. 1987) under the CO_2 and climate-change conditions used for New Zealand, the values in Table 6 result.

Table 6 *Calculated change in photosynthesis and stomatal conductance under the average changes generated under the 3 emission scenarios used here. The calculated change in photosynthesis ignores a range of possible feedback processes that could reduce or enhance the initial response. The relative conductance change per °C warming would be the relevant measure to use for comparison in Figure 36c*

Emission scenario	Simulation year	Temperature change (°C)	CO_2 conc. (ppmv)	Relative photosyn.	Relative stomatal conductance	Relative conductance per °C warming
	1990	0	353	0	0	0
A1B	2040	0.93	483	10.4	-19.3	-20.8
A2		0.93	481	10.2	-19.1	-20.6
B1		0.73	457	8.7	-16.0	-21.9
A1B	2090	2.07	674	19.5	-37.4	-18.1
A2		2.56	754	22.0	-42.9	-16.7
B1		1.32	538	13.5	-25.6	-19.4

Overall, stomatal closure by elevated CO_2 together with the relatively slight increases in temperature for New Zealand mean there is likely to be stomatal closure in most stands. This is even more pronounced in the near term as changes in CO_2 concentration (that initiate stomatal closure and thus reduce transpiration rate) occur faster than changes in temperature (that act to increase transpiration rates). These numbers are only a guide, as canopies will also change in other ways in response to climatic changes which can further change either atmospheric conditions, such as relative humidity, or plant photosynthetic rates through changes in foliage development or available nutrition.

4.2.4 Responses of photosynthesis to CO_2 concentration

Of all the aspects of atmospheric and climate change, the increase in atmospheric CO_2 concentration is the most certain. What is still uncertain, however, is the way plants respond to that change.

It has been shown in many experimental studies that C_3 photosynthesis responds strongly to CO_2 concentration, with photosynthesis typically increasing by 25–75% for doubling

atmospheric CO_2 concentration (e.g., Kimball 1983; Cure & Acock 1986; Drake 1992; Luxmoore et al. 1993; Kirschbaum 2000a, 2004; Urban 2003; Nowak et al. 2004). These include observations on trees and persist even after inclusion of the effects of the often-observed photosynthetic down regulation (Gunderson & Wullschleger 1994).

Recent work has also shown sustained growth increases for plants fumigated in 'free air CO_2 enrichment' (FACE) experiments (Nowak et al. 2004). This has been observed in wheat fields (Garcia et al. 1998) and in largely undisturbed forests (Herrick & Thomas 2001; Gunderson et al. 2002). These responses are consistent with theoretical understanding of the effect of CO_2 concentration on photosynthesis at the leaf and stand level (McMurtrie et al. 1992; Long et al. 1996). At the same time, many individual studies show specific deviations from mean responses that can sometimes be linked to specific factors such as nutrient availability and sometimes remain still unresolved (Nowak et al. 2004).

While the CO_2 response can generally be moderately variable in interaction with other limiting factors in the environment (Kirschbaum 1999; Körner et al. 2007), the modelled response shows less variability across New Zealand because other environmental limitations are not too variable, e.g., temperature is moderate and most sites – with some exceptions – experience no or only moderate degrees of water limitation. Nutrition is also generally adequate, either because of the inherent good fertility of soils or because of some supplemental fertiliser application or inclusion of legumes on sites with known fertility limitations. For most of New Zealand's current plantation forest, the possibility of a restricted response to CO_2 through nutrient limitations is low. Current plantations show a medium to high nutrient level in their foliage as a result of active management against nutrient deficiency. Consequently, in our model comparisons against observed growth rates, site fertility was only a weak determinant of growth at different sites (Figure 37). There were a small number of sites in Northland with extremely low soil nitrogen concentrations. Growth on these sites was probably limited by nutrition, but for other sites in the country there was almost no relationship with soil nitrogen, indicating that for most forestry sites in New Zealand, nutrition is currently adequate. The same will probably be valid for forests established in the future as they are likely to be planted on farmland with often good nutrient levels.

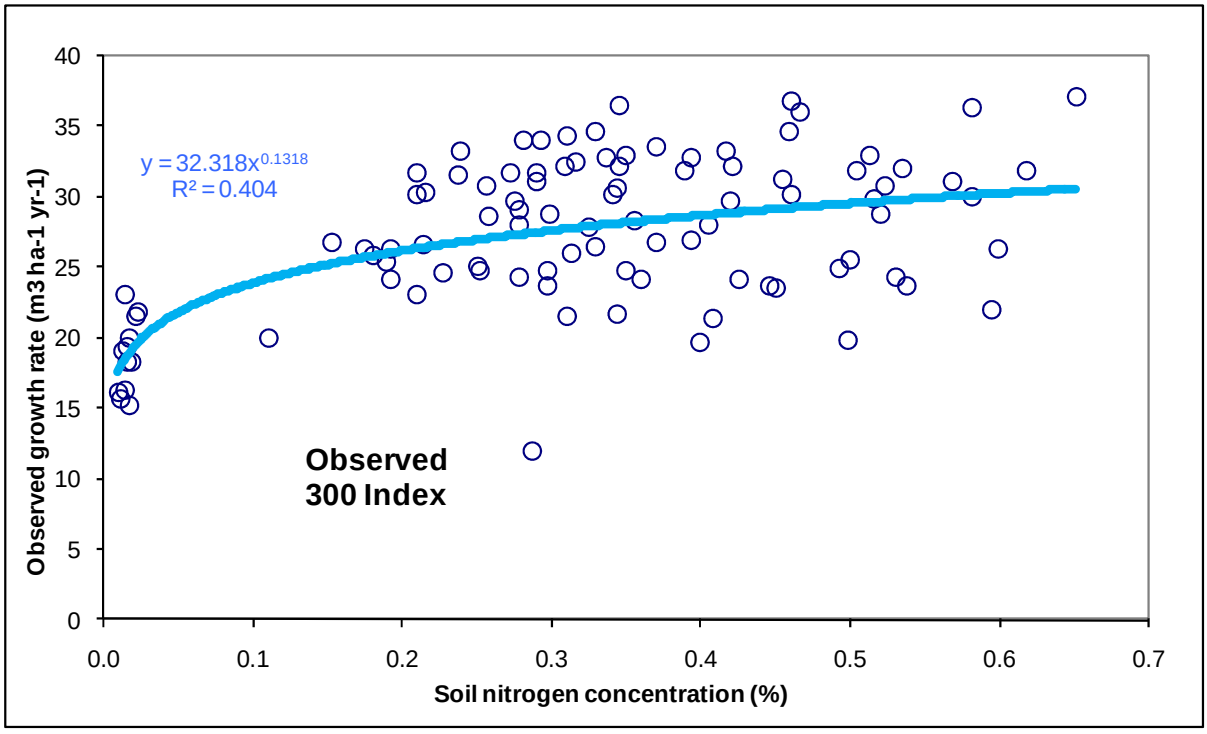

Figure 37 Observed growth rate of the 101 PSP plots expressed as a function of soil nitrogen concentration of the top 5 cm observed at those sites.

4.2.4.1 Mature plant responses to CO_2 concentration

For logistic constraints, most research on CO_2 responses of plants has so far been carried out on young plants, or species of smaller mature sizes. It leaves the question whether mature stands would respond to increasing CO_2 concentration in the same way as young stands. The answer to that question is complicated by the fact that stand growth normally slows as stands mature but the reasons for that slowing are not well understood (Ryan et al. 1997). Depending on the physiological causes of age-related declines in productivity, and the age over which a response to CO_2 is assessed, a range of possible apparent response patterns to CO_2 fertilisation can be obtained (Kirschbaum 2005).

For instance, if maturity-related decreases in productivity are actually a function of stand size (rather than stand age), a stand grown under elevated CO_2 might be affected by these size-related growth reductions at an earlier age than a stand grown under lower CO_2. An apparent growth response to CO_2 might then be obtained if growth is normalised for differences in stand size. For stands of the same age, however, growth may be no different between high and low-CO_2 grown stands because any direct CO_2 stimulation of productivity could be negated by the size-related reduction in productivity.

Experimental evidence on this important question is very limited owing to the logistic constraints of modifying the whole environment of a large tree canopy. Some of the small number of observations indicate on-going growth enhancements (e.g., Delucia et al. 2005); others indicate on-going stimulation of carbon gain, with most of the extra carbon used for greater root growth and below-ground allocation (Norby et al. 2004); and yet others indicate either a brief stimulation that is not sustained over subsequent years (e.g., Asshoff et al. 2006 for European beech but no change for hornbeam and European oak) or a stimulation that

diminishes over time (30 years) or stand size (Hättenschwiler et al. 1997). Another study (Tognetti et al. 2000) found no significant increase in radial stem growth due to CO_2 enrichment over a long period of growth. Interestingly, in the same experiment where Asshoff et al (2006) did not find significant growth differences based on tree ring and basal area growth Zotz et al. (2005) found CO_2 enhancement of photosynthesis of around 40% in the third year of the experiment. In cases where growth enhancements are not sustained, it is not clear whether this is due to nutrient feed-backs, size-related feed-backs or other factors like allocation shifts that might make mature stands less responsive to increasing CO_2. There is no New Zealand-specific study of mature tree CO_2 responses for plantation tree species, and our current knowledge is based on overseas studies.

For the present simulations, responses to CO_2 were assumed to be sustained throughout the growth of stands other than for conditions where the combination of environmental factors led to adverse consequences for the nutrient or water cycle. It is also well-known that tree growth slows down as trees grow beyond their peak ages or sizes, but there was no indication in our calibration data sets that such limits would start to affect tree growth at ages or sizes within the normal rotation lengths used in New Zealand.

Based on these observations under current growth conditions, the relevant parameters were set to remain non-limiting even under conditions where growth might be enhanced through better environmental growth conditions. If that extrapolation from the current observed data set had not been valid, it could have led to some overestimation of the beneficial growth responses into the future.

4.2.4.2 Photosynthetic down regulation for plants in high CO_2 environments

Many workers who have exposed plants to elevated CO_2 concentration have observed a degree of photosynthetic down regulation over exposure times of weeks or longer (e.g., Gunderson & Wullschleger 1994; Long et al. 1996; Wolfe et al. 1998). Part of this phenomenon has been explained as an experimental artefact in that downward acclimation tends to be more pronounced if plants are grown in smaller pots (Arp 1991; Thomas & Strain 1991). In pines, there was no down regulation in current-year needles but only in newly grown needles that developed under changed atmospheric conditions (Turnbull et al. 1998).

More generally, plants regulate their various processes for an overall balance. If one of their required constituents, namely carbon, becomes more readily available as a result of increased CO_2, the question arises whether the plant can utilise that extra resource. If plants are grown with restricted root volumes then carbohydrate supply even under normal CO_2 may be in adequate supply so that excess carbohydrate cannot be utilised and plants down-regulate their photosynthetic capacity to again match supply and a limited demand (Erice et al. 2006). It is therefore consistent to find that degree of down-regulation increases with diminishing root zones, and little down-regulation is observed when the source–sink balance is manipulated in favour of creating more sinks (Erice et al. 2006), or for plants that are grown in larger pots or in the field (Arp 1991; Drake et al. 2004).

However, even under natural conditions, a degree of ‘downward acclimation’, in this case through reduced internal nutrient status, has to be expected if increased photosynthetic carbon gain cannot be matched by similarly increased nutrient supply. This would result in lower foliar nutrient concentrations and consequently reduced inherent photosynthetic rates (e.g.,

Rastetter et al. 1992, 1997; Kirschbaum et al. 1994, 1998; Wolfe et al. 1998). It is unclear whether there is additional downward acclimation in addition to these readily understood processes.

This uncertainty about down regulation raises the question whether such effects as CO_2 fertilisation should be included in modelling tree growth under climate change. We have dealt with that issue by presenting simulations with maximum and minimum likely outcome for growth under CO_2 by modelling climate-change effects with and without the effects of CO_2 fertilisation.

4.2.5 Climate change effects on soils processes

Plants also require nutrients, especially nitrogen and phosphorus. Most nitrogen and phosphorus is derived from the decomposition of soil organic matter. In the decomposition of soil organic matter, CO_2 is released to the atmosphere and any excess nitrogen and phosphorus is mineralised and becomes available for plant uptake. If plants are able to fix more carbon through increased CO_2 concentration, but nutrient uptake is limited, plant internal nutrient status declines as is usually observed experimentally (e.g., Drake 1992; Tissue et al. 1993). This provides a primary negative feed-back effect on plant responses to increasing CO_2 concentration. Plants that fix more carbon also produce more litter which adds to soil organic matter and immobilises nutrients. This reduces the nutrients available for plant uptake and provides a secondary negative feed-back effect (Rastetter et al. 1992, 1997; Comins & McMurtrie 1993; Kirschbaum et al. 1994, 1998), and process more recently termed 'progressive nitrogen limitation' (Luo et al. 2004).

These two processes restrict the possible positive response of plant productivity to increasing CO_2 concentration. However, temperature increases can also play a role. There are likely to be only slight direct effects of increasing temperature on plant function, but temperature can stimulate the rate of organic matter decomposition and mineralisation of nitrogen (Kirschbaum 2004). With increasing temperature, more nutrients can become available for plant uptake, and that can stimulate plant productivity independent of any direct physiological plant responses to increasing temperature (Schimel et al. 1990).

An increase in nutrient availability via better mineralisation with increasing temperature means that trees might be sufficiently supplied with, e.g., nitrogen for enhanced growth depending on the nutritional status that the trees experience now. For New Zealand's plantation forestry, nutrient deficiencies, especially of nitrogen, phosphorus and boron, are considered as manageable growth limiting factors. Consequently, noticeable nitrogen limitations are essentially confined to some site in Northland (Fig. 37), and and there were no indications of phosphorus limitations in our primary data set at all (data not shown).

4.2.6 Integrating responses to temperature, CO_2, nutrition and water availability in a modelling approach

Forest growth is ultimately determined by the interacting cycles of carbon, water and nutrients. Plants grow by fixing CO_2 from the atmosphere, but in the diffusive uptake of CO_2, trees inevitably lose water. Water can be replenished from the soil as long as adequate soil

water is available. Otherwise, further water loss must be prevented by stomatal closure which then also limits CO_2 fixation.

The relativities between water loss and carbon gain are affected by temperature, which affects the vapour pressure deficit and transpiration rate, and by CO_2 concentration, which affects the rate of photosynthesis. With increasing temperature, more water is lost per unit carbon gained, and with increasing CO_2 concentration, more carbon can be gained per unit water lost.

The required amounts of nitrogen and phosphorus are mainly derived from the decomposition of soil organic matter. Nutrient supply is both a co-limitation that affects the primary response to aspects of climate change, and nutrient supply can be directly affected by climatic changes. All these interactions and feedbacks should be modelled through a process-based model that has the capability to integrate these linkages.

4.2.7 Linkages and possible effects

Based on current knowledge of interactions and feedback between the important components and processes and the projections of changes in climate and CO_2 concentration for New Zealand overall trends regarding the impacts have been assessed above. Changes vary over New Zealand due to a combination of prevailing key limitations and the nature of climatic changes. The relative rates of increases in CO_2 concentration compared with changes in temperature and rainfall are particularly important.

Photosynthesis will respond strongly to the increase in CO_2, which is expected to increase the growth rate of trees. Responsiveness to CO_2 is strongly influenced by the nutritional status of stands, but in the generally fertile conditions in New Zealand, the CO_2 fertilisation effect can be strongly expressed. CO_2 fertilisation can generally be enhanced under water limited situations. However, as water stress does not play an important role in New Zealand, and because of the general good nutrient status, the CO_2 fertilisation effect is ubiquitous and moderately strong.

With expected warmer winter temperatures, the growing period in New Zealand will increase and an expansion of the plantation forest estate to higher altitudes will therefore be possible. Vapour pressure deficit will change with temperature and could lead to increased transpiration if that effect were not negated by CO_2-induced stomatal closure, probably leading to slight decreases in transpiration rate despite greater evaporative demand. Changes in the amount and timing of precipitation could potentially play a critical role for future growth of stands in New Zealand, but anticipated changes even out to 2090 are generally small under any of the 12 GCMs used and are unlikely to play an important role.

4.2.8 Modelling approach

The integration of these multiple factors and their feedbacks to each other and to actual tree growth was done with the process-based model CenW that explicitly links these components. The CO_2 response and subsequent feedback effects are a major part of the modelling exercise, and are necessary to provide a balanced assessment of the combined interactions between temperature, nutrient and water balance changes under future climate scenarios.

Running such a model under various climate scenarios for New Zealand's conditions has allowed the study of the response of our plantation forests to the expected changes. Process-based models allow projections beyond our range of current experience. However, even for a process-based model, testing and comparisons against current-day observations are important steps to build confidence in the model's ability to capture reality. These could be done fairly successfully for changes in temperature and precipitation.

For responses to CO_2, however, this is much more difficult. Numerous experiments have been conducted where plants have been exposed to elevated CO_2. While, these experiments usually show growth responses that are the basis of the current simulations, results also diverge. While some reasons for different findings have been identified, others remain elusive. For obvious logistic reasons, observations are particularly sparse for tall and mature trees, limiting the confidence of predictions of CO_2 responses to stands of trees over extended periods. The ability to model the complex feedback under a CO_2 enriched atmosphere is certainly important if down-regulation does not occur. We currently cannot exclude this option, which reduces the suite of models that can be used for running such a scenario.

5 General discussion

We produced productivity surfaces for both indigenous forest species, and for *P. radiata*. The two plant groups experience very different growth conditions, with pines grown in plantations and indigenous forests mostly occur in mixed stands of unmanaged forests. These different growing conditions necessitated the use of different modelling approaches to describe the growth of the different stands types, with the modelling of indigenous forests concentrating on accounting for the biotic interactions between target species and their neighbouring and competing plants, whereas pine-growth modelling could focus more strongly and directly on the physiological determinants of stand growth.

Growth of the two different plant types differed significantly; with pine growth rates many times higher than that of indigenous forests (cf. Figure 18, 23). Such a large difference was not unexpected because the two forest types are affected by very different growth limitations. Indigenous forest trees grow in competition with neighbours and unspecified and unmeasured other understorey species. Some of these competitive interactive effects can be accounted for in the modelling but others remain unaccounted for reduction in potential productivity. Productivity in indigenous forests can also be reduced through pests and diseases and herbivory (both by invertebrates and introduced mammalian herbivores). Also, many forests grow on impoverished sites with poor nutrition and steep, rocky or otherwise difficult conditions. Stands growing under these diverse conditions contributed to the observed growth in measured stands.

Pines, on the other hands, are grown in plantations where inter-tree competition is controlled and minimised through careful management of stand stocking and placement of individual trees. Competition from weeds is also minimised by managers through weed control of variable intensity. Pines as exotic species are also generally fairly unaffected by pests, diseases and herbivory. Fertility in most measured stands was also reported as being adequate (Figure 37), partly due to the selection by forests managers of sites with better perceived growth potential and partly to the prevention of fertility problems by supplemental fertiliser addition or planting of legumes.

For pines, it is therefore easier to see relationships between growth and the underlying physiological drivers of growth, with limitations due to temperature and water stress that can be related to broad-scale patterns of temperature and water availability (Figures 22, 23). These surfaces also display small-scale variability due to soil properties, such as differences in water holding capacity that are most noticeable in the water-limited regions of the eastern part of the South Island. Pine growth could also be limited by high rainfall (Figures 22, 23). This pattern was clearly seen in the observations of pine growth, but a physiological explanation is still elusive.

In contrast, the growth of indigenous forest species was much more uniform across the country (Figure 18). This pattern probably indicates that under more favourable conditions, competitive interactions between trees increase so that the potential positive effect of more favourable abiotic conditions cannot express itself in the growth of individual species.

We used a stem density of 2,500 stems ha^{-1} for estimating carbon gain of indigenous forests since this stem density is commonly used in indigenous forest restoration planting. A variety of stem density values were tried, varying from 1,500 to 10,000 stems per hectare. Estimated carbon gain did not vary considerably across different densities since growth became more

rapidly constrained by stand basal area at higher densities. The lack of mortality and size-asymmetric competition is a limitation imposed by a lack of mortality models for most of the species studied. However given the relatively short modelling period (30 years) it is unlikely that this will have altered estimated carbon gain appreciably. It is unclear whether the omission of size-asymmetric competition may have affected estimated carbon gain. In mature forests, the majority of carbon is generally contributed by a few large individuals, with some evidence that the presence of emergent trees might enhance carbon storage in live biomass (Keith et al., 2009), but it is unlikely this effect would be seen within 30 years.

The parameterised model for pine growth could then also be applied to climate-change simulations. Overall, the emerging picture was reassuring, with the simulations indicating no dramatic decreases in productivity in any region under any scenario. Without considering increasing CO_2, there were generally some productivity losses in the warm north and gains in the cooler south (Figures 27, 28), but all changes were generally moderate (Figure 29), reflecting the fact that pines in New Zealand currently experience growth conditions well within their suitability envelope and the anticipated climatic changes in New Zealand are generally fairly mild (Figures 25, 26; Table 5).

If one considers increasing CO_2 as well, and if the CO_2 fertilisation effect can fully express itself under typical growth conditions, then expected growth trends become positive in all regions and under all scenarios (Figures 30, 31), with growth responses for currently highly productive sites of about 15% by 2040 and 25–30% by 2090 (Figure 32). It must be stressed, however, that these large positive responses are contingent on a strong plant-physiological response and on the maintenance of adequate soil fertility as growth responses would otherwise be curtailed by nutrient feedback effects.

On the negative side, climate change is likely to lead to a loss of soil organic matter (Figure 33), principally due to the stimulation of organic matter decomposition by higher temperature. Such organic matter losses can be partly prevented by the stimulation of plant productivity by elevated CO_2, which would also increase plant litter inputs and reduce soil organic matter losses (Figure 33).

Climate change is likely to affect other abiotic and biotic factors in addition to the plant physiological factors simulated here, and that, in turn, may affect plantation growth and productivity. These factors include weeds, insects, pathogens and the risks from wind and fire. Climate change is likely to increase fire risk and that the length of the fire season in most areas of New Zealand, but especially in eastern areas due to increasing temperature and slightly decreasing rainfall (Watt et al. 2008).

It is difficult to forecast changes in wind speeds, and to the extent that scenarios have been produced, they present a divergent picture, with increasing wind damage in some regions and decreasing wind damage in others. Upper and eastern parts of the North Island may periodically be subject to more severe extra-tropical cyclones (Watt et al. 2008). Changes in wind could potentially be very important, but at this stage, it is not yet possible to make confident predictions of the severity or even the direction of any changes.

Biotic factors are also likely to be strongly influenced by climate change as the distribution of weeds, insects and pathogens is strongly determined by climatic conditions. Climatic changes are therefore likely to result in shifts in the geographic range of many species. Potential problems could be posed by the introduction of new species or the release of potentially

damaging species from their currently limited distribution in the far north of New Zealand. These problems are common for weed species, insect pests and diseases.

There are also a range of possible interactions between abiotic and biotic factors, which need to be considered in order to gain a full understanding of likely climate change effects on productivity. It is generally considered that most of these interactions are likely to have an overall negative impact on plantation productivity. The work reported here could address only the direct physiological effects of climate change on forest productivity, but it would be highly desirable to probe in greater depth into the possible interactions between forest productivity and various stresses in order to get a fuller appreciation of the totality of possible climate change impacts.

These forest productivity surfaces can help forestry to be both fully integrated within land-use decisions and widely used in adapting to and reducing the impacts of climate change. As with exotic forests, the production of a productivity surface for indigenous species will reduce landowner uncertainty and encourage Afforestation/Reforestation (A/R) activity coincident with co-benefits such as increased resilience of adjacent agricultural land to extreme weather events (PCE 2002) in the form of erosion control, improved water quality, and enhanced biodiversity.

6 Acknowledgements

We would like to thank Gerard Horgan, Robert Holdaway and Ian Payton for many useful comments and suggestions on this report.

7 References

Allen LH 1990. Plant responses to rising carbon dioxide and potential interactions with air pollutants. Journal of Environmental Quality 19: 15–34.

Arneth A, Kelliher FM, McSeveny TM, Byers JN 1998a. Assessment of annual carbon exchange in a water-stressed *Pinus radiata* plantation: an analysis based on eddy covariance measurements and an integrated biophysical model. Global Change Biology 5: 531–545.

Arneth A, Kelliher FM, McSeveny TM, Byers JN 1998b. Fluxes of carbon and water in a *Pinus radiata* forest subject to soil water deficit. Australian Journal of Plant Physiology 25: 557–570.

Arneth A, Lloyd J, Santruckova H, Bird M, Grigoryev S, Kalaschnikov YN, Gleixner G, Schulze ED 2002. Response of central Siberian Scots pine to soil water deficit and long-term trends in atmospheric CO_2 concentration. Global Biogeochemical Cycles 16: 1–13.

Arp WJ 1991. Effects of source-sink relations on photosynthetic acclimation to elevated CO_2. Plant Cell and Environment 14: 869–875.

Asshoff R, Zotz G, Körner C 2006. Growth and phenology of mature temperate forest trees in elevated CO_2. Global Change Biology 12: 848–861.

Baisden WT 2006. Agricultural and forest productivity for modelling policy scenarios: evaluating approaches for New Zealand greenhouse gas mitigation Journal of the Royal Society of New Zealand 36: 1–15.

Ball JT, Woodrow IE, Berry JA 1987. A model predicting stomatal conductance and its contribution to the control of photosynthesis under different environmental conditions. In: Biggins J ed. Progress in photosynthesis research. Dordrecht, The Netherlands, Martin-Nijhoff Publishers. Pp. 221–224.

Battaglia M, Bruce J, Brack C, Baker T 2009. Climate change and Australia's plantation estate: analysis of vulnerability and preliminary investigation of adaptation options. Report prepared for Forest and Wood Products Australia Ltd, Melbourne. 125 p.

Beets PN, Kimberley MO, McKinley RB 2007. Predicting wood density of *Pinus radiata* annual growth increments. New Zealand Journal of Forestry Science 37: 241–266.

Beets P, Peltzer D, Sutherland A, Trotter C, Mason N 2009. Chapter Four. Indigenous forest sinks and mitigation options. In: Carbon stocks and changes in New Zealand's soils and forests, and implications of post-2012 accounting options for land-based emissions offsets and mitigation opportunities. Landcare Research Report LC0708/174, prepared for the Ministry of Agriculture and Forestry, pp. 79-118.

Burnham KP, Anderson RS 2002. Model selection and multimodel inference: A practical information-theoretic approach. New York, Springer-Verlag.

Comins HN, McMurtrie RE 1993. Long-term biotic response of nutrient-limited forest ecosystems to CO_2-enrichment; equilibrium behaviour of integrated plant-soil models. Ecological Application 3: 666–681.

Coomes DA, Allen RB 2007. Effects of size, competition and altitude on tree growth. Journal of Ecology 95: 1084–1097.

Coomes DA, Allen RB, Scott NA, Goulding C, Beets P 2002. Designing systems to monitor carbon stocks in forests and shrublands. Forest Ecology and Management 164: 89–108.

Cure JD, Acock B 1986. Crop responses to carbon dioxide doubling: a literature survey. Agricultural and Forest Meteorology 38: 127–145..

Curtis PS, Wang X 1998. A meta analysis of elevated CO_2 effects on woody plant mass, form, and physiology. Oecologia 113: 299–313.

Dawson TE, Mambelli S, Plamboeck AH, Templer PH, Tu KP 2002. Stable isotopes in plant ecology. Annual Review of Ecology and Systematics 33: 507–559.

Delucia EH, Moore DJ, Norby RJ 2005. Contrasting responses of forest ecosystems to rising atmospheric CO_2: implications for the global C cycle. Global Biogeochemical Cycles 19: Article GB3006.

Drake BG 1992. A field study of the effects of elevated CO_2 on ecosystem processes in a Chesapeake Bay wetland. Australian Journal of Botany 40: 579–595.

Drake BG, Gonzalez-Meler MA, Long SP 1997. More efficient plants: a consequence of rising atmospheric CO_2? Annual Review of Plant Physiology and Plant Molecular Biology 48: 609–639.

Dungan RJ, Norton DA, Duncan RP 2001. Seed rain in successional vegetation, Port Hills Ecological District, New Zealand. New Zealand Journal of Botany 39: 115-124.

Duquesnay A, Breda N, Stievenard M, Dupouey JL 1998. Changes of tree-ring $\delta^{13}C$ and water-use efficiency of beech (*Fagus sylvatica* L.) in north-eastern France during the past century. Plant, Cell and Environment 21: 565–572.

Easdale TA, Kunstler G 2010. NZ Waitutu. Description of basic behaviours and species specific parameters for alluvial terraces. Version 1.

Elith J, Leathwick JR, Hastie T 2008. A working guide to boosted regression trees. Journal of Animal Ecology 77: 802–813.

Erice G, Irigoyen JJ, Pérez P, Martínez-Carrasco R, Sánchez-Díaz M 2006. Effect of elevated CO_2, temperature and drought on photosynthesis of nodulated alfalfa during a cutting regrowth cycle. Physiologia Plantarum 126: 458–468.

Farquhar GD, von Caemmerer S 1982. Modelling of photosynthetic response to environmental conditions. In Physiological Plant Ecology II. Water Relations and Carbon Assimilation, Encyclopedia of Plant Physiology, New Series Vol. 12B (Lange, O.L, Nobel, P.S., Osmond, C.B. and Ziegler, H., eds.) Springer-Verlag, Berlin, Heidelberg, New York, pp. 549-588.

Garcia RL, Long SP, Wall GW, Osborne CP, Kimball BA, Nie GY, Pinter PJ, Lamorte RL, Wechsung F 1998. Photosynthesis and conductance of spring-wheat leaves: field response to continuous free-air atmospheric CO_2 enrichment. Plant, Cell and Environment 21: 659–669.

Gunderson CA, Sholtis JD, Wullschleger SD, Tissue DT, Hanson PJ, Norby RJ 2002. Environmental and stomatal control of photosynthetic enhancement in the canopy of a sweetgum (*Liquidambar styraciflua* L.) plantation during 3 years of CO_2 enrichment. Plant, Cell and Environment 25: 379–393.

Gunderson, C.A. and Wullschleger, S.D. 1994. Photosynthetic acclimation in trees to rising atmospheric CO_2: a broader perspective. Photosynth. Res. 39: 369-388.

Hall GMJ, Hollinger DY 2000. Simulating New Zealand forest dynamics with a generalized temperate forest gap model. Ecological Applications 10: 115–130.

Hall GMJ, McGlone MS 2006. Potential forest cover of New Zealand as determined by an ecosystem process model. New Zealand Journal of Botany 44: 211-232.

Hall GMJ, Wiser SK, Allen RB, Beets PN, Goulding CJ 2001. Strategies to estimate national forest carbon stocks from inventory data: the 1990 New Zealand baseline. Global Change Biology 7: 389–403.

Hättenschwiler S, Miglietta F, Raschi A, Körner C 1997. Thirty years of *in situ* tree growth under elevated CO_2: a model for future forest responses? Global Change Biology 3: 436–471.

Hellmers H, Rook DA 1973. Air temperature and growth of *P. radiata* seedlings. New Zealand Journal of Forestry Science 3: 271–285.

Herrick JD, Thomas RB 2001. No photosynthetic down-regulation in sweetgum trees (*Liquidambar styraciflua* L.) after three years of CO_2 enrichment at the Duke FACE experiment. Plant, Cell and Environment 24: 53–64.

Hollinger DY 1990. Forestry and forest ecosystems. In: Climatic change – impacts on New Zealand. New Zealand Climate Change Programme. Wellington, Ministry for the Environment. 244 p.

Hurst JM, Richardson SJ, Wiser SK, Allen RB 2007. Growth, mortality and recruitment of New Zealand's indigenous timber species. Landcare Research Contract Report LC0708/19.

Hutchinson MF 2010. *ANUSPLIN*, http://cres.anu.edu.au/outputs/anusplin.php. {Last accessed in October 2010}.

Jackson DS, Gifford HH 1974. Environmental variables influencing the increment of radiata pine (1) Periodic volume increment. New Zealand Journal of Forestry Science 4(1): 3–26.

Jarvis PG, McNaughton KG 1986. Stomatal control of transpiration: scaling up from leaf to region. Advances in Ecological Research 15: 1– 49.

Keith H, Mackey BG, Lindenmayer DB 2009. Re-evaluation of forest biomass carbon stocks and lessons from the world's most carbon-dense forests. Proceedings of the National Academy of Sciences 106: 11635-11640.

Kimball BA 1983. Carbon dioxide and agricultural yield: an assemblage and analysis of 430 prior observations. Agronomy Journal 75: 779–788.

Kimberley MO, Beets PN 2007. National volume function for estimating total stem volume of *Pinus radiata* stands in New Zealand. New Zealand Journal of Forestry Science 37: 355–371.

Kirschbaum MUF 1999a. CenW, a forest growth model with linked carbon, energy, nutrient and water cycles. Ecological Modelling 118: 17–59.

Kirschbaum MUF 1999b. Modelling forest growth and carbon storage with increasing CO_2 and temperature. Tellus 51B: 871–888.

Kirschbaum MUF 1999c. The effect of climate change on forest growth in Australia. In: Howden SM, Gorman JT eds Impacts of global change on Australian temperate forests. Working Paper Series 99/08. Pp. 62–68.

Kirschbaum MUF 2000. Forest growth and species distributions in a changing climate. Tree Physiology 20: 309–322.

Kirschbaum MUF 2004. Direct and indirect climate-change effects on photosynthesis and transpiration. Plant Biology 6: 242–253.

Kirschbaum MUF 2005. A modeling analysis of the interactions between forest age and forest responsiveness to increasing CO_2 concentration. Tree Physiology 25: 953–963.

Kirschbaum MUF, Paul KI 2002. Modelling carbon and nitrogen dynamics in forest soils with a modified version of the CENTURY model. Soil Biology & Biochemistry 34: 341–354.

Kirschbaum MUF, Guo LB, Gifford RM 2008a. Observed and modelled soil carbon and nitrogen changes after planting a *Pinus radiata* stand onto former pasture. Soil Biology and Biochemistry 40: 247–257.

Kirschbaum MUF, Guo LB, Gifford RM 2008b. Soil-carbon changes after reforestation. Constraints on the carbon balance imposed by nitrogen dynamics. Forest Ecology and Management 255: 2990–3000.

Kirschbaum MUF, King DA Comins HN, McMurtrie RE, Medlyn BE, Keith H, Pongracic S, Murty D, Keith H, Raison RJ, Khanna PK, Sheriff DW 1994. Modelling forest response to increasing CO_2 concentration under nutrient-limited conditions. Plant, Cell and Environment 17: 1081–1099.

Kirschbaum MUF, Medlyn B, King DA, Pongracic S, Murty D, Keith H, Khanna PK, Snowdon P, Raison JR 1998. Modelling forest-growth response to increasing CO_2 concentration in relation to various factors affecting nutrient supply. Global Change Biology 4: 23–42.

Kirschbaum MUF, Simioni G, Medlyn BE, McMurtrie RE 2003. On the importance of including soil nutrient feed-back effects for predicting ecosystem carbon exchange. Functional Plant Biology 30: 223–237.

Körner C, Morgan J, Norby R 2007. CO_2 fertilization: when, where, how much? In: Canadell JG, Pataki DE, Pitelka LF eds Terrestrical ecosystems in a changing world. Berlin/Heidelberg, Springer Verlag. Pp. 9–21.

Kouwenberg LLR, McElwain JC, Kurschner WM, Wagner F, Beerling DJ, Mayle FE, Visscher H 2003. Stomatal frequency adjustment of four conifer species to historical changes in atmospheric CO_2. American Journal of Botany 90: 610–619.

Leathwick JR, Whitehead D 2001. Soil and atmospheric water deficits and the distribution of New Zealand's indigenous tree species. Functional Ecology 15: 233–242.

Leathwick JR, Wilson GH, Rutledge D, Wardle P, Morgan FJ, Johnston K, McLeod M, Kirkpatrick R 2003. Land environments of New Zealand. Auckland, David Bateman.

Long SP, Osborne CP, Humphries SW 1996. Photosynthesis, rising atmospheric carbon dioxide concentration and climate change. In: Breymeyer AI, Hall DO, Melillo JM, Ågren GI eds SCOPE 56 – Global change: effects on coniferous forests and grasslands. Chichester, John Wiley & Sons Ltd. Pp. 121–159.

Lucas R, Kirschbaum MUF 1999. Australia's forest carbon sink: threats and opportunities from climate change. In: Howden SM, Gorman JT eds Impacts of global change on Australian temperate forests. Working Paper Series, 99/08. Pp. 119–125.

Luo Y, Su B, Currie WS, Dukes JS, Finzi A, Hartwig U, Hungate B, McMurtrie RE, Oren R, Parton WJ, Pataki DE, Shaw MR, Zak DR, Field CB 2004. Progressive nitrogen limitation of ecosystem responses to rising atmospheric carbon dioxide. BioScience 54: 731–739.

Luxmoore RJ, Wullschleger SD, Hanson PJ 1993. Forest responses to CO_2 enrichment and climate warming. Water, Air, and Soil Pollution 70: 309–323.

Madgwick HAI 1994. *Pinus radiata* - Biomass, Form and Growth. Published by HAI Madgwick, Rotorua, 428 pp.

MAF 2010. National Exotic Forest Regional Yield Tables. http://www.maf.govt.nz/mafnet/publications/nefd/yield-tables.htm {last accessed in August 2010)

Magnani F, Consiglio L, Erhard M, Nole A, Ripullone F, Borghetti M 2004. Growth patterns and carbon balance of *Pinus radiata* and *Pseudotsuga menziesii* plantations under climate change scenarios in Italy. Forest Ecology and Management 202: 93–105.

Marshall JD, Monserud RA 1996. Homeostatic gas-exchange parameters inferred from $^{13}C/^{12}C$ in tree rings of conifers. Oecologia 105: 13–21.

Martin P, Rosenberg N, McKenney MS 1989. Sensitivity of evapotranspiration in a wheat field, a forest and a grassland to changes in climate and direct effects of carbon dioxide. Climatic Change 14: 117–151.

Mason, N.W.H., Carswell, F.E., Overton, J.M., Briggs, C.M. & Hall, G.M.J. (2010) Estimation of current and potential carbon stocks and potential Kyoto-compliant carbon gain on conservation land *Science for Conservation,* (In press**)**.

McKenney MS, Rosenberg NJ 1993. Sensitivity of some potential evapotranspiration estimation methods to climate change. Agricultural and Forest Meteorology 64: 81–110.

McMurtrie RE, Comins HN, Kirschbaum MUF, Wang Y-P 1992. Modifying existing forest growth models to take account of effects of elevated CO_2. Australian Journal of Botany 40: 657–677.

McMurtrie RE, Rook DA, Kelliher FM 1990. Modelling the yield of *Pinus radiata* on a site limited by water and nitrogen. Forest Ecology and Management 30: 381–413.

Medlyn BE, Barton CVM, Broadmeadow MSJ, Ceulemans R, De Angelis P, Forstreuter M, Freeman M, Jackson SB, Kellomäki S, Laitat E, Rey A, Roberntz P, Sigurdsson BD,

Strassemeyer J, Wang K, Curtis PS, Jarvis PG 2001. Stomatal conductance of forest species after long-term exposure to elevated CO_2 concentration: a synthesis. New Phytologist 149: 247–264.

MfE 2008. Climate change effects and impacts assessment: A guidance manual for local government in New Zealand. 2nd ed. Prepared by Mullan B, Wratt D, Dean S, Hollis M, Allan S, Williams T, Kenny G, MfE staff. Wellington, Ministry for the Environment. Report ME870. 167 p.

Monserud RA, Marshall JD 2001. Time-series analysis of $\delta^{13}C$ from tree rings. I. Time trends and autocorrelation. Tree Physiology 21: 1087–1102.

Monteith JL 1965. Evaporation and environment. Symposium of the Society of Experimental Biologists. 19: 205–234.

Morison JIL 1985. Sensitivity of stomata and water use efficiency to high CO_2. Plant, Cell and Environment 8: 467–474.

Nash JE, Sutcliffe JV 1970. River flow forecasting through conceptual models. 1. A discussion of principles. Journal of Hydrology 10: 282–290.

Nowak RS, Ellsworth DS, Smith SD 2004. Functional responses of plants to elevated atmospheric CO_2 – do photosynthetic and productivity data from FACE experiments support early predictions? New Phytologist 162: 253–280.

Norby RJ, Ledford J, Reilly CD, Miller NE, O'Neill EG 2004. Fine-root production dominates response of a deciduous forest to atmospheric CO_2 enrichment. Proceedings of the National Academy of Science 101: 9689–9693.

Pacala SW, Canham CD, Saponara J, Silander JA, Kobe RK, Ribbens E 1996. Forest models defined by field measurements: II. Estimation, error analysis and dynamics Ecological Monographs 66: 1–43.

Parton WJ, Schimel DS, Cole CV, Ojima DS, 1987. Analysis of factors controlling soil organic matter levels in Great Plains grasslands. Soil Science Society of America Journal 51: 1173–1179.

Payton IJ 2007. Forest carbon tables to determine carbon dioxide (CO_2) emissions resulting from the deforestation of pre-1990 indigenous forest land. *Landcare Research Contract Report: LC0708/052.*

Prentice IC, Farquhar GD, Fasham MJR, Goulden ML, Heimann M, Jaramillo VJ, Kheshgi HS, Le Quéré C, Scholes RJ, Wallace DWR 2001. The carbon cycle and atmospheric carbon dioxide. In: Houghton JT et al. eds Climate change 2001: the scientific basis. Contribution of Working Group I to the Third Assessment Report of the Intergovernmental Panel on Climate Change Cambridge UK and New York, Cambridge University Press, pp. 99–181.

Post WM, Pastor J 1996. Linkages: an individual-based forest ecosystem model. Climatic Change 34: 253–261.

Rahmstorf S, Cazenave A, Church JA, Hansen JE, Keeling RF, Parker DE ,Somerville RCJ 2007. Recent climate observations compared to projections. Science 316: 709.

Rastetter EB, Ågren GI, Shaver GR 1997. Responses of N-limited ecosystems to increased CO_2: a balanced-nutrition, coupled-element-cycles model. Ecological Applications 7: 444–460.

Rastetter EB, McKane RB, Shaver GR, Melillo JM 1992. Changes in C storage by terrestrial ecosystems: how C-N interactions restrict responses to CO_2 and temperature. Water, Air & Soil Pollution 64: 327–344.

Richardson B, Whitehead D, McCracken IJ 2002. Root-zone water storage and growth of *Pinus radiata* in the presence of a broom understorey. New Zealand Journal of Forestry Science 32: 208–220.

Rook DA, Whitehead D 1979. Temperature and growth of *Pinus radiata*. Proceedings of the Agronomy Society of New Zealand 9: 109–112.

Rook DA, Carson M J 1978. Temperature and irradiance and the total daily photosynthetic production of the crown of a *Pinus radiata* tree. Oecologia 36(3): 371–382.

Roxburgh SH, Barrett DJ, Berry SL, Carter JO, Davies ID, Gifford RM, Kirschbaum MUF, M^{c}Beth BP, Noble IR, Parton WG, Raupach MR, Roderick ML 2004. A critical overview of model estimates of net primary productivity for the Australian continent. Functional Plant Biology 31: 1043–1059.

Rundgren M, Björck S 2003. Late-glacial and early Holocene variations in atmospheric CO_2 concentration indicated by high-resolution stomatal index data. Earth and Planetary Science Letters 213: 191–204.

Ryan MG, Binkley D, Fownes JH 1997. Age-related decline in forest productivity: patterns and processes. Advances in Ecological Research 27: 213–262.

Sabaté S, Gracia CA, Sánchez A 2002. Likely effects of climate change on growth of *Quercus ilex*, *Pinus halepensis*, *Pinus pinaster*, *Pinus sylvestris* and *Fagus sylvatica* forests in the Mediterranean region. Forest Ecology and Management 162: 23–37.

Sands PJ, 1995. Modelling canopy production. II. From single-leaf photosynthesis parameters to daily canopy photosynthesis. Australian Journal of Plant Physiology 22, 603–614.

Schimel DS, PartonWJ, Kittel TGF, Ojima DS, Cole CV, 1990. Grassland biogeochemistry: Links to atmospheric processes. Climatic Change 17, 13–25.

Simioni G, Ritson P, McGrath J, Kirschbaum MUF, Copeland B, Dumbrell I 2008. Predicting wood production and carbon sequestration of *Pinus radiata* plantations in south-western Australia: application of a process-based model. Forest Ecology and Management 255: 901–912.

Simioni G, Ritson P, Kirschbaum MUF, McGrath J, Dumbrell I, Copeland B 2009. Predicting the carbon budget of tree plantations under climate change: the case study of *Pinus radiata* in south-western Australia. Tree Physiology 29: 1081–1093.

Soares P, Tomé M, Skovsgaard JP, Vanclay JK 1995. Evaluating a growth model for forest management using continuous forest inventory data. Forest Ecology & Management 71: 251–265.

SRES 2000. Special Report on Emissions Scenarios. A Special Report of Working Group III of the Intergovernmental Panel on Climate Change. Cambridge University Press, Cambridge, UK.

Tait A, 2008. Future projections of growing degree days and frost in New Zealand and some implications for grape growing. Weather and Climate 28: 17–36.

Tait A, Liley B 2009. Interpolation of daily solar radiation for New Zealand using a satellite-derived cloud cover surface. Weather and Climate 29: 70–88.

Tait A, Henderson R, Turner R, Zheng X 2006. Thin-plate smoothing spline interpolation of daily rainfall for New Zealand using a climatological rainfall surface. International Journal of Climatology 26: 2097–2115.

Thomas RB, Strain BR 1991. Root restriction as a factor in photosynthetic acclimation of cotton seedlings grown in elevated carbon dioxide. Plant Physiology 96: 627–634.

Thornthwaite CW 1948. An approach towards a rational classification of climate. Geographical Review 38: 55–94.

Tissue DT, Thomas RB, Strain BR 1993. Long-term effects of elevated CO_2 and nutrients on photosynthesis and Rubisco in loblolly pine seedlings. Plant, Cell and Environment 16: 859–865.

Tognetti R, Cherubini P, Innes JL 2000. Comparative stem growth rates of Mediterranean trees under background and naturally enhanced ambient CO_2 concentrations. New Phytologist 146: 59–74.

Turnbull MH, Tissue DT, Griffin KL, Rogers GND, Whitehead D 1998. Photosynthetic acclimation to long-term exposure to elevated CO_2 concentration in *Pinus radiata* D. Don. is related to age of needles. Plant, Cell and Environment 21: 1019–1028.

Urban O 2003. Physiological impacts of elevated CO_2 concentration ranging from molecular to whole plant responses. Photosynthetica 41: 9–20.

Wakelin S, Beets P (2009). Chapter Three. Exotic forest sinks and mitigation options. In: Carbon stocks and changes in New Zealand's soils and forests, and implications of post-2012 accounting options for land-based emissions offsets and mitigation opportunities. Landcare Research Report LC0708/174, prepared for the Ministry of Agriculture and Forestry, pp. 21-78.

Walker S, King N, Monks A, Williams S, Burrows L, Cieraad E, Meurk C, Overton JM, Price R, Smale M 2009. Secondary woody vegetation patterns in New Zealand's South Island dryland zone. New Zealand Journal of Botany 47: 367-393.

Watt MS, Whitehead D, Richardson B, Mason EG, Leckie AC 2003. Modelling the influence of weed competition on the growth of young *Pinus radiata* at a dryland site. Forest Ecology and Management 178: 271–286.

Watt MS, Kimberley MO, Coker G, Richardson B, Estcourt G 2007. Modelling the influence of weed competition on growth of young *Pinus radiata*. Development and parameterization of a hybrid model across an environmental gradient. Canadian Journal of Forest Research 37: 607–616.

Watt MS, Kirschbaum MUF, Paul TSH , Tait A, Pearce HG, Brockerhoff EG, Moore JR, Bulman LS, Kriticos DJ 2008. The effect of climate change on New Zealand's planted forests. Impacts, risks and opportunities. Client Report CC MAF POL-2008-07 (106-1) prepared for the Ministry of Agriculture and Forestry, 149 pp.

Watt MS, Palmer DJ, Kimberley MO, Höck BK, Payn TW, Lowe DJ 2010. Development of models to predict *Pinus radiata* productivity throughout New Zealand. Canadian Journal of Forest Research 40: 488–499.

Whitehead D, Leathwick JR, Walcroft AS 2001. Modeling annual carbon uptake for the indigenous forests of New Zealand. Forest Science 47: 9–20.

Whitehead D, Kelliher FM, Frampton CM, Godfrey MJS 1994. Seasonal development of leaf area in a young, widely-spaced *Pinus radiata* D. Don stand. Tree Physiology 14: 1019–1038.

Wilde RH, Willoughby EJ, Hewitt AE 2000. Data manual for the national soils database spatial extension. Landcare Research New Zealand Ltd. Available online at: http://www.landcareresearch.co.nz/databases/nzlri.asp {Last accessed October 2010}

Wolfe DW, Gifford RM, Hilbert D, Luo YQ 1998. Integration of photosynthetic acclimation to CO_2 at the whole-plant level. Global Change Biology 4: 879–893.

Woodward FI 1987. Stomatal numbers are sensitive to increases in CO_2 from pre-industrial levels. Nature 327: 617–618.

Zotz G, Pepin S, Körner C 2005. No down-regulation of leaf photosynthesis in mature forest trees after three years if exposure to elevated CO_2. Plant Biology 7: 369–374.

Appendix 1 – Parameters for *Pinus radiata* simulations and other modelling details

The runs of CenW benefitted from previous work where the model had been parameterised for *P. radiata* stands in Australia. Hence, the parameterisation of the previous work of Kirschbaum (1999) and Kirschbaum et al. (2008a), which had also proved to be useful for the work of Simioni et al (2007, 2008) with *P. radiata* in Western Australia. However, each data set has some particularly strong emphasis on some aspects of model performance or another. The present data set consisted of few observations from each stand, but rather of observations from many stands across a wide range of environmental conditions. The challenges of that new data set required the development of a small number of new modelling routines, which are described in Appendix 2, and a revised parameterisation to obtain best description of the full present data set. The final parameter set is given in Table A1.

Table A1 *Main parameters used in the simulations of P. radiata*

Parameter description	***P. radiata***	**Units**
Minimum foliage turn-over	0.05	yr^{-1}
Fine-root turn-over	0.8	yr^{-1}
Branch turn-over	0.04	yr^{-1}
Bark turn-over	0.04	yr^{-1}
Low-light senescence limit	0.5	MJ m^{-2} d^{-1}
Max daily low-light senescence	0.0025	d^{-1}
Max drought foliage death rate	0.14	% d^{-1}
Mycorrhizal uptake	4.5	g kg^{-1} d^{-1}
Soil water stress threshold	0.4	-
Respiration ratio	0.37	-
Specific leaf area	5	m^2 $(kgDW)^{-1}$
Foliage albedo	7	%
Transmissivity	1	%
Loss as NMVOC	0.5	%
Threshold N concentrations (N_o)	10	gN $(kgDW)^{-1}$
Non-limiting N concentration (N_{sat})	15	gN $(kgDW)^{-1}$
Ball-Berry stomatal parameter (unstressed)	8.0	-
Ball-Berry stomatal parameter (stressed)	4.0	-
Foliage clumping - range decrease	0.42	-
Canopy width dependence on dbh (intercept)	0.75	-
Canopy width dependence on dbh (slope)	0.14	-
Age-based decline	None	
Temperature response (T_{min})	5.5	°C
Temperature response ($T_{opt, lower}$)	16.0	°C
Temperature response ($T_{opt, upper}$)	21.0	°C
Temperature response (T_{max})	40.0	°C
Temperature damage (Frost)	1.0	°C
Temperature damage (Scorch)	30.0	°C
Temperature damage (Sensitivity)	0.15	-
Temperature damage (Repair rate)	1.0	-
Heavy-rain damage (threshold)	60.0	mm d^{-1}
Heavy-rain damage (Sensitivity)	0.13	-
Heavy-rain damage (Repair rate)	0.75	-
Water-logging threshold	0.98	-
Water-logging sensitivity	1.0	-
Biological N fixation	None	

Table A1 (cont.) *Main parameters used in the simulations of P. radiata*

Parameter description	***P. radiata***	**Units**
Foliage: branch ratio	0.7	-
Stem: branch	3.6	-
Coarse roots: stem wood	0.2	-
Bark: stem wood	0.1	-
Allocation to seed and seed capsules	0.01	-
Allocation to pollen	0.01	-
Minimum wood allocation	0.1	-
Fine root: foliage ratio (nitrogen-unstressed)	0.35	-
Fine root: foliage ratio (nitrogen-stressed)	0.7	-
Stemwood : foliage [N] ratio	0.1	-
Bark : foliage [N] ratio	0.1	-
Branch : foliage [N] ratio	0.23	-
Fine root : foliage [N] ratio	0.45	-
Foliar lignin concentration	25	%
Root lignin concentration	25	%
Atmospheric N deposition	3.0	kgN ha^{-1} yr^{-1}
Volatilisation fraction	0.05	-
Leaching fraction	0.5	-
Litter water-holding capacity	0.75	g gDW^{-1}
Mulching effect of litter	5.0	% tDW^{-1}
Canopy aerodynamic resistance	15	s m^{-1}
Canopy rainfall interception	0.3	mm LAI^{-1}
Organic matter transfer in the soil for top three layers, decreasing with depth	5, 3, 1	% cm^{-1} yr^{-1}
Organic matter transfer from surface to soil	20	% yr^{-1}
Critical C:N ratio	7.5	
Decomposition rate adjustment	1.0	
Ratio of C:N ratios in structural and metabolic pools	5	
Exponential term in lignin inhibition	3	
Residual decomposition under dry conditions	0.1	
Mineral N immobilised	10	% d^{-1}

Table A1 (cont.) *Main parameters used in the simulations of P. radiata*

Parameter description	***P. radiata***	**Units**
Foliage: branch ratio	0.7	-
Stem: branch	3.6	-
Coarse roots: stem wood	0.2	-
Bark: stem wood	0.1	-
Allocation to seed and seed capsules	0.01	-
Allocation to pollen	0.01	-
Minimum wood allocation	0.1	-
Fine root: foliage ratio (nitrogen-unstressed)	0.35	-
Fine root: foliage ratio (nitrogen-stressed)	0.7	-
Stemwood : foliage [N] ratio	0.1	-
Bark : foliage [N] ratio	0.1	-
Branch : foliage [N] ratio	0.23	-
Fine root : foliage [N] ratio	0.45	-
Foliar lignin concentration	25	%
Root lignin concentration	25	%
Atmospheric N deposition	3.0	kgN ha^{-1} yr^{-1}
Volatilisation fraction	0.05	-
Leaching fraction	0.5	-
Litter water-holding capacity	0.75	g gDW^{-1}
Mulching effect of litter	5.0	% tDW^{-1}
Canopy aerodynamic resistance	15	s m^{-1}
Canopy rainfall interception	0.3	mm LAI^{-1}
Organic matter transfer in the soil for top three layers, decreasing with depth	5, 3, 1	% cm^{-1} yr^{-1}
Organic matter transfer from surface to soil	20	% yr^{-1}
Critical C:N ratio	7.5	
Decomposition rate adjustment	1.0	
Ratio of C:N ratios in structural and metabolic pools	5	
Exponential term in lignin inhibition	3	
Residual decomposition under dry conditions	0.1	
Mineral N immobilised	10	% d^{-1}

Standard silviculture used for generating productivity surfaces.

Initial planting: 1000 stems/ha
Thinning at age 5 to 500 stems/ha (removal of stands of average sized trees)
Thinning at age 8 to 300 stems/ha (removal of stands of average sized trees)
Clearfelling at age 30.

CO_2 concentrations

CO_2 concentrations were increased linearly throughout respective 30-year simulations whereas other environmental variables were held constant. This was done because the change in CO_2 concentration is relatively predictable and steady, whereas the small changes in other environmental variables are likely to be less than normal environmental variability over respective 30-year simulation periods. The actual concentrations and linear approximations were obtained from Prentice et al. (2001), based on simulations with the Bern model, and are shown in Table A1.1.

Table A1.1 *CO_2 concentrations used for simulations of current (1990) and future plant productivity.*

		CO_2 conc. (ppm)	Initial CO_2 concentration	Annual increase in CO_2 concentration
	1990	353	331	1.5
A1B	2040	483	426.8	3.75
A2		481	422.5	3.9
B1		457	419.5	2.5
A1B	2090	674	626	3.2
A2		754	638.5	7.7
B1		538	530.5	0.5

Appendix 2 – New modeling routines introduced into CenW.

For the present work, a number of new routines had to be introduced to better describe the environmental effects on a number of key stand properties. These are very briefly described in the following.

Wood density

Wood density varies with age and stand stocking. More importantly, in the present context, wood density can also vary significantly with environmental variables, especially temperature and soil fertility (Beets et al. 2007). Variation can be substantial, with wood density varying from 350 to 500 kgDW m^{-3} across a range of ages, stand stocking and temperatures (Beets et al. 2007). To be able to model stand volume increments across the range of environmental conditions in New Zealand and to follow stand growth with changing stocking and increasing age, it was necessary to explicitly account for those variables. The wood density model of Beets et al. (2007) was therefore essentially implemented in CenW.

Height–diameter relationships

As for wood density, the allometric relationships between tree height and diameter vary considerably across the range of environmental conditions in New Zealand. This could be seen in the range of height:diameter ratios in the data set (Figure 19), for example. To account for this variation, new algorithms were developed and implemented in CenW. These new routines and their derivation have been described in the scientific paper of Watt and Kirschbaum (in preparation). A copy of the draft paper is given in Appendix 3.

Weed module

Initial runs of the model indicated clearly that early growth of stands was consistently overestimated whereas later-age growth could be described more adequately. It was considered that a major reason for that pattern was related to weed competition during early growth (Watt et al. 2007), and it was therefore considered necessary explicitly to include a weed-competition module. The simplest workable form of that module was selected.

It allows for:

1. competition for light, with the relative competitiveness of weeds and *P. radiata* determined by their respective heights;
2. competition for nutrients, with their relative competitiveness determined by their relative fine-root abundance, but with introduction of an additional term that reduces the competitiveness of *P. radiata* based on stocking density and ameliorated by the development of a coarse-root network. Hence, at first, weeds are more competitive because they are assumed to be distributed as thousands of seedlings across the whole site whereas pine seedlings initially explore only a small proportion of the whole site, corresponding to the soil near the spots where they have been planted.
3. water use to be increased by the additional leaf area contributed by weed foliage. Hence, water stress is more likely during early development even when trees themselves would take up only a small amount of water.

Excess Water Limitation

It was apparent that *P. radiata* performs poorly under conditions of excess soil water or frequent and high rainfall (Figure 20). While the pattern is clearly evident from the growth data, its exact physiological cause is not readily apparent. This was dealt with by introducing two new photosynthetic limitations, one related to water logging and the other directly to the experience of heavy rainfall. Hence, maximum photosynthetic carbon gain, A_{max}, was calculated as:

$A_{max} = f(N_{lim}, W_{lim}, C_{lim}, T_{lim}, T_d, R_d)$

where N_{lim}, W_{lim}, C_{lim} and T_{lim} are limitations due to foliar nitrogen concentrations, water availability, CO_2 concentration and temperature, and T_d, R_d are additional damage functions due to frost or scorch damage (for T_d), and R_d is the new damage functions due to intense rainfall, calculated as:

$R_d = s_R * D_r$

where s_R is a sensitivity term describing the reduction in carbon gain per unit of rain damage and D_r are accumulated rain damage units, the change of which is calculated as:

$dD_r = (R - R_{lim}) - D_{repair}$ if $R > R_{lim}$

$dD_r = -D_{repair}$ if $R <= R_{lim}$

where R is daily rainfall, R_{lim} is a threshold below which heavy rainfall does not cause damage to plants and D_{repair} is a rate at which the damage can be repaired.

Water-logging is included as part of the calculations of water limitations. So, if the soil is not too dry, water limitation, W_{lim}, can instead be calculated as:

$W_{lim} = s_L * (S_w - L_{lim})$ if $S_w > L_{lim}$

where s_L is the water-stress sensitivity to water logging, S_w is the proportional amount of soil water (0..1) and L_{lim} is the limiting amount of soil water that determines the onset of water logging limitations.

Appendix 3 – Moving beyond simple linear allometric relationships between tree height and diameter

(Draft paper submitted to *Ecological Modelling*)

Michael S. Watt[a*] and Miko U. F. Kirschbaum[b]

[*a]Scion, PO Box 29237, Fendalton, Christchurch, New Zealand

[b]Landcare Research, Private Bag 11052, Palmerston North 4442, New Zealand

*Corresponding author.
E-mail address: michael.watt@scionresearch.com
Address for correspondence:
Michael S. Watt
Scion
PO Box 29237
Christchurch
New Zealand
Tel.:+64 3 364 2949; Fax: +64 3 364 2812

Running title: Allometric relationships in *Pinus radiata*

Abstract
Allometric relationships are used across a broad range of ecological disciplines as they provide a convenient means of scaling height (*H*) as a function of diameter (*D*). In these functions, it is commonly assumed that log transformed diameter and height are linearly related, with a constant slope across environmental gradients. It is also widely thought that the elastic similarity model, in which $H \propto D^{2/3}$, holds true for all tree species, as this is a functional relationship that describes mechanical stability under self weight. Despite the wide use of these functions, little research has undertaken a rigorous intra-species evaluation of the applicability of these functions or the underlying theory. Here, we evaluate the applicability of these models to measurements from *Pinus radiata* plots covering broad intra- and inter-stand environmental variation, and refine these models to make them more generally applicable.

Our results show that the slope between height and diameter ranges two-fold (0.73 − 1.43), which clearly violates the assumptions of both allometric relationships and the elastic similarity model. A large proportion of the variation in slope (R^2 = 0.72) was found to be explained by significant positive relationships with stand density, degree of topographical exposure, ratio of soil carbon to nitrogen, and air temperature. There was also a significant increase in *H*/*D* with increasing age. Addition of a slope sub-model and an age modifier into a standard allometric relationship significantly improved model fit to the data without unduly complicating the model form. We discuss implications of this research in the context of allometric scaling theory and offer an alternative theory that accounts for the observed results.

Key words: allometry; diameter; elastic similarity model; environmental impacts; height; stocking

1. Introduction

Allometric relationships are often used to describe height–diameter relationships in forest trees as they are convenient to use and allow determination of height over a wide size range. Using these functions, height, *H*, can be determined from,

$$\ln(H) = \beta + \alpha \ln(D) \quad (1)$$

where *D* is diameter at breast height and α and β are species-specific allometric constants.

While the parameters α and β can be considered empirical, they can also be linked into a theoretical framework related to the biophysical constraints on plant growth and function. The morphology of light-demanding conifers grown in even aged stands is largely determined by two countervailing pressures. Rapid height growth in competition with other trees is advantageous to access a greater share of solar radiation and maintain an upper canopy position. However, preferential carbon allocation to height at the expense of diameter is limited by hydraulic and mechanical considerations. The Euler Buckling equation (Greenhill, 1881) has been widely used to describe the critical height (H_{crit}) that a vertical tree stem can reach before it elastically buckles under its own weight as,

$$H_{crit} = C\left(\frac{E}{\rho}\right)^{1/3} D^{2/3} \quad (2)$$

where ρ is the density of green wood, *E* is modulus of elasticity (also known as Young's modulus), *D* is stem diameter and *C* is a constant of proportionality (Greenhill, 1881). The safety factor defines the margin by which critical height exceeds actual height, *H*, and is defined as, H_{crit}/H.

Assuming that density specific stiffness (E/ρ) and the safety factor remain constant with increases in diameter, Equation 2 predicts that scaling of plant height (*H*), will be proportional to the 2/3 power of stem diameter (i.e. $H \propto D^{2/3}$), which equates in the allometric relationship (Equation 1) to a value of 2/3 (0.66) for the slope parameter (α). This forms the basis for the elastic similarity model proposed by McMahon (1973) and McMahon and Kronauer (1976), and subsequently used to scale diameter with height in conifers and dicots (Dean and Long, 1986; Rich et al., 1986; Norberg, 1988; Bertram, 1989).

Despite the evident simplicity of allometric relationships, and the compelling theoretical foundation provided by the elastic similarity model, little research has tested the applicability of these functions for plantation-grown species across broad environmental gradients. Among plantation-grown species, *Pinus radiata* D. Don provides a useful case study as it is the most widespread plantation conifer within the Southern Hemisphere and has been the subject of considerable research. The utility of allometric relationships or the elastic similarity model has not been comprehensively examined for *P. radiata* grown under standard plantation conditions. However, wide inter- and intra-specific stand variation in *H*/*D* (Waghorn et al., 2007a; Watt and Zoric, in press) and E/ρ (Watt et al., 2006; Waghorn et al., 2007c; Watt et al., 2009), and increases in both of these properties with age (Lasserre et al., 2009; Watt and Zoric, in press) have been reported previously. These observations suggest that the underpinning assumptions of the elastic similarity model may not be valid. This variation in *H*/*D* also suggests that allometric relationships, with a constant slope between height and diameter, may not be applicable across a range of environmental and stand conditions.

Here we apply the allometric relationship to time series height-diameter measurements from *P. radiata* plots covering a wide range of environments, stand densities and plantation ages. We tested the accuracy of the allometric relationship and elastic similarity model in predicting height from diameter and the general applicability of these relationships across intra- and inter-stand environments. Using these data, we modified the traditional allometric relationship to a more sophisticated algorithm that is applicable to a more diverse set of stand conditions and ages, yet still retains a relatively simple structure. The form of the final model is compared with that of the elastic similarity model and we discuss implications of this research in the context of allometric scaling theory.

2. Methods and materials

2.1 Permanent sample plots used

A total of 84 permanent sample plots that covered a wide range (Table 1), including almost all the environments in which plantations are grown within New Zealand, were selected for the study (Fig. 1). These plots were predominantly established in forests managed under operational silvicultural regimes and as such represent the range in stand densities and dimensions typically found throughout plantations within New Zealand.

As two separate models were created (see section 2.4) the dataset was split into two groups comprising data with diameter < 10 cm and diameter ≥ 10 cm. For trees with diameter < 10 no modifications were made to the data. For the trees with diameter ≥ 10 only plot data with at least four sequential measurements at a relatively constant stand density were included so that intra-plot relationships between height and diameter at the plot level could be accurately determined (see section 2.4 model description). After these data were screened there was one set of time series data at a constant stand density for each of the 84 plots. For the retained plots there were on average nine repeated measurements (range = four to 16), spaced on average two years apart (range one – six years). Within these plots the age at which measurements were taken ranged from 5 to 32 years after planting, while stand density ranged from 103 to 913 stems ha^{-1}. Although there was a general decline in stand density with increasing age the relationship between these two variables was insignificant and relatively weak ($R^2 = 0.11$).

2.2 Measurements

For each plot, forty soil cores were taken from the upper 50 mm of mineral soil following canopy closure. These samples were bulked to provide a single soil sample for each plot. Soil samples were air-dried and passed through a 2-mm sieve, then weighed and analysed. Carbon and nitrogen were analysed on a LECO CNS-2000 (LECO, Michigan, US).

From the coordinates of each of these permanent sample plots, data were extracted from biophysical GIS surfaces that described meteorological data and topographical exposure (described below). Meteorological data used in analyses were obtained from thin-plate spline surfaces (Hutchinson and Gessler, 1994) fitted to meteorological station data (Leathwick and Stephens, 1998), at a spatial resolution of 100 m^2. Average monthly and annual values were extracted from these climate raster surfaces for windspeed, solar radiation, total rainfall, mean, minimum, maximum air temperature and vapour pressure deficit.

From these surfaces, mean maximum spring temperature ($T_{spr\ max}$) and topographical exposure (topex) were found to be important determinants of H/D (see model description). As previously described (Hannah et al., 1995), topex was determined using GIS from digital terrain maps as the sum of measured angles from the point of reference (plot centre) to a

distance of 1 km over the eight major compass bearings (N, NE, E, etc.). Topex has been found previously to be an accurate predictor of windspeed (Hannah et al., 1995) as declinations (negative values), values of 0 and inclinations (positive values) respectively distinguish exposed hilltops, flat areas and sheltered gullies.

2.3 Model diagnostics and analysis

A range of diagnostic tests were undertaken on the developed models (see section 2.4 for model description). Model comparisons were made using the coefficient of determination (R^2). Model gains in precision were determined using an *F*-test, with the significance tested for each improved model against the residual sum of squares for the simpler model. Residuals were plotted against independent variables and predicted values to determine model bias for all developed models. The Shapiro-Wilk test was used to determine if residuals for the final model were normally distributed, with values over $P = 0.05$ supporting the null hypothesis that the residuals were from a normal distribution (Hatcher and Stepanski, 1994). To ensure tests of significance were not subject to temporal autocorrelation the R^2 and significance tests were determined from a randomly selected subset of the data that included one observation per plot. All model coefficients were determined from the full dataset.

Following Niklas et al. (1994), reduced major axis (RMA) regression analyses were used to re-estimate slope, α_{RMA}, so that values found here could be directly compared with those predicted from the elastic similarity model. Using this method α_{RMA} was determined from α/r where α and r are, respectively, slope and the correlation coefficient determined under the ordinary least squares method used here. Unless otherwise stated, all values of α refer to that determined under ordinary least squares.

2.4 Model description

All modelling was undertaken using SAS (SAS-Institute-Inc., 2000). Examination of the data showed that for small trees with diameter < 10 cm, there was a strong linear relationship between height and diameter (Fig. 2). Consequently, the relationship over this range was modelled using Equation 3 with the following parameters for α and β,

$$\ln(H) = 0.600 + 0.511 \ln(D) \quad (3)$$

Equation 3 accounted for 91% of the variance in the data (Fig. 2). Although trees with diameter < 10 cm data covered a wide range in environmental conditions, stand density (350–1890 stems ha^{-1}) residuals were normally distributed and exhibited little correlation with either predicted values, stand density or a wide range of environmental variables (data not shown).

For trees with $D \geq 10$ cm, the relationship between diameter and height was relatively linear, with some curvature at greater diameters (Fig. 2). A linear model of the following form was fitted to the data:

$$\ln(H) = 1.79 + \alpha_2 \ln(D - 2.30) \quad (4)$$

Through subtracting 2.30 (log transformed value of 10 cm) from diameter, and setting the *y*-axis intercept to 1.79 (predicted value of height at 10 cm from equation 3) predictions of height below and above 10 cm were linked. This base model (Model 1) had a fitted slope (α_2) of 1.00 (Table 2) and accounted for 77% of the variance in the data (Fig. 2; Table 2).

Examination of plots of residuals against both stand density and environmental variables indicated some bias in Model 1 (data not shown). We therefore re-formulated the model by developing a sub-model of slope (α_2) that was a function of both stand density and environmental variables. Plot-level values of slope for this model were estimated by fitting Equation 4 to the multiple measurements of height and diameter over constant stand densities within each plot. This fitting procedure yielded a total of 84 plot-level observations of slope (one value per plot), covering a range of stand densities (109–913 stems ha^{-1}), that were used to develop the slope sub-model.

Using these plot level values, a multiple regression model of slope was developed using the general linear modelling procedure. Environmental variables and stand density were introduced sequentially into the model starting with the variable that exhibited the strongest correlation, until further additions were not significant. Variable selection was undertaken manually, one variable at a time, and plots of residuals were examined prior to variable addition to ensure that the next variable was included in the model used the least biased functional form. The final model of slope included stand density (S), mean maximum spring air temperature ($T_{spr.\ max}$), soil CN ratio and topex (X_t), combined in the following formulation,

$$\alpha_2 = 0.094 + 3.22 \times 10^{-4} S + 0.033 T_{spr.\ max} + 0.016 CN + 0.0012\ X_t \quad (5)$$

The final model with these variables accounted for 72% of the variance in slope, α_2 (Table 3). The variables stand density, $T_{spr\ max}$, CN ratio and topex all exhibited highly significant (P<0.001) positive linear relationships with slope and had respective partial R^2 values of 0.45, 0.10, 0.11 and 0.06 (Table 3). The variance inflation factor for all variables was less than 10, indicating that multi-collinearity was within acceptable limits (Der and Everitt, 2001). Residuals from this model were normally distributed (Shapiro-Wilk P = 0.59) and exhibited little apparent bias with either predicted values or any of the independent variables in the model. Residuals exhibited little apparent bias with any of the environmental variables that were not included in the model, and none of these variables would have significantly (P=0.05) improved the final model. Spring mean maximum temperature was a substantially better predictor that annual mean or annual mean maximum temperatures (data not shown).

Substitution of estimates of slope from Equation 5 into Equation 4, significantly improved Model 1 (P<0.001) and accounted for a further 61% of the remaining variance in the annual data, improving the R^2 by 0.14, from 0.77 to 0.91 (Table 2). Residuals from this revised model (Model 2) exhibited little apparent bias with independent variables. However, there was a positive relationship between residuals and stand age, a (data not shown). Inclusion of a in the model as a polynomial term in the following formulation was found to correct this bias:

$$\ln(H) = 1.79 + \alpha_2 \ln(D - 2.30) - 0.0105a + 6.22 \times 10^{-3} a^2 \quad (6)$$

Age was added directly into the allometric equation, rather than in the sub-model describing slope (Equation 5), as plot level estimates of slope typically covered a wide range in stand ages.

This final model formulation described in Equation 6 (Model 3) significantly improved (P<0.001) Model 2 (Equation 5), and predicted values of height from model 3 were strongly related to actual height (Fig. 3) accounting for 92% of the variance in the data (Table 2). Residuals from Model 3 were normally distributed (Shapiro Wilk P = 0.29) and found to exhibit little apparent bias with any independent variables in the model or predicted values (data not shown).

2.5 Sensitivity analyses for the final model

The effect of environmental variables and stand density on height was examined through partial response functions generated by the final model. Two sets of figures were generated. The first set of figures sequentially examined the effect of stand density, $T_{spr\ max}$, CN ratio and topex on *H*/*D* across the full range of each variable. In the generation of this response function, mean values in the dataset were used for diameter (34.1 cm), age (15.1 years) and the other three independent variables ($T_{spr\ max}$, CN ratio and topex) in the model (see Table 1 for mean values). In the second set of figures, height was predicted across the recorded range in diameter in the data, for mean, minimum and maximum values of the three environmental variables and stand density. This analysis was undertaken as it illustrates how variation in each variable influences height across the range in diameter. In this set of figures age was scaled as a function of diameter so that realistic values of height were obtained.

The influence of age on height was examined using partial response functions in a separate figure. Again, because of the co-variation of age and diameter, it was not appropriate to simply express the variation of height across the age range while keeping diameter constant at a mean value. Instead, to factor out the effect of diameter, variation in height across the range in age was determined for a series of constant diameters of 20, 30, 40 and 50 cm. For each diameter, the partial response function was generated over the observed age range in the data. All environmental variables and stand density were held constant at their average values for the dataset (see Table 1).

3. Results

3.1. Model comparisons

Our data covered a wide variation in tree height (range of 2 to 45 m), diameter (range of 1 to 65 cm), stand age (3–32.2) and stand densities (109–1890 stems ha^{-1}). Stems with diameters of less than 10 cm clearly had a lower slope than those greater than 10 cm (Figure 2) and allometry across this diameter range was not sensitive to environment or stand density.

Of the trees with diameters greater than 10 cm, a simple linear allometric relationship accounted for 77% of variation (Table 2). This slope for this relationship of 1.0 clearly exceeded 0.66, as predicted by the elastic similarity model (Fig. 2), using ordinary least squares. Under reduced major axis regression the slope was even higher at 1.14 (α_{RMA} = 1.00/0.88). Substantial gains in model accuracy, to an R^2 of 0.91 were obtained through expressing plot level slope (which ranged widely from 0.73 to 1.43) as a function of the four key controlling variables, spring mean maximum air temperature, soil C:N ratio, topographic exposure and stand density (Table 3). A further small but significant improvement was obtained through explicitly including stand age in the calculation of height (Table 2). This final model accounted for 92% of the variance in height, and was relatively unbiased with respect to predicted values (Fig. 3).

3.2 Partial response functions

Partial response functions show predicted *H*/*D* increased relatively linearly with all variables controlling slope and was most sensitive to stand density (Fig. 4a) and C: N ratio (Fig. 4c). Plots of height against diameter show a similar degree of sensitivity between independent variables. At an average diameter of 34 cm, predictions of height ranged by 9.8 m or 54% across the C:N range in the data (Fig. 5c). As environmental and stand factors appeared to have no influence on the height-diameter relationship in very young trees of up to 10 cm

diameter (Fig. 2), the effect of the identified controlling variables became increasingly important as diameter increased beyond 10 cm. For the C:N ratio, these increases ranged from no effect at diameter of 10 cm to 70% at diameter of 45cm (Fig. 5c), which was the largest diameter at which the complete range in C:N ratio was represented in the data. At an average diameter, ranges in predicted height for stand density, $T_{spr,\ max}$ and topex were, respectively, 37% (7.0 m), 29% (5.3 m), and 22% (4.2m) (Figs. 5a, b, d). At the maximum diameter at which the complete range in each variable was present in the data, variation in height for stand density, T_{max} and topex, reached respective ranges of 39% (7.2 m), 38% (9.4 m) and 23% (4.6 m) (Figs. 5a, b, d, respectively).

Similarly, the effect of age on height was most marked for older trees (Fig. 6). There was little effect of age on height up to 12 years, after which there was an exponential increase in height with increasing age (Fig. 6). This was most evident for larger values of diameter. For a diameter of 50 cm, predicted height increased in response to the age values represented in the data from 30.6 m at 14 years to 42.9 m at 32.2 years (Fig. 6).

4. Discussion

Allometric relationships have been successfully used to describe height as a function of tree diameters across broad size ranges (Parresol, 1999; Zianis, 2008). Consequently, a large body of literature has been developed around the assumption that allometric equations are generalisable (Enquist, 2002). However, results presented here clearly show that the parameters in allometric relationships are not constant but can vary significantly with both stand and environmental conditions. We found a two-fold variation in the slope parameter (0.73 − 1.43) between plots that was largely attributable to both intra- and inter-specific stand variation in stand density and environmental conditions. Results also suggest that even when allometric relationships are confined to a single site, the assumption of linearity between height and diameter may be invalid, as even for a constant diameter and values of other variables, height can vary considerably with tree age. This was confirmed by a large number of plots within our dataset that showed a distinct upward curvature in the relationship between height and diameter with increasing stand age. It is also in apparent in the upward curvature in the overall data set (Fig. 2).

It has long been recognised that *H*/*D* increases markedly with stand density in a wide range of plantation-grown pine and spruce species (for review see Sjolte-Jorgansen (1967)). For example, measurements taken from a 17-year-old *P. radiata* stand density trial show a two-fold increase in *H*/*D* (0.46 m cm^{-1} to 1.03 cm m^{-1}) over a range of 209 to 2,551 stems ha^{-1} (Waghorn et al., 2007c). This wide-reported intra-stand variation in *H*/*D* for plantation-grown *Pinaceae* species provides empirical confirmation that allometric equations with a single value for slope are not an adequate description of allometry.

As topex has been previously found to be strongly negatively related to mean wind speed (Hannah et al., 1995; Ruel et al., 1998), the inclusion of topex in our model of allometry most likely reflects the impact of wind on tree morphology (i.e. low topex is associated with high wind speed). This result is consistent with reported observations that show wind to have a significant effect on both tree morphology and biomechanical properties. Reported morphological effects of wind drag are increased stem radial growth, particularly in the direction of the constant force and reduced height extension (Jacobs, 1954; Telewski and Jaffe, 1986b; a; Telewski, 1989), resulting in reductions in *H*/*D*. Wind-induced alterations to stem biomechanical properties include increases in microfibril angle, second moment of cross-sectional area and quantity of reaction wood and reductions in the modulus of elasticity (Nicholls, 1982; Telewski and Jaffe, 1986b; Pruyn et al., 2000). These responses are thought to be developmental adaptations that reduce bending stresses acting on the stem

by increasing the second moment of cross-sectional area and reducing the speed specific drag of the crown (Petty and Swain, 1985; Telewski and Jaffe, 1986b; Niklas, 1992).

The impact of wind speed on *H*/*D* described here may also partially account for the effects of stand density on *H*/*D*. Previous research has shown that high stand densities lower stem deflection through both reducing wind speed within the canopy (Raupach, 1992; Green et al., 1995) and damping stem oscillations through increasing the number of collisions with neighbours (Milne, 1991). This reduced lateral force and stem deflection allows trees to obtain a greater height for a given diameter (see later discussion). As indicated by previous research, increases in *H*/*D* with increasing stand density are also likely to be attributable to reductions in available radiation (Watt et al., 2009). Preferential allocation of carbon to height growth under low light is likely to be a survival mechanism in light demanding conifers to avoid overtopping by neighbouring trees.

Among the environmental variables found to significantly influence the slope of the logarithmic *H*/*D* relationship, CN ratio had the strongest influence. Previous research is consistent with our findings showing that *H*/*D* increases as site fertility declines (Snowdon and Benson, 1992; Bergh et al., 1999; Watt et al., 2009). The positive relationship found here between air temperature and *H*/*D* also agrees with previous findings and could be attributable to the increases in density-specific stiffness (*E*/ρ) that occur with increasing air temperature (Watt et al., 2006; Watt et al., 2009). Increases in modulus of elasticity provide greater stability under both self weight and external lateral forces allowing trees to obtain greater *H*/*D* (Lachenbruch et al., in press).

At a broader functional level, all the variables included in the final allometry model have been found previously to exhibit significant positive correlations with either *E* or *E*/ρ (Telewski and Jaffe, 1986b; Watt et al., 2006; Waghorn et al., 2007b; Lasserre et al., 2009; Watt et al., 2009). This provides strong supporting evidence for the developed model of stem allometry as increases in *H*/*D*, predicted by increases in all variables need to be accompanied by increases in the *E*/ρ and strength to provide stability under lateral force or self weight (Moore et al., in press). Previous detailed research in *P. radiata* confirms the strong positive relationship between *H*/*D* and both *E* and *E*/ρ (Watt et al., 2006; Waghorn et al., 2007c; Lasserre et al., 2009; Watt et al., 2009) but also shows that these increases in *E*/ρ are not sufficient to maintain constant safety margins, as predicted by Euler Buckling, within *P. radiata* (Watt et al., 2006).

The wide variation in scaling between height and diameter found here suggests that assumptions underpinning the elastic similarity model are incorrect. Perhaps the most limiting aspect of the elastic similarity model is that it is predicated on buckling under self-weight as the limiting process and does not consider the influence of lateral external loads, predominantly caused by wind. Lichteneegger (1999) showed mathematically that increases in tree height for a given diameter (*H*/*D*) are possible under lower external loads and in trees with higher strength, a property that is strongly and positively related to the modulus of elasticity (Niklas, 1992). This is supported by empirical observations (e.g., (Putz et al., 1983)) showing that trees that fail by stem fracture in wind storms have lower wood density, strength and modulus of elasticity than trees that are uprooted.

The wide environmental conditions under which stands are grown create a considerable range in lateral loads. Young stands at high stand densities growing in sheltered areas are likely to experience much lower lateral loads and self weight than older, exposed stands grown at low stand densities. If we assume that tree height is close to the value that can be supported for a given diameter without undue risk of stem breakage, then the variation in *H*/*D* found here may at least partially reflect variation in lateral loads. Increases in the modulus of elasticity provide a means of mitigating the effects of lateral loads and self weight

on tree stability, which accounts for higher values of *H*/*D* in older age stands or those growing in warm environments.

In conclusion, we investigated variation in the height–diameter relationship of *P. radiata* stands growing across New Zealand under a range of environmental conditions. Our individual observations were taken from stands covering a variety of ages, stand densities and growing conditions. This allowed us to refine existing allometric relationships and develop a new description that links *H*/*D* explicitly to key environmental drivers and stand properties. As the derived relationships are based on a large number of individual observations they are robust. The variables selected to describe *H*/*D* are also physiologically sound and consistent with theory on tree stability. Greater height growth in trees is of clear competitive advantage in allowing greater access to radiation for taller trees, but height growth is constrained by mechanical limitations. Our observations suggest that trees growing in more sheltered positions (i.e. denser stands or those less exposed in the landscape) or that have higher density-specific stiffness (i.e. older trees or trees experiencing warmer temperatures) can attain greater values of *H*/*D*.

Acknowledgements

This research was funded by Ministry of Agriculture and Forestry under contract No. SLMACC C09X0902. We are grateful to David Palmer for constructing Figure 1. We gratefully acknowledge and thank Carolyn Andersen for her assistance in obtaining permissions from the forestry companies involved and for the PSP data extraction. We are also indebted to numerous forestry companies and private owners for supporting this research.

References

Bergh, J., Linder, S., Lundmark, T. and Elfving, B., 1999. The effect of water and nutrient availability on the productivity of Norway spruce in northern and southern Sweden. Forest Ecology and Management, 119:51-62.

Bertram, J.E.A., 1989. Size-dependent differential scaling in branches: the mechanical design of trees revisited. Trees: Structure and Function, 3:241-253.

Dean, T.J. and Long, J.N., 1986. Validity of the constant-stress and elastic instability principles of stem formation in *Pinus contorta* and *Trifolium pratense*. Annals of Botany 58:833-840.

Der, G. and Everitt, B.S., 2001. A Handbook of Statistical Analyses Using SAS. Chapman and Hall, CRC, 360 pp.

Enquist, B.J., 2002. Universal scaling in tree and vascular plant allometry: Toward a general quantitative theory linking plant form and function from cells to ecosystems. Tree Physiology, 22:1045-1064.

Green, S.R., Grace, J. and Hutchings, N.J., 1995. Observation of turbulent air flow in three stands of widely spaced Sitka spruce. Agricultural and Forest Meteorology. 74:205-225.

Greenhill, A.G., 1881. Determination of the greatest height consistent with stability that a vertical pole or mast can be made, and of the greatest height to which a tree of given proportions can grow. Proceedings of the Cambridge Philosophical Society, 4:65-73.

Hannah, P., Palutikof, J.P. and Quine, C.P., 1995. Predicting windspeeds for forest areas in complex terrain. In: Coutts MP, Grace J (eds) Wind and trees. Cambridge University Press, Cambridge, pp 113-129.

Hatcher, L. and Stepanski, E.J., 1994. A step by step approach to using the SAS system for univariate and multivariate statistics. SAS Institute Inc., Cary, NC, 552 pp.

Hutchinson, M.F. and Gessler, P.E., 1994. Splines-more than just a smooth interpolator. Geoderma, 62:45-67.

Jacobs, M.R., 1954. The effect of wind sway on the form and development of *Pinus radiata* D. Don. Australian Journal of Botany, 2:35-51.

Lachenbruch, B., Moore, J.R. and Evans, R., in press. Radial changes in wood: The structure and function of juvenile vs. mature wood in woody plants.

Lasserre, J.P., Mason, E.G., Watt, M.S. and Moore, J.R., 2009. Influence of initial planting spacing and genotype on microfibril angle, basic density, fibre properties and modulus of elasticity in *Pinus radiata* D.Don corewood. Forest Ecology and Management, 258:1924-1931.

Leathwick, J.R. and Stephens, R.T.T., 1998. Climate surfaces for New Zealand. Landcare Res. Contract Report LC9798/126. Landcare Research, Lincoln, New Zealand 19 pp.

Lichtenegger, H., Reiterer, A., Stanzl-Tschegg, S.E. and Fratzl, P., 1999. Variation of cellulose microfibril angles in softwoods and hardwoods - a possible strategy of mechanical optimization. Journal of Structural Biology, 128:257-269.

McMahon, T.A., 1973. Size and shape in biology. Science, 179:1201-1204.

McMahon, T.A. and Kronauer, R.E., 1976. Tree structures: deducing the principle of mechanical design. Journal of Theoretical Biology 59:443-446.

Milne, R., 1991. Dynamics of swaying of *Picea sitchensis*. Tree Physiology, 9:383-399.

Nicholls, J.W.P., 1982. Wind action, leaning trees and compression wood in *Pinus radiata* D. Don. Australian Forest Research, 12:75-91.

Niklas, K., 1994. Plant Allometry – the scaling of form and process. University of Chicago Press. 395 pp.

Niklas, K.J., 1992. Plant biomechanics: an engineering approach to plant form and function. University of Chicago Press, Chicago.

Norberg, R.A., 1988. Theory of growth geometry of plants and self thinning of plant populations: geometric similarity, elastic similarity, and different growth modes of plant parts. American Naturalist 131:220-256.

Parresol, B.R., 1999. Assessing tree and stand biomass: A review with examples and critical comparisons. Forest Science, 45:573-593.

Petty, J.A. and Swain, C., 1985. Factors influencing stem breakage in conifers in high winds. Forestry, 58:75-84.

Pruyn, M.L., Ewers, B.J., III and Telewski, F.W., 2000. Thigmomorphogenesis: changes in the morphology and mechanical properties of two *Populus* hybrids in response to mechanical perturbation. Tree Physiology, 20:535-540.

Putz, F.E., Coley, P.D., Lu, K., Montalvo, A. and Aiello, A., 1983. Uprooting and snapping of trees, Structural determinants and ecological consequences. Canadian Journal of Forest Research, 13:1011-1020.

Raupach, M.R., 1992. Drag and drag partition on rough surfaces. Boundary-layer Meteorology, 60:375-395.

Rich, P.M., Helenurm, K., Kearns, D., Morse, S.R., Palmer, M.W. and Short, L., 1986. Height and stem diameter relationships for dicotyledonous trees and arborescent palms of Costa Rica tropical wet forest. Bulletin of the Torrey Botanical Club, 113:241-246.

Ruel, J.C., Pin, D. and Cooper, K., 1998. Effect of topography on wind behaviour in a complex terrain. Forestry (Oxford), 71:261-265.

SAS-Institute-Inc., 2000. SAS/STAT User's Guide: Version 8. Volumes 1, 2 and 3. SAS Institute Inc., Cary, North Carolina, 3884 pp.

Sjolte-Jorgensen, J., 1967. The influence of spacing on the growth and development of coniferous plantations. International Review of Forestry Research., 2:43-94.

Snowdon, P. and Benson, M.L., 1992. Effects of combinations of irrigation and fertilisation on the growth and above-ground biomass production of *Pinus radiata*. Forest Ecology and Management, 52:87-116.

Telewski, F.W., 1989. Structure and function of flexure wood in *Abies fraseri*. Tree Physiology, 5:113-121.

Telewski, F.W. and Jaffe, M.J., 1986a. Thigmomorphogenesis: anatomical, morphological and mechanical analysis of genetically different sibs of *Pinus taeda* in response to mechanical perturbation. Physiologia Plantarum. 66:219-226.

Telewski, F.W. and Jaffe, M.J., 1986b. Thigmomorphogenesis: field and laboratory studies of Abies fraseri in response to wind or mechanical perturbation. Physiologia Plantarum. 66:211-218.

Waghorn, M.J., Mason, E.G. and Watt, M.S., 2007a. Assessing interactions between initial stand stocking and genotype on growth and form of 17 year old *Pinus radiata* in Canterbury. New Zealand Journal of Forestry, 52:24-30.

Waghorn, M.J., Mason, E.G. and Watt, M.S., 2007b. Influence of initial stand density and genotype on longitudinal variation in modulus of elasticity for 17-year-old *Pinus radiata*. Forest Ecology and Management, 252:67-72.

Waghorn, M.J., Watt, M.S. and Mason, E.G., 2007c. Influence of tree morphology, genetics, and initial stand density on outerwood modulus of elasticity of 17-year-old *Pinus radiata*. Forest Ecology and Management 244:86-92.

Watt, M.S., Clinton, P.W., Parfitt, R.L., Ross, C. and Coker, G.W.R., 2009. Modelling the influence of site and weed competition on juvenile modulus of elasticity in *Pinus*

radiata across broad environmental gradients. Forest Ecology and Management, 258:1479-1488.

Watt, M.S., Moore, J.R., Facon, J.P., Downes, G.M., Clinton, P.W., Coker, G., Davis, M.R., Simcock, R., Parfitt, R.L., Dando, J., Mason, E.G. and Bown, H.E., 2006. Modelling environmental variation in Young's modulus for *Pinus radiata* and implications for determination of critical buckling height. Annals of Botany, 98:765-775.

Watt, M.S. and Zoric, B., in press. Development of a model describing modulus of elasticity across environmental and stand density gradients in plantation grown *Pinus radiata* within New Zealand. Canadian Journal of Forest Research.

Zianis, D., 2008. Predicting mean aboveground forest biomass and its associated variance. Forest Ecology and Management, 256:1400-1407.

Table 1. Variation in stand level data including variables used in the final model. Shown is the mean and standard deviation (in brackets) and range. The range in stocking is shown for trees with diameter ≥ 10 cm.

Variable	Mean	Range
Rainfall (mm yr^{-1})	1361 (432)	660 – 2124
Mean av. annual temp. (°C)	11.8 (2.4)	8.4 – 15.9
Mean min. annual temp. (°C)	7.1 (2.6)	3.3 – 12.1
Mean max. annual temp. (°C)	16.6 (2.1)	13.1 – 19.9
Mean max. spring temp. (°C)	16.3 (1.7)	12.8 – 19.1
Stand density (stems ha^{-1})	366 (186)	109 – 913
Topex (degrees)	3.1 (35)	67.5 – 72.2
CN ratio	17.4 (4.5)	10 – 32.2

Table 2. Model parameters and statistics for the models describing tree height. Shown under significance are F-values and P categories, with *** denoting significance at P = 0.001. Also shown are cumulative and partial (in brackets) R2 values. Models 1, 2: ln H = 1.79 + α2 ln(D − 2.30); Model 3: ln H = 1.79 + α2 ln (D − 2.30) + γ age + ε age2

Model No.	Model parameters			Model statistics	
	α_2	γ	ε	Significance	R^2
1	1.00			273***	0.77 (0.77)
2	*			105***	0.91 (0.14)
3	*	-0.011	6.37×10^{-3}	9.3***	0.92 (0.01)

*Equation form and values for slope (α_2) are given in Table 3.

Table 3. Model statistics for sub-model developed for the slope parameter (α_2) described by $\alpha_2 = \tau + \eta S + \kappa T_{spr\ max} + \lambda CN + \mu X_t$. Parameter values and variable partial R^2 and cumulative R^2 values (in brackets) are shown. For the significance category the *F* values and *P* categories from an *F*-test, are shown, with asterisks *** representing significance at $P < 0.001$. The variance inflation factor (VIF) is also shown.

Para.	Value	Variable	Units	R^2	Signif.	VIF
τ	0.094					
η	3.22×10^{-4}	Stocking (*S*)	stems ha^{-1}	0.45 (0.45)	5.7***	1.30
κ	0.033	Mean max. spring temp. ($T_{spr\ max}$)	°C	0.55 (0.10)	5.7***	1.19
λ	0.016	CN ratio (*CN*)		0.66 (0.11)	6.7***	1.39
μ	0.0012	Topex (X_t)	degrees	0.72 (0.06)	4.0***	1.28

Figure legends

Figure 1. New Zealand map showing location of the stands used in this study. Note that due to the very close proximity some plots are obscured on this figure.

Figure 2. Relationship between diameter and actual (symbols) and predicted (lines) height for trees with diameter (D) < 10 cm (filled circles; dashed line), and ≥ 10 cm (open circles solid line). Linear lines of best fit shown include ln (H) = 0.60 + 0.51 ln (D) for data with D < 10 cm and ln (H) = 1.79 + 1.00 ln (D − 2.3) for data with $D \geq 10$ cm. The dotted line shows separation of data into D < 10 cm and $D \geq 10$ cm.

Figure 3. Relationship between predicted and actual height for the final model. The1:1 line is shown as a solid line.

Figure 4. Partial response functions showing variation in predicted height/diameter as a function of (a) stand density, (b) mean maximum spring air temperature, $T_{\text{spr max}}$, (c) CN ratio and (d) topographical exposure, Topex. Figures a – d were generated at the mean diameter (34.1 cm) and the range for each variable in the dataset (see Table 1 for ranges).

Figure 5. Partial response functions showing model generated predicted height across the recorded range in diameters for minimum (thick solid line), mean (solid line) and maximum (dashed line) (a) stand density (b) mean maximum spring air temperature, $T_{\text{spr. max}}$, (c) CN ratio and (d) topographical exposure, topex (see Table 1 for ranges in these variables). Age, a, was scaled as a function of tree diameter, D, using a = 65.2 − 44.3 ln (D)+ 8.4 ln $(D)^2$ to ensure that age-diameter combinations remained within a realistic range. The dotted line shown on all graphs shows the mean diameter in the dataset (34.1 cm).

Figure 6. Partial response function showing the relationship between age and predicted tree height for a range of tree diameters, D. For each diameter the range in age over which the partial response function has been generated reflects the age range in the data, ±1 cm of the target diameter. These partial response functions were generated using mean values for stand density (34.1 cm) and all environmental variables (see Table 1 for values).

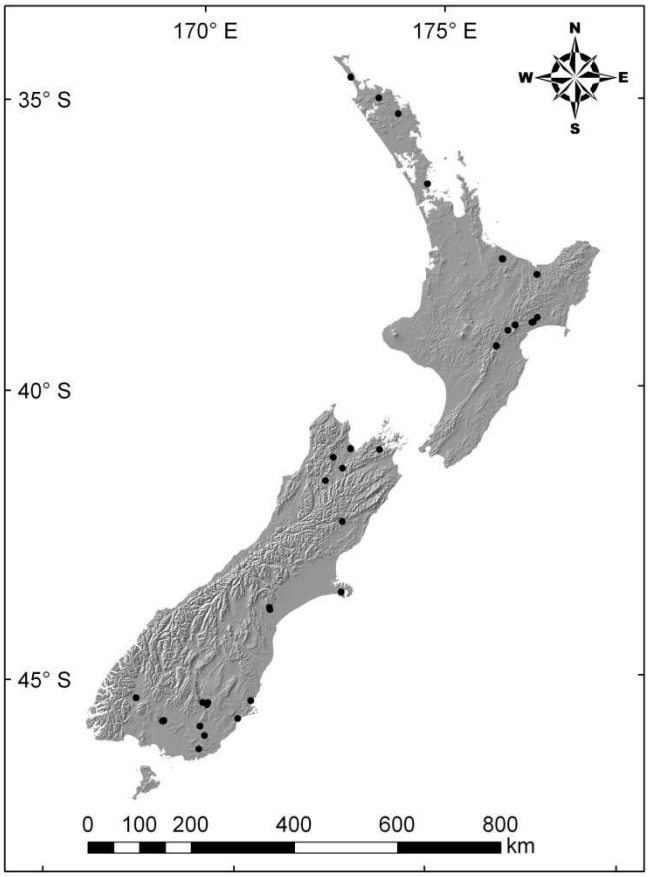

Figure 1

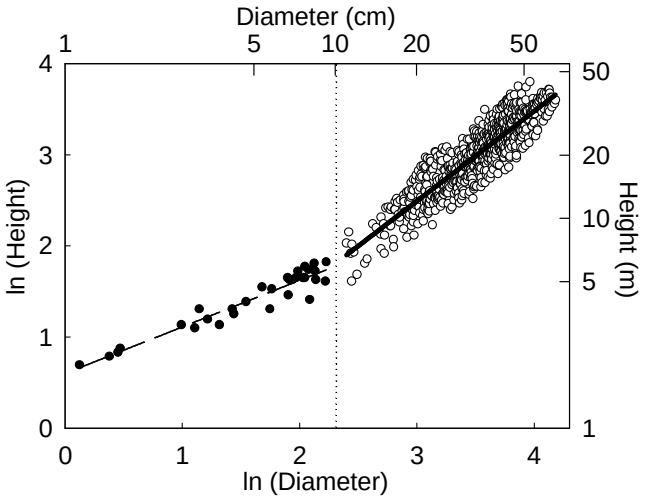

Figure 2

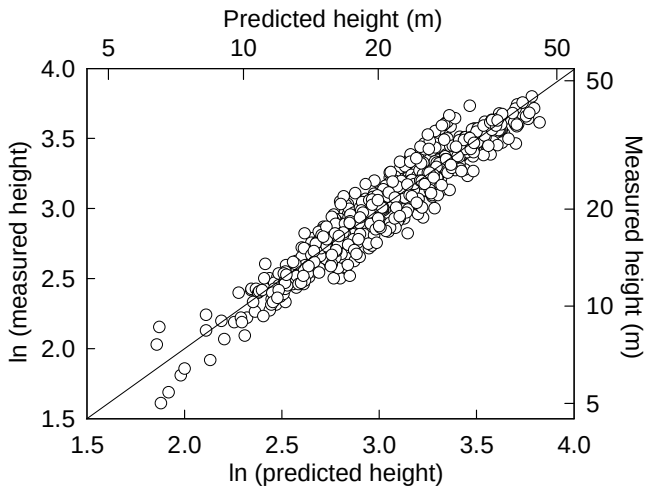

Figure 3

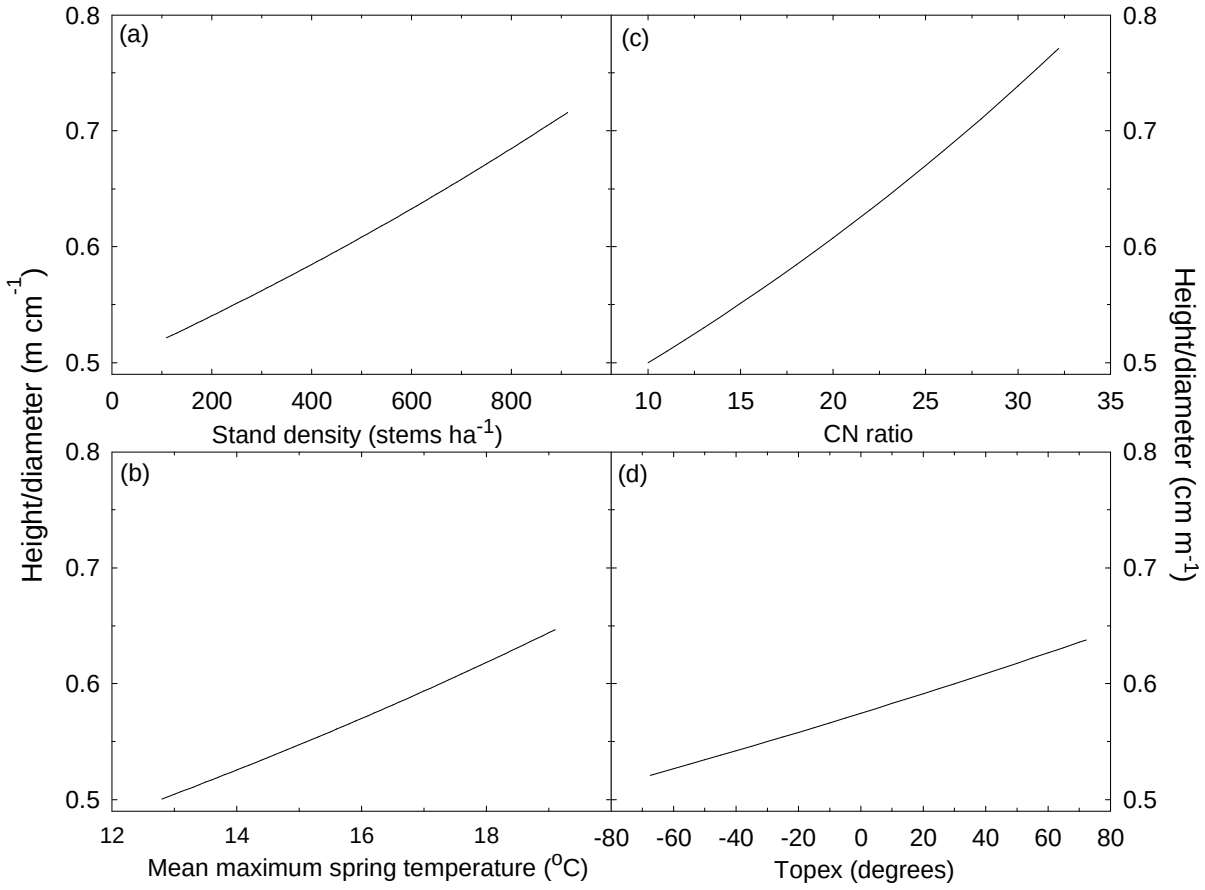

Figure 4

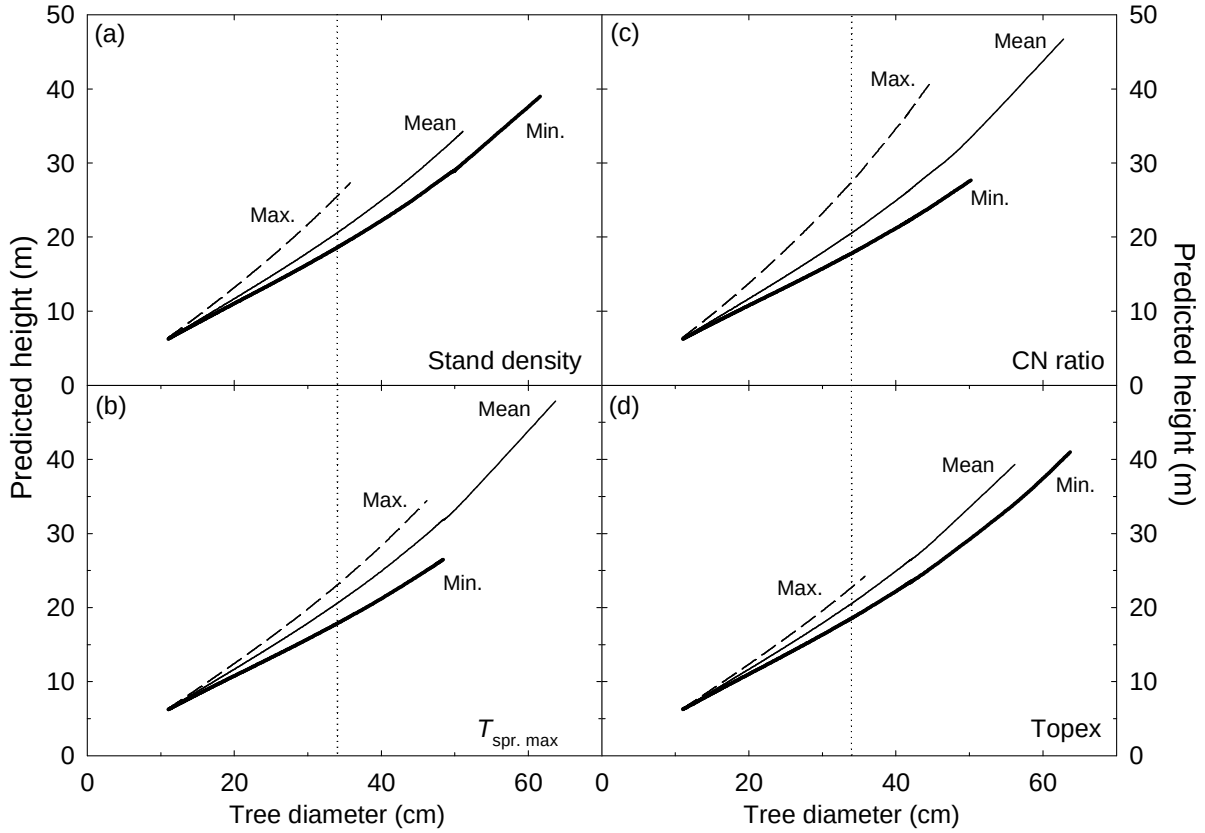

Figure 5

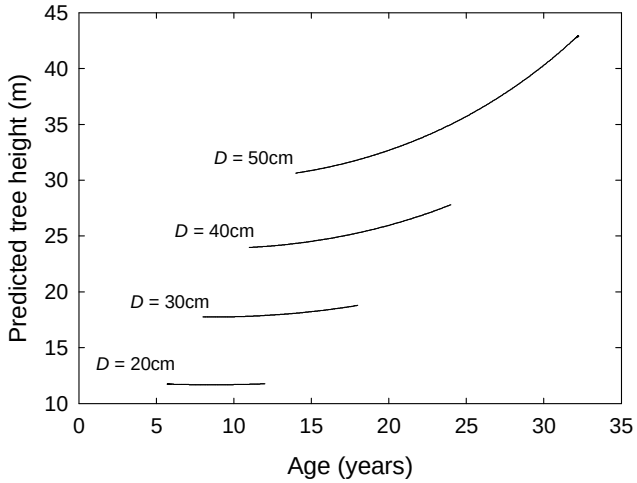

Figure 6

Appendix 4 – Some more details of model- data comparisons for the *Pinus radiata* model

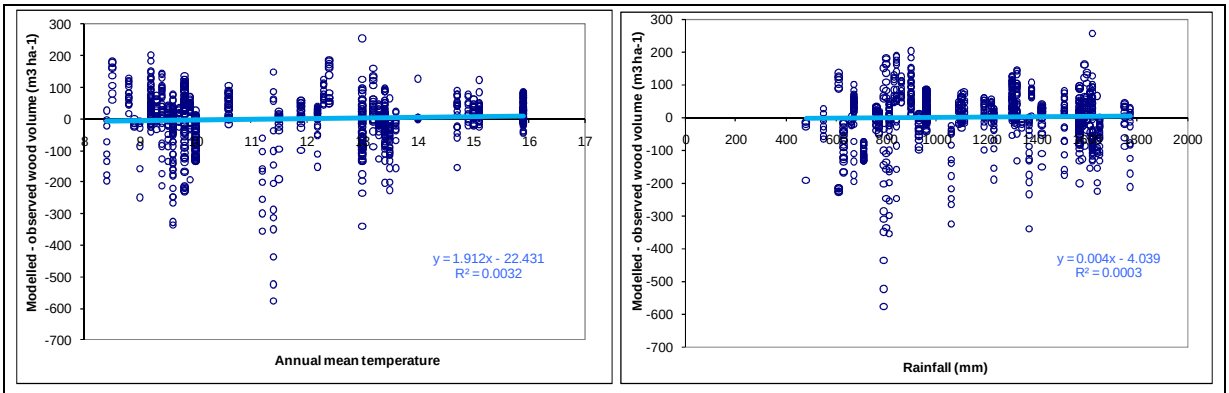

Fig A2.1 Residual values (modelled - observed) for stem volume plotted against annual mean air temperature and total annual rainfall. The blue lines are lines fitted to the data, showing that the effects of temperature and rainfall are fully accounted for in the model simulations.

There was no remaining bias in the plot of residuals against mean annual air temperature and total annual precipitation, the two key environmental drivers.

Appendix 5 – Further details of the modeling indigenous forest growth

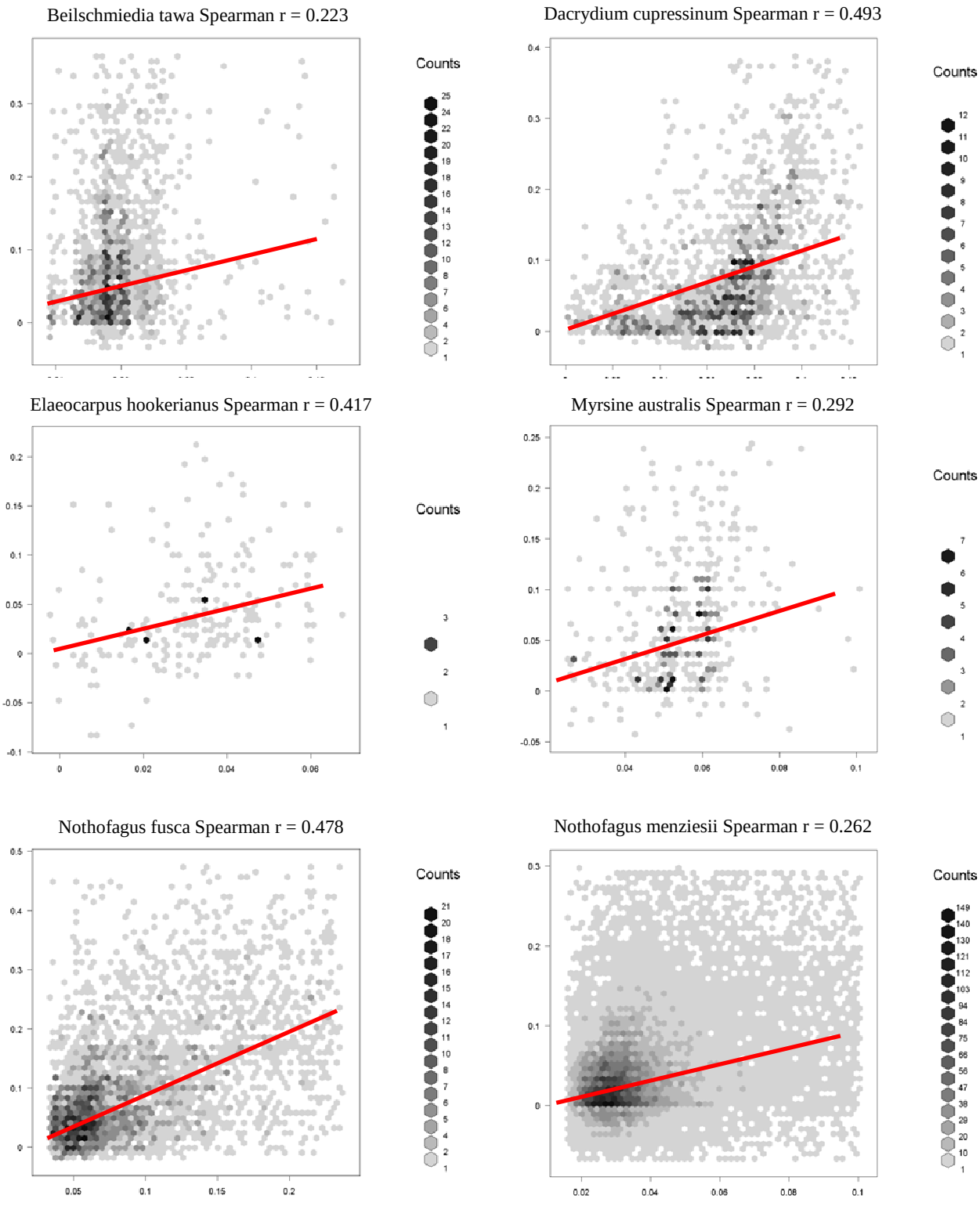

Figure A5.1. Observed and predicted annual growth in diameter (cm) clipped to 95% confidence intervals for both observed and predicted. Red lines indicate a 1:1 relationship between observed and predicted. To better reveal the distribution of individual stems in the plot, stems are grouped into hexagons. Darker hexagons contain more stems (in accordance with the legend for each plot).

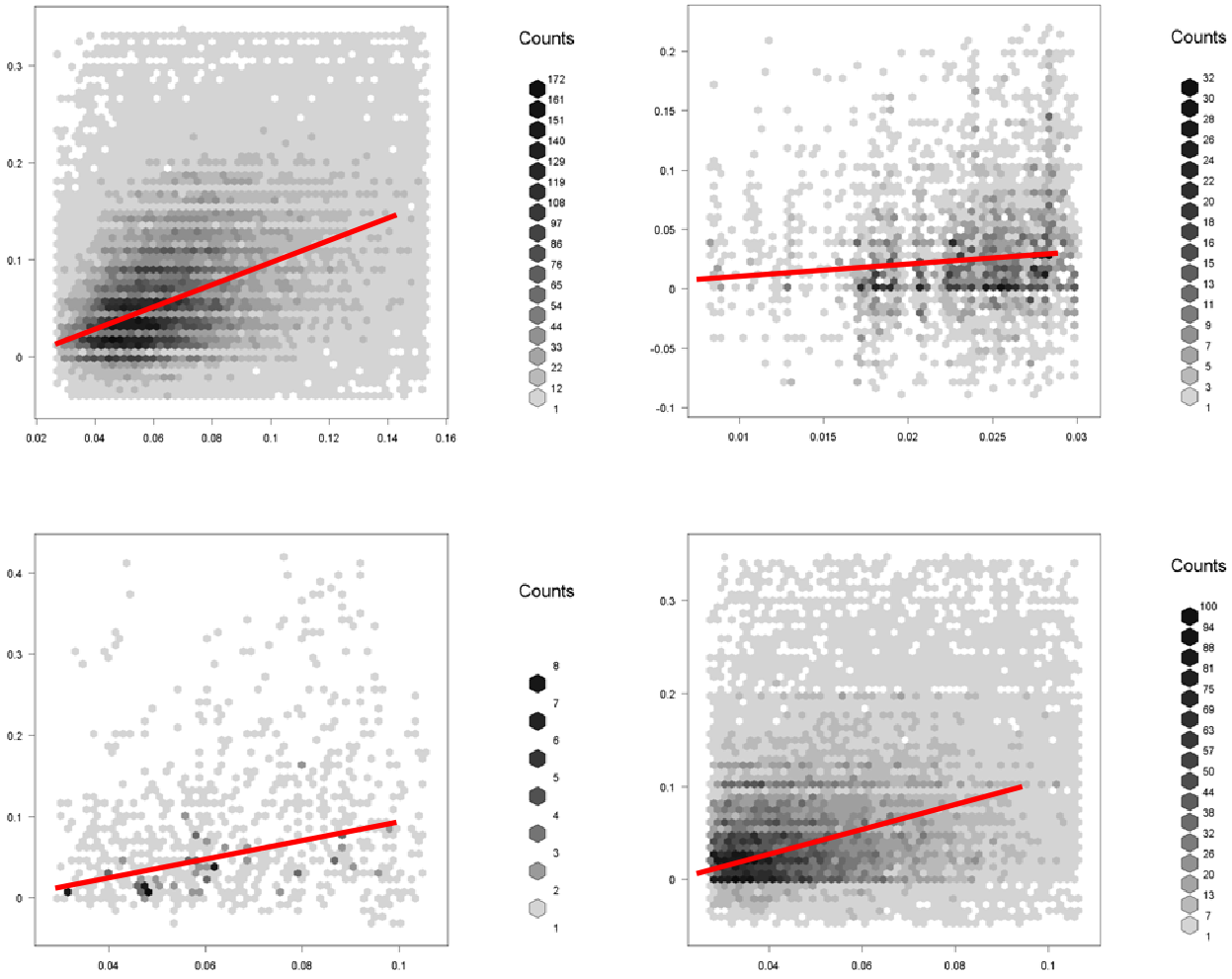

Figure A5.1 (cont.)

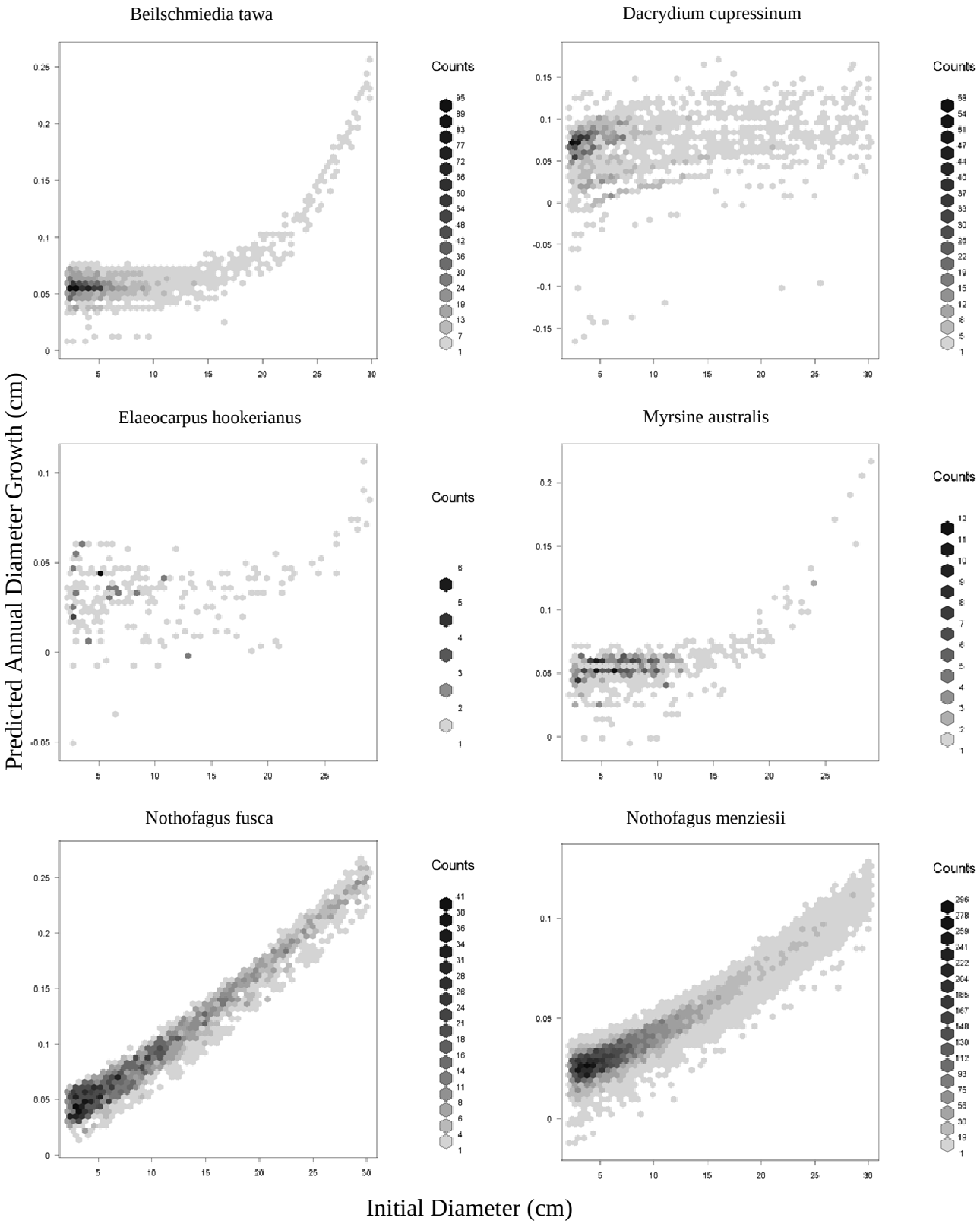

Figure A5.2 Predicted annual growth in diameter (cm) of individual stems against their initial diameter (cm) for selected species. A function, Growth = a +b(Diameter)^c + d(Basal Area) was fitted, with b and c constrained to be non-negative, and d constrained to be non-positive. Shading indicates density of stems within each hexagon according to the legend for each species.

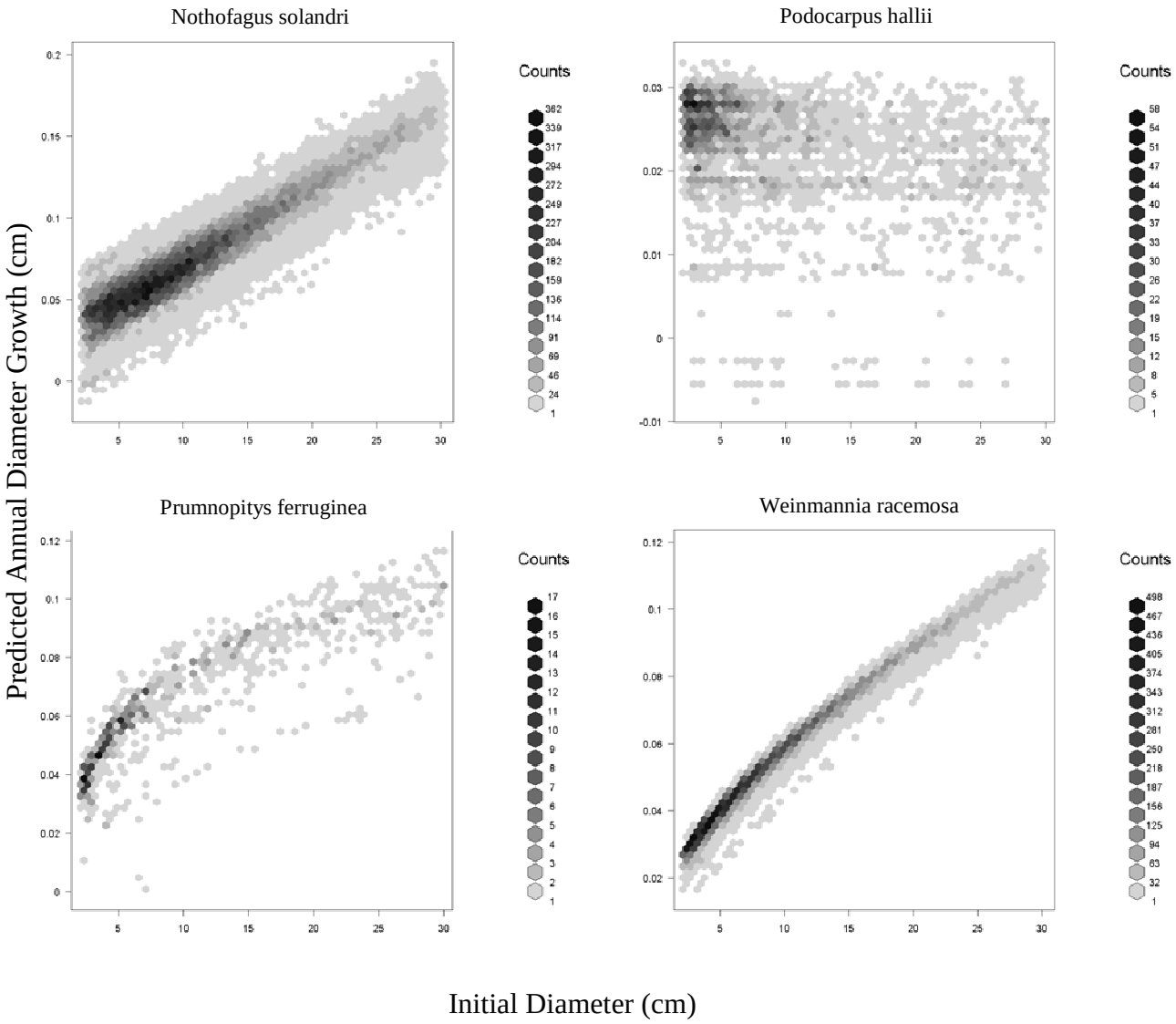

Figure A5.2 (cont.)

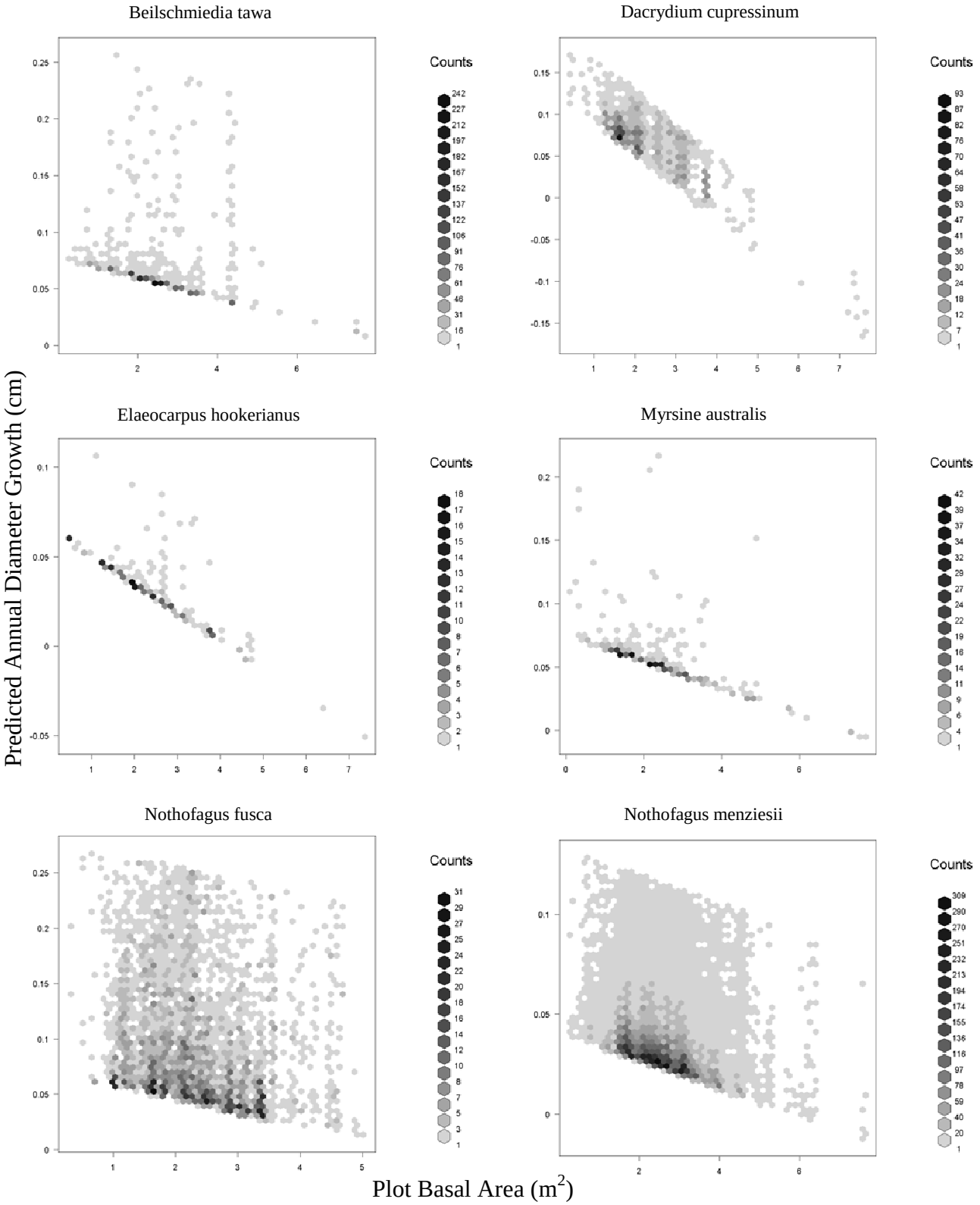

Figure A5.3 Predicted growth in diameter (cm) of individual stems against initial total basal area within 0.04ha plots in which they occurred. Predictions were obtained by fitting the model described in the legend of Figure A5.2.

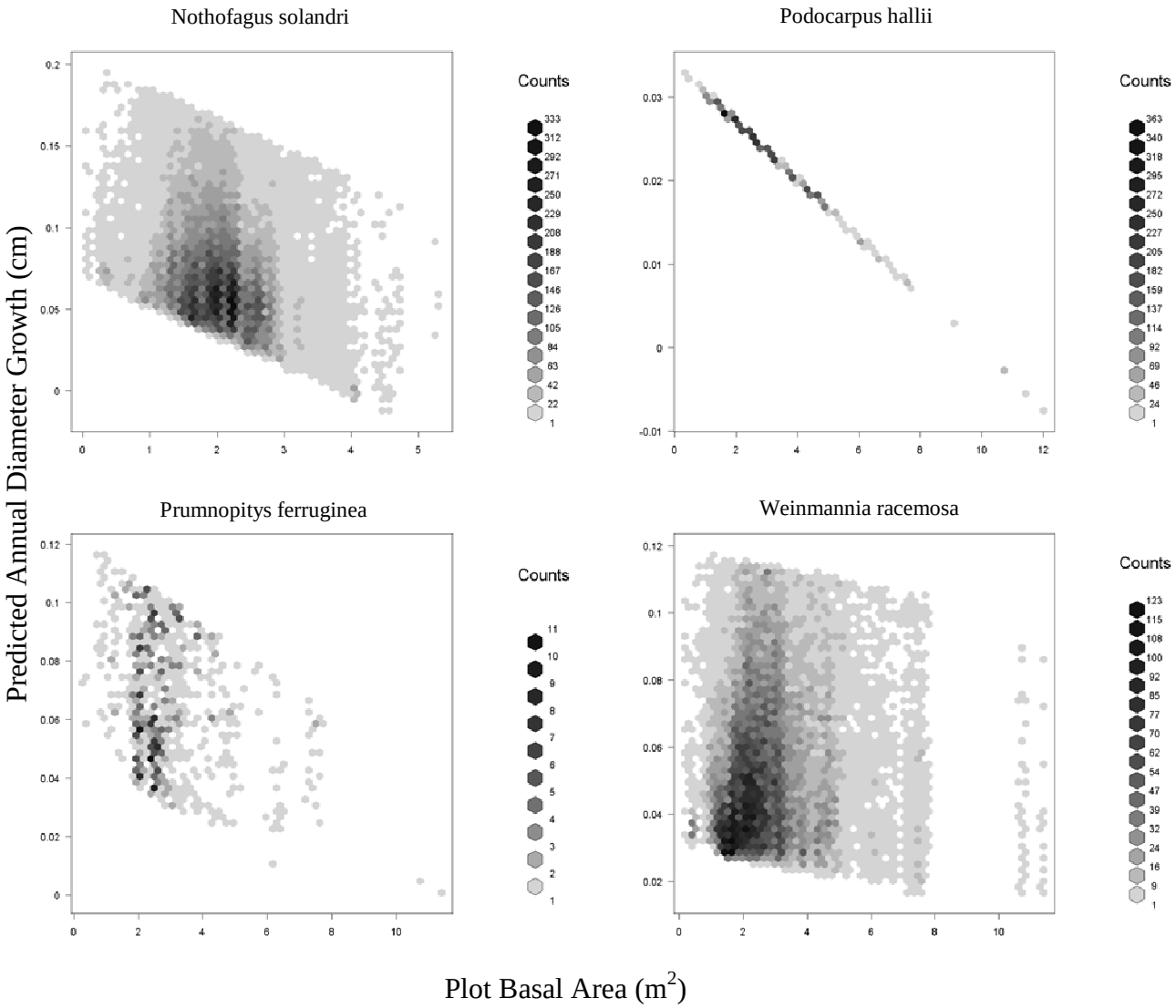

Figure A5.3 (cont.)

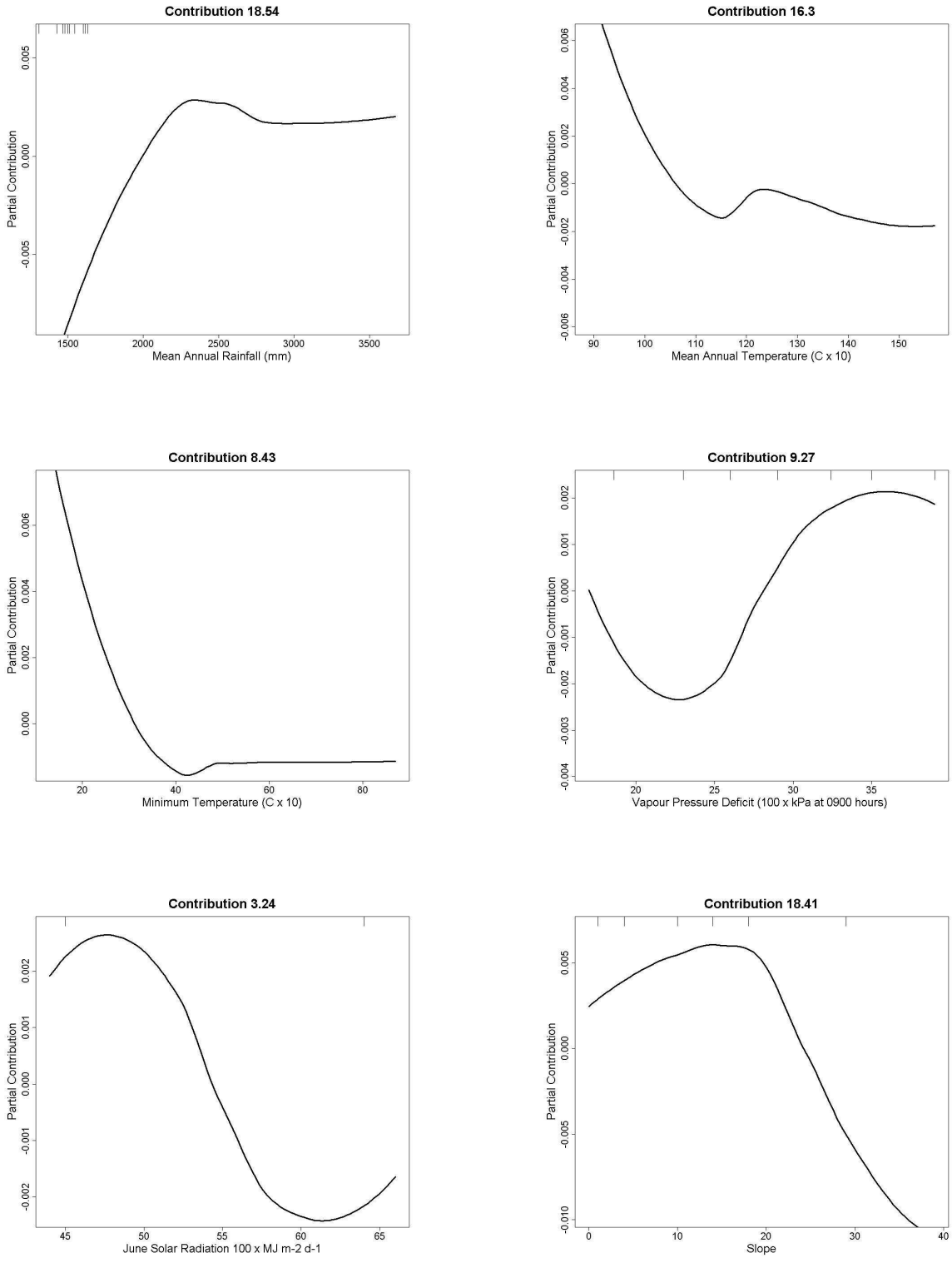

Figure A5.4a Smoothed partial contributions of key environmental variables to predicted mean deviance in diameter growth for *Beilschmiedia tawa* in 0.04 ha plots in boosted regression tree models.

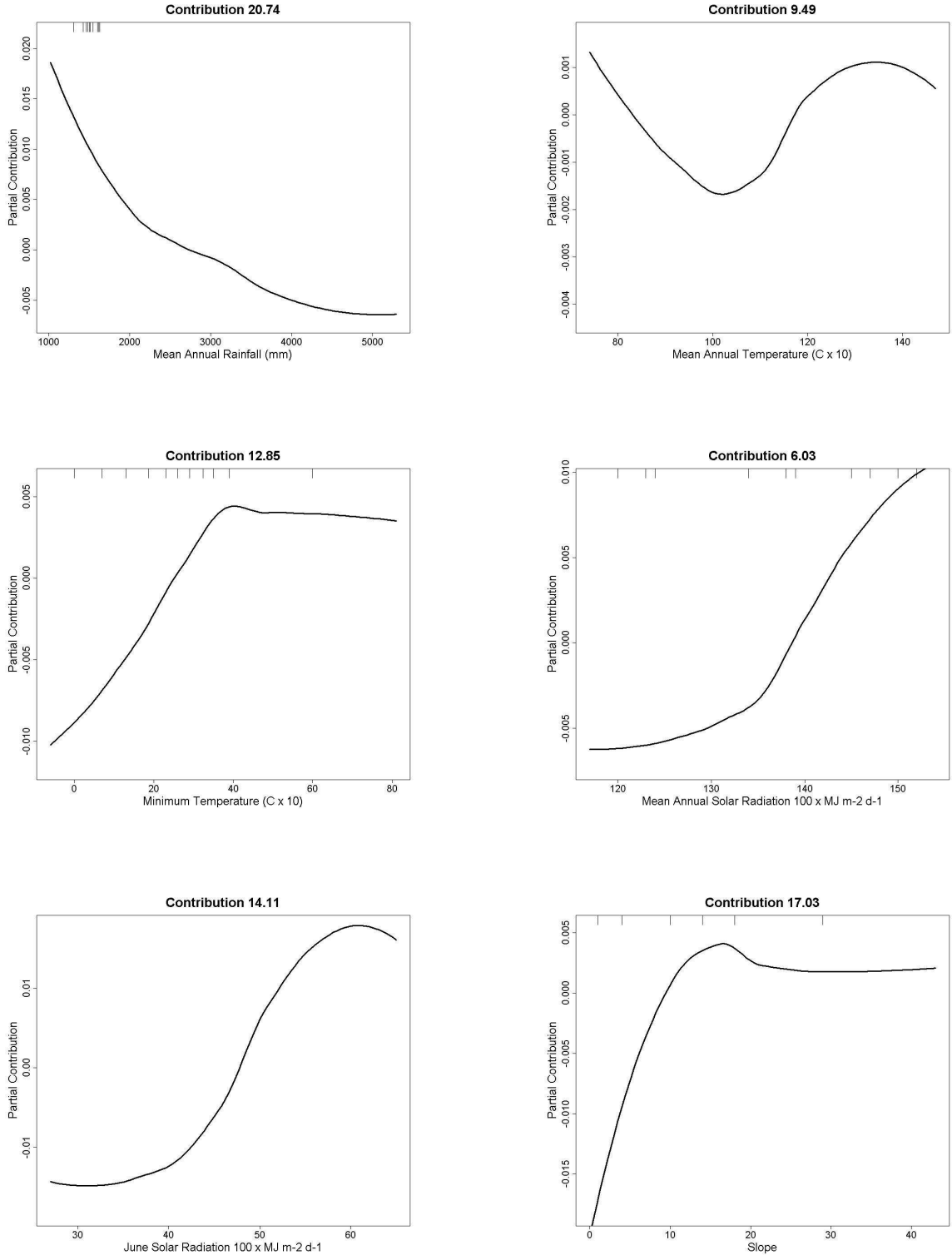

Figure A5.4b Smoothed partial contributions of key environmental variables to predicted mean deviance in diameter growth for *Dacrydium cupressinum* in 0.04 ha plots in boosted regression tree models.

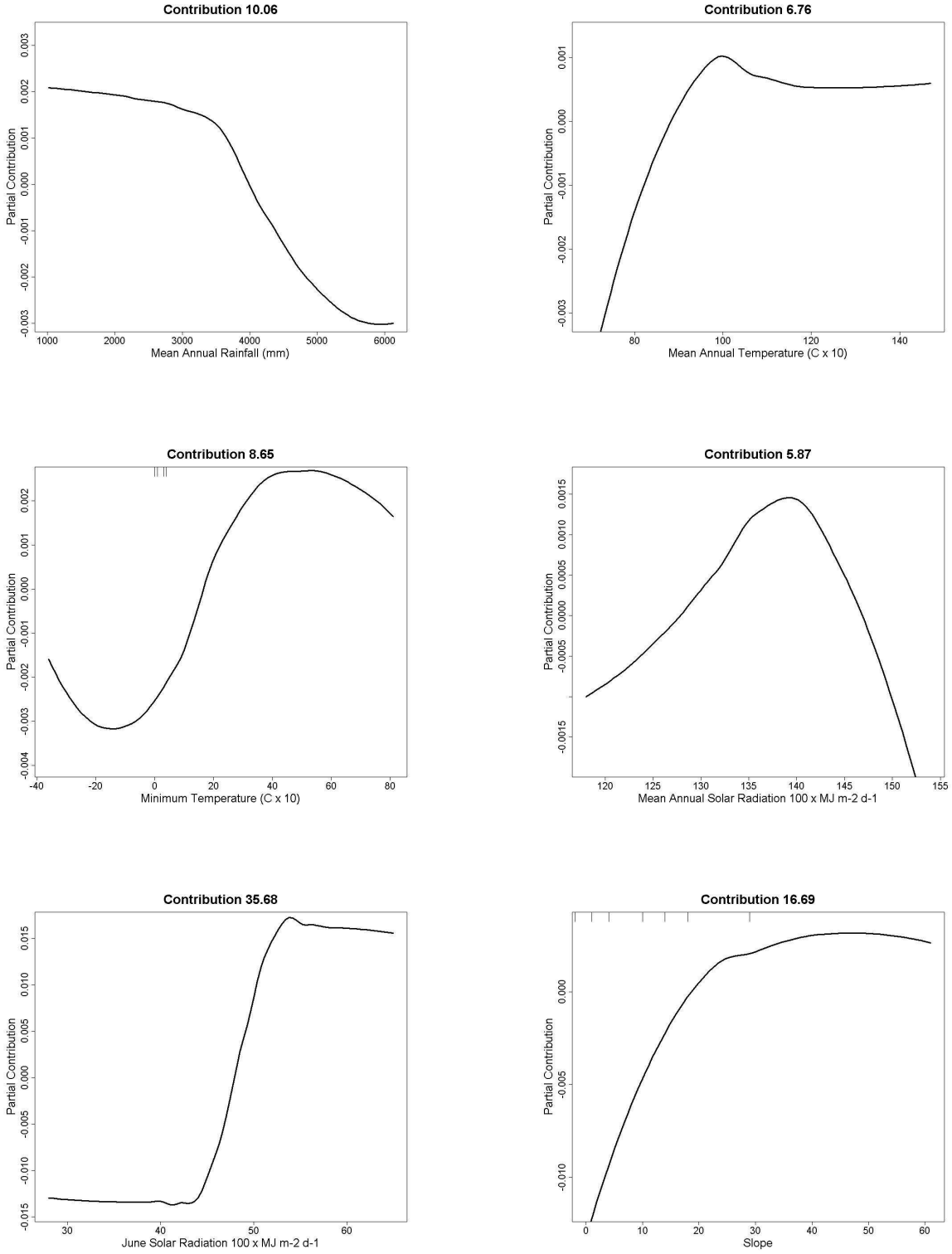

Figure A5.4c Smoothed partial contributions of key environmental variables to predicted mean deviance in diameter growth for *Elaeocarpus hookerianus* in 0.04 ha plots in boosted regression tree models.

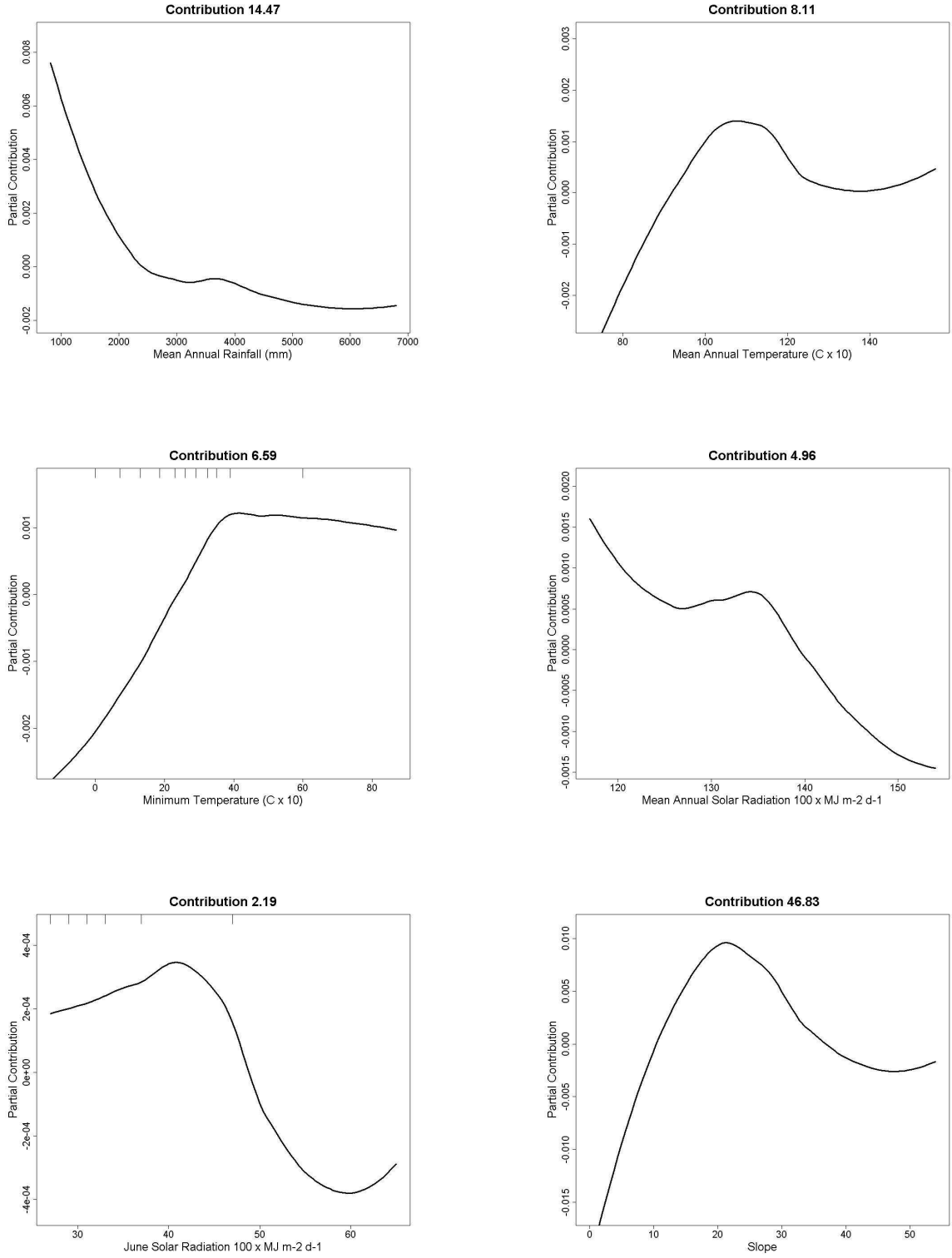

Figure A5.4d Smoothed partial contributions of key environmental variables to predicted mean deviance in diameter rowth for *Myrsine australis* in 0.04 ha plots in boosted regression tree models.

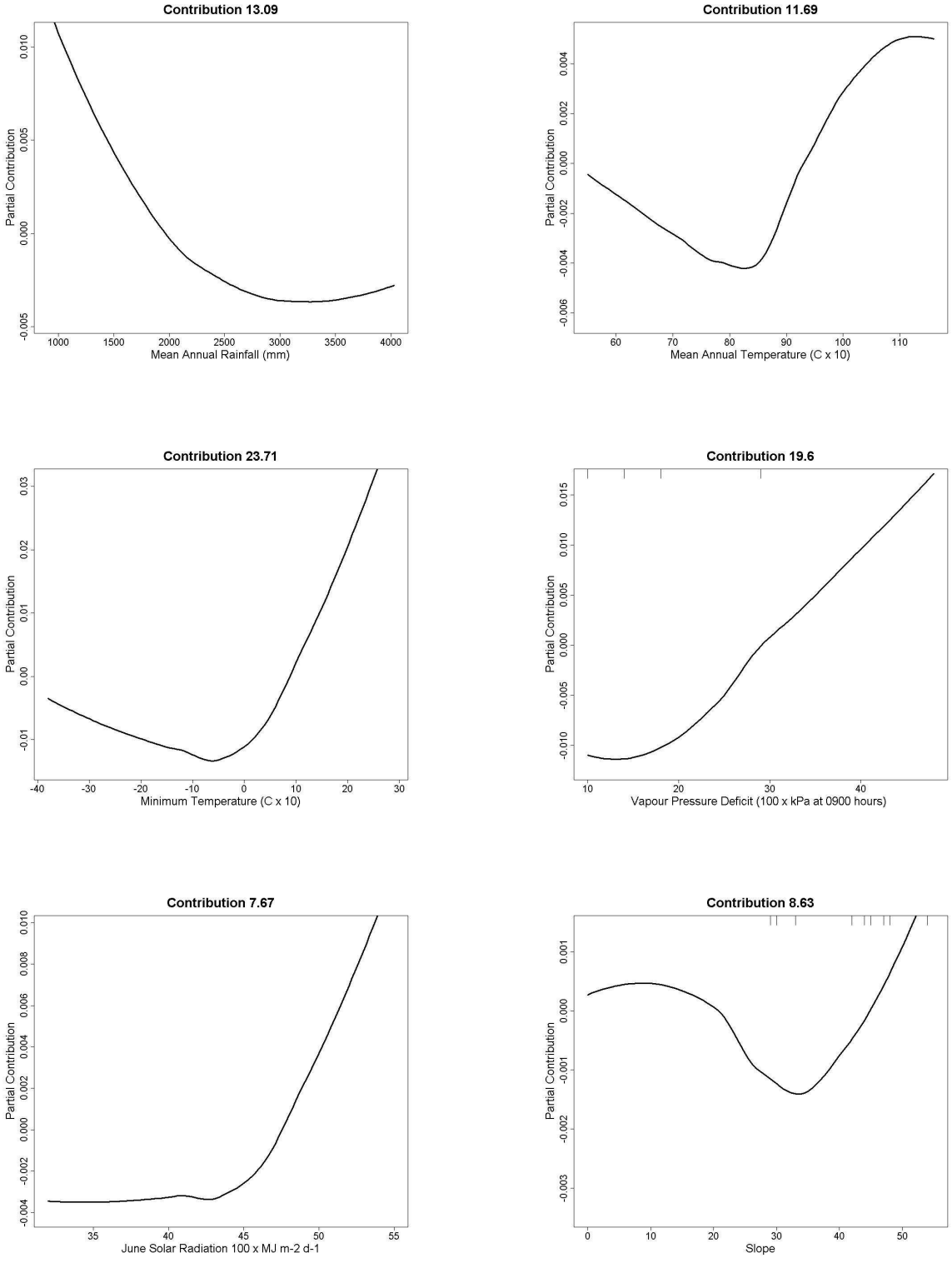

Figure A5.4e Smoothed partial contributions of key environmental variables to predicted mean deviance in diameter growth for *Nothofagus fusca* in 0.04 ha plots in boosted regression tree models.

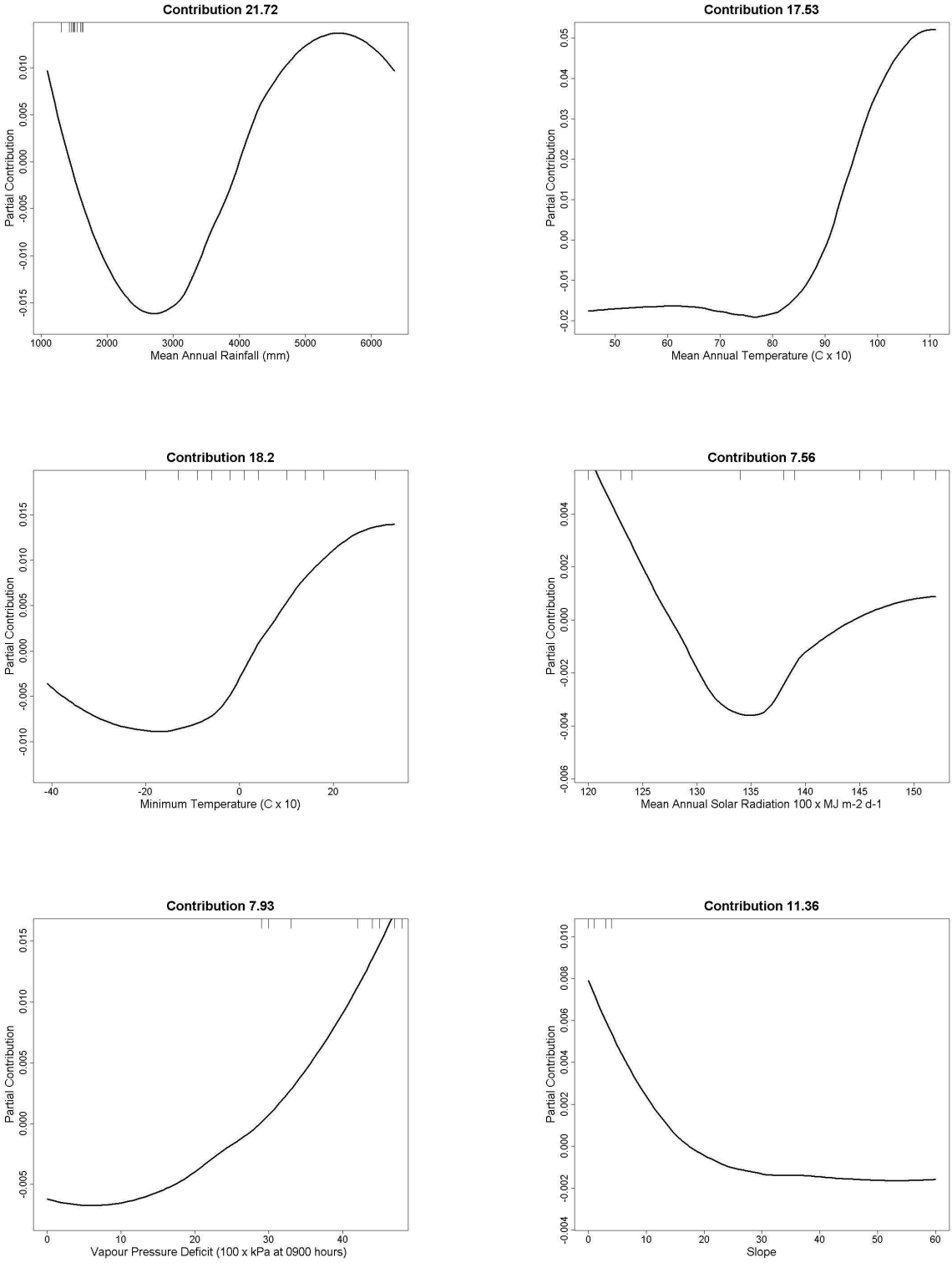

Figure A5.4f Smoothed partial contributions of key environmental variables to predicted mean deviance in diameter growth for *Nothofagus menziesii* in 0.04 ha plots in boosted regression tree models.

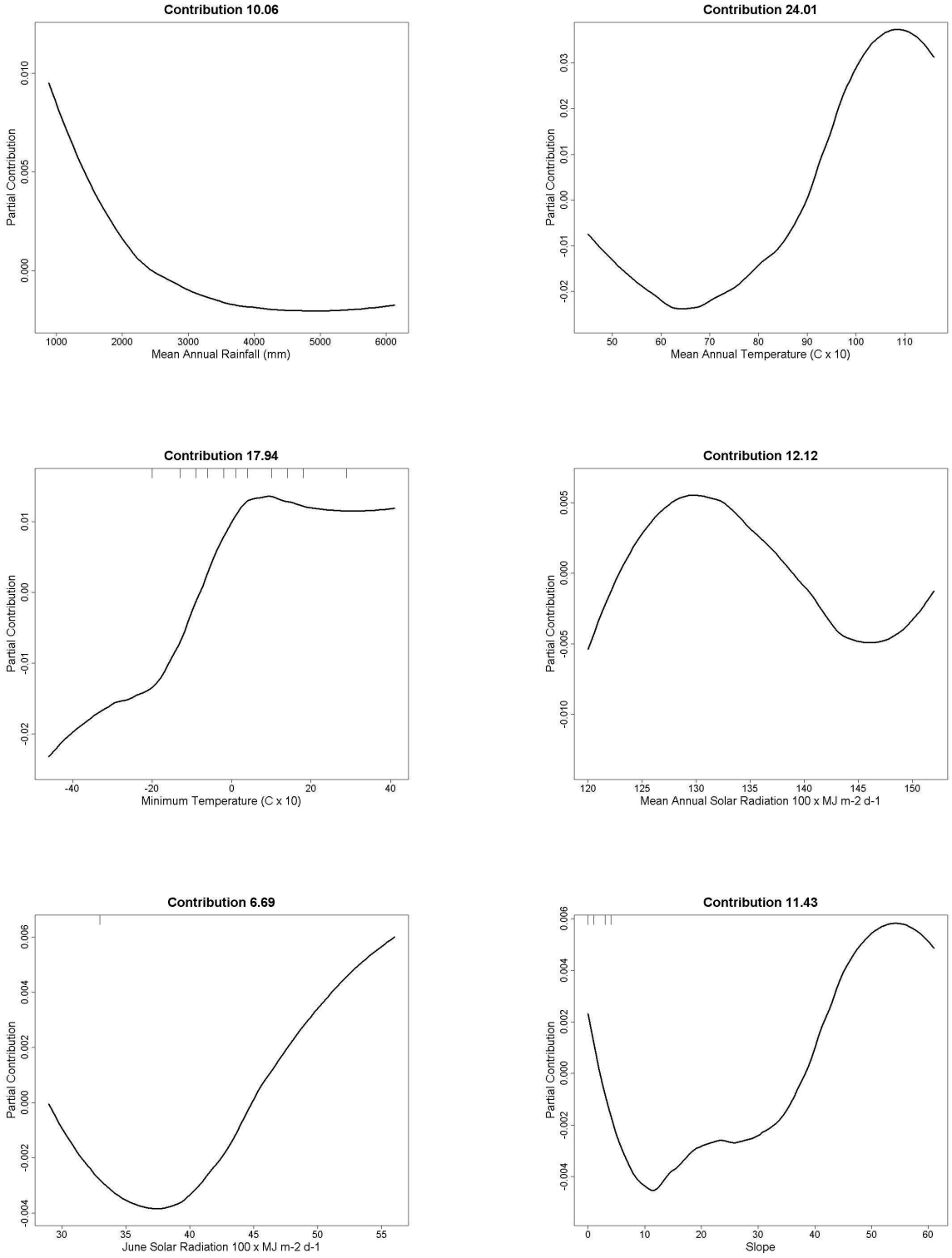

Figure A5.4g Smoothed partial contributions of key environmental variables to predicted mean deviance in diameter growth for *Nothofagus solandri* in 0.04 ha plots in boosted regression tree models.

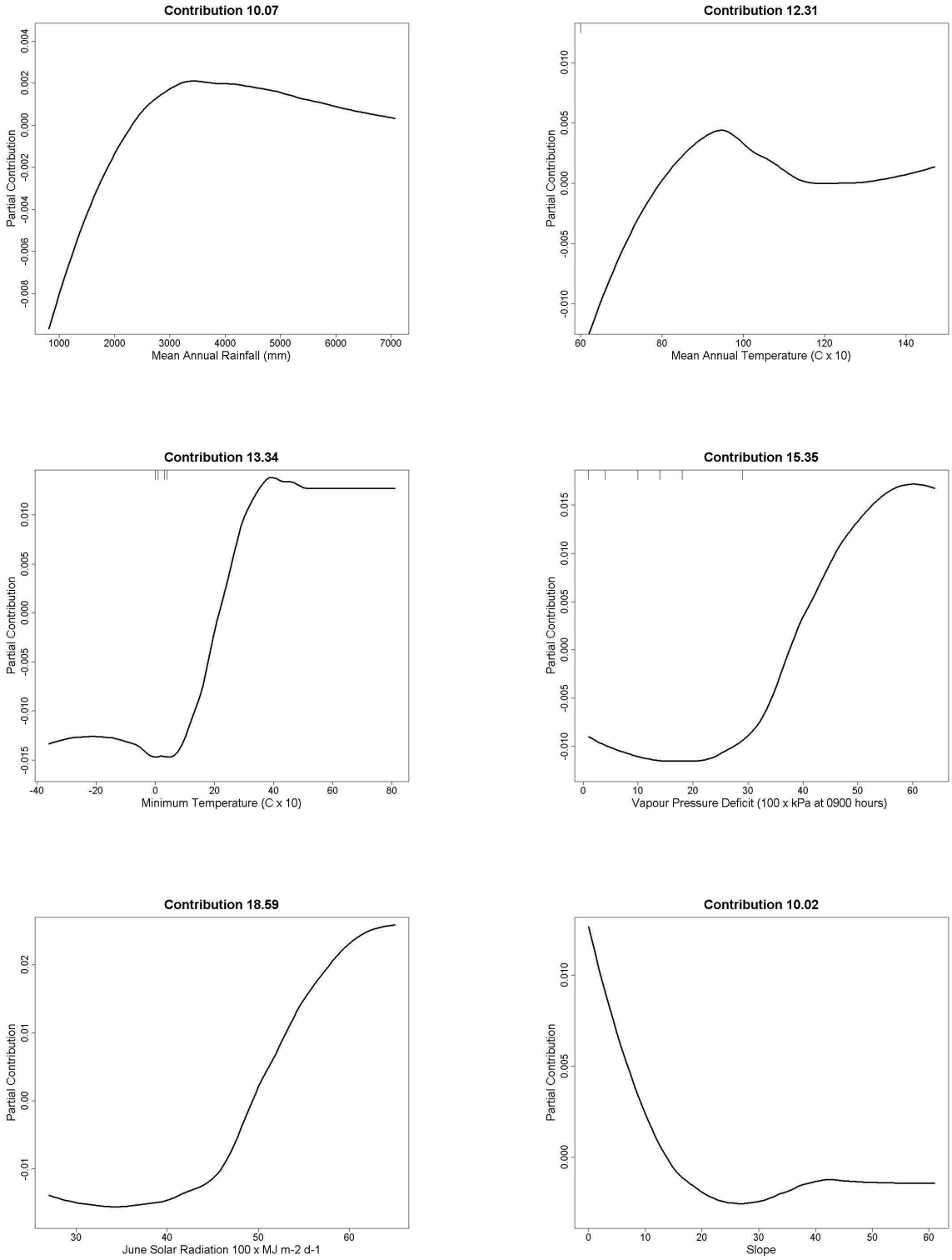

Figure A5.4h Smoothed partial contributions of key environmental variables to predicted mean deviance in diameter growth for *Podocarpus hallii* in 0.04 ha plots in boosted regression tree models.

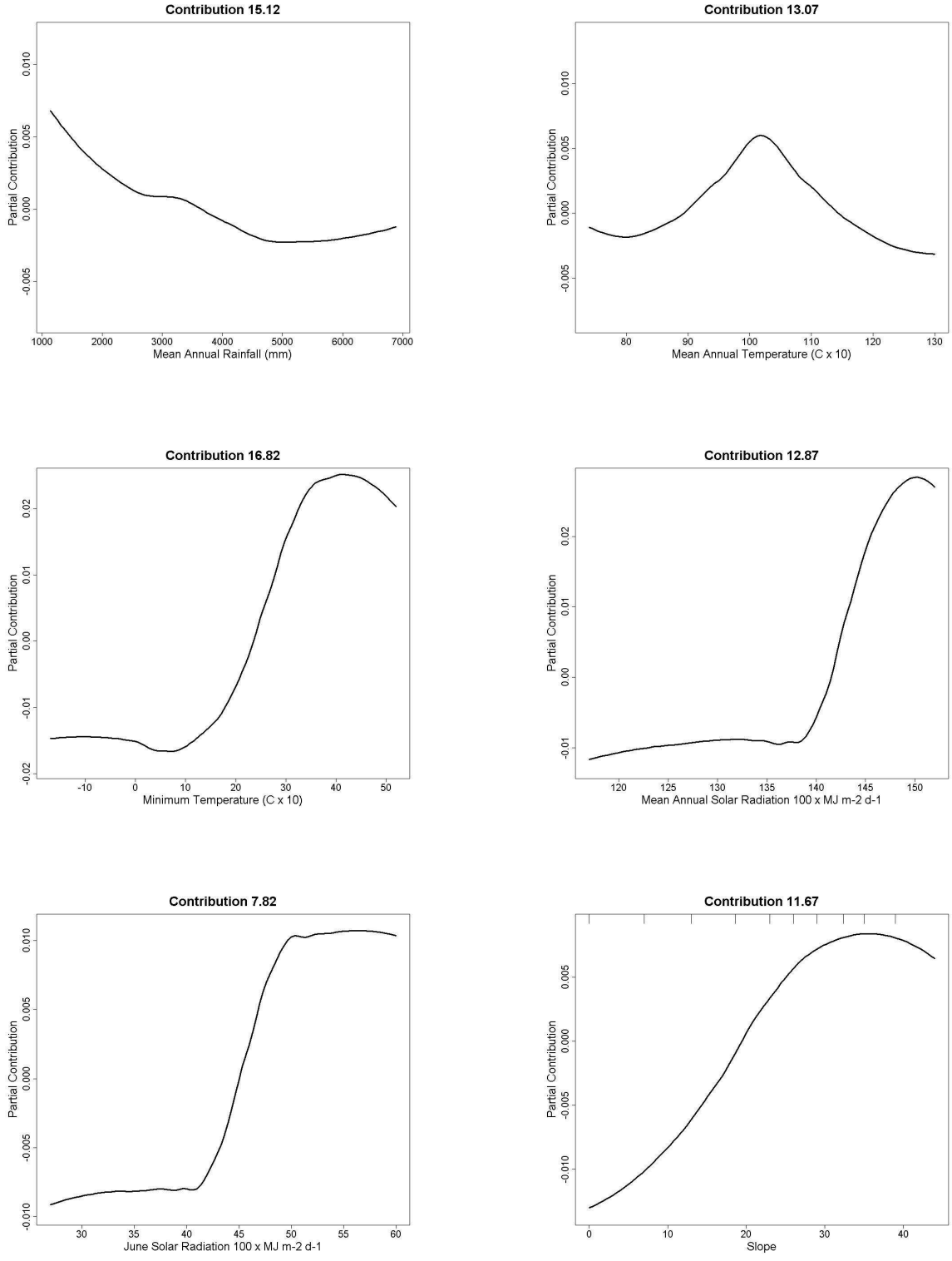

Figure A5.4i Smoothed partial contributions of key environmental variables to predicted mean deviance in diameter growth for *Prumnopitys ferruginea* in 0.04 ha plots in boosted regression tree models.

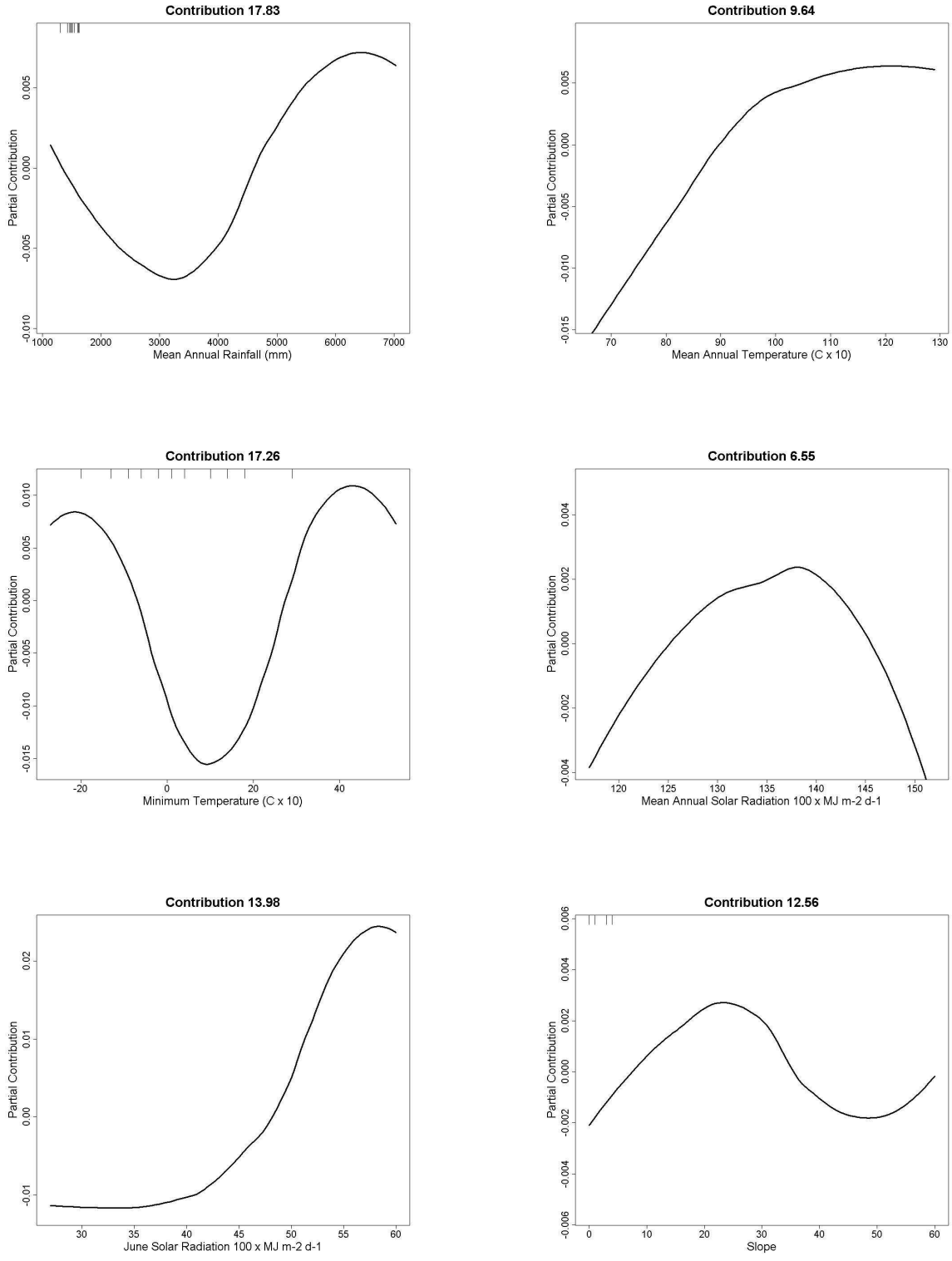

Figure A5.4j Smoothed partial contributions of key environmental variables to predicted mean deviance in diameter growth for *Weinmannia racemosa* in 0.04 ha plots in boosted regression tree models.